TIME VARIATION STUDIES

OF THE COSMIC RAY PHOTON COMPONENT DEEP IN THE ATMOSPHERE

A Thesis

Submitted to

Faculty of Graduate Studies, University of Manitoba, in partial fulfillment of the requirements of the Degree of Doctor of Philosophy.

By

Fook-Kit Chin

Winnipeg, Manitoba

August, 1966

ACKNOWLEDGEMENTS

The writer wishes to express his gratitude to Professor S. Standil, the supervisor, for his continuing guidance and valuable suggestions during the time of this research and the preparation of this thesis.

Sincere thanks are due to Mr. R. S. Foulds for his technical assistance in maintaining the electronics throughout the experiments.

Grateful acknowledgements are extended to Northern Electric Co. Ltd. not only for their grant of a research fellowship to the writer during 1962-1963, but also for their personal concerns which have become a constant source of encouragement.

Acknowledgements are also made with thanks to the National Research Council of Canada for the financial support to this research, to Dr. H. Carmichael for the supply of Deep River neutron monitor data, and to the Department of Transport, Winnipeg for the supply of daily weather reports.

A B S T R A C T

The results of a study on the atmospheric effect and the solar diurnal variation of sea level cosmic ray photons with energies between 3.8 and 183 MeV, using a large NaI (Tl) crystal total absorption spectrometer, are presented and discussed.

Long term observations show that the atmospheric effects of the sea level cosmic ray photons are mainly barometric. The energy dependence of the barometric coefficients was established and is explained in terms of a simple absorption model.

The energy relationships of solar diurnal amplitudes and times of maximum were also found. The results are interpreted taking into account the effect of the earth's magnetic field and the Axford-Parker theory by assuming a one-to-one correspondence between the energy of the detected photons and the "effective" energy of the primaries from which they arise.

C O N T E N T S

CHAPTER I

INTRODUCTION

Although the time variation of cosmic radiation was studied as early as 1930, it is not until the last fifteen years that it has fully developed into a new and special field of cosmic ray research, lying at the boundary of geophysics, solar physics and astrophysics. The rapid expansion of this field is mostly due to the great advancement in cosmic radiation detection techniques and the associated instrumentation which have made possible an accurate continuous recording. The establishment of this field as a new branch of research must also be credited to the revelation of the geophysical and astrophysical aspects of the cosmic radiation and to the tremendous collective efforts in experimentation during the IGY year. Further great progress in this field will rely on the findings from satellites and space probes, especially if they can be operated on a continuous basis.

Undoubtedly, the time variation of cosmic radiation has been verified as a sensitive tool in attempts at understanding the state of distribution of matter and energy and the cosmic dynamic processes in outer space. It can provide information about the distribution of cosmic ray sources in space, the cosmic ray gradient in the galaxy, particles of solar origin, dynamics of the solar wind, magnetic fields in the interplanetary and galactic media, geomagnetic field and the terrestrial atmosphere since these studies of cosmic radiation can be explained in terms of electrodynamics, plasma physics, solar atmospheric conditions, structures of the galaxy, geomagnetism and meteorology. Studying the

time variation of cosmic radiation at the earth, we can infer the situations in the vicinity of earth and sun, in the interplanetary space, and in the galaxy. With further advances in this field, the origin of cosmic radiation will be disclosed.

Even though the satellites and space probes have become powerful instruments for cosmic ray research in this era, their potency in the study of the time variation of cosmic radiation has not yet been fully utilized. Up to the present time, ground cosmic ray detectors still play the most important role in such research because of their efficiency in a continuous collection of data.

Situated deep in the atmosphere, cosmic ray monitors observe essentially the secondary cosmic ray components. By means of the method of coupling constants, the amplitude of variation in different secondary components can be used to estimate the variation in the primary energy spectrum (Dorman 1957, see Appendix A). As most of the secondary component detectors record the integral effect of the primaries as a result of their deficiency in differential energy discrimination, they are sensitive only to a certain primary energy region according to the energy dependence of their coupling constants. Consequently, the determination of the energy dependence of the primary variation will require extensive data of various secondary components. Better accuracy will be obtained if these secondary components have a substantial difference in the energy dependence of their coupling constants. At present, the nucleonic and hard components are the two most popular ones which yield reliable information in connection with the primary cosmic radiation of low energy.

The existence of cosmic ray photons near sea level has long been recognized theoretically and experimentally. However, the study of

such photons has been very far behind the general advancement in cosmic ray research, probably because of the late development of methods to effect its separation from the other cosmic ray components. Earlier work on the sea level photons has been performed to study their absorption coefficients in matter (Janossy et al. 1940, and Regener 1940) and their energy spectrum (Janossy et al. 1940, Clay et al. 1951, Chou 1953, Cernigoi et al. 1954, and Kameda 1960). Since 1950, common interest in cosmic ray photons has been shifting to the understanding of primary photons. In 1951, Perlow et al. reported that rocket experiments show 0.1% of the energy flux above the atmosphere in the form of photons. During a balloon flight on March 20, 1958, a gamma-ray burst of 2×10^{-5} ergs/sec cm^2 from a solar flare was detected (Peterson et al. 1959). Having measured the primary photons at balloon altitudes with emulsions, Fowler et al. (1963), Kird (1963) and Abraham et al. (1963) also arrived at the conclusion that the contribution of photons in the primary component is negligibly small. The experimental results of the Explorer XI (Kraushaar et al. 1963) indicates an upper limit of 3×10^{-4} particles cm^{-2} sec^{-1} $sterad^{-1}$ for primary photons of energy greater than 100 MeV. In recent years, a number of workers (Maze et al. 1960, Firkowski et al. 1962, 1963, Gawin et al. 1963, Gawin et al. 1965) have given evidence on primary photons by studying showers with a low content of penetrating particles. Local sources of high energy photons have also been searched for by Cocconi (1960), Chudakov et al. (1963), and Kraushaar et al. (1963). In general, primary photons have been reported to have very low intensity.

So far there are suprisingly few reports on the time variation of photons near sea level. As primary photons are negligible in quantity, sea level photons are mainly the end product of the nuclear and electromagnetic interactions between the primaries and the atmosphere. The

significance of such a study is obvious. It can provide information about the coupling processes between the primary and the sea level photons and serve as a secondary component for the determination of the variation in the primary energy spectrum. At the University of Manitoba, a large NaI (Tl) crystal total absorption spectrometer has been designed by Standil et al. (1959) primarily for the study of the photon component near sea level. With this spectrometer the solar flare event of May 4, 1960 was recorded (Standil et al. 1961), the pressure coefficients of the photon component near sea level were determined for photon energies greater than 7 and 35 MeV (Bukata et al. 1962), and a day-night comparison of the photon intensity was investigated (Chin et al. 1962). Results obtained encouraged a further study of the sea level photons with the spectrometer. With the acquisition of a 400 channel pulse height analyser in 1962, it became possible to perform a time study on the differential energy spectra of the photons on a continuous basis, and work was started on the daily variation of the photon component. Data have been analysed to determine the atmospheric effect and the solar diurnal variation for such a component. In particular, the energy dependence of the barometric coefficients and of the solar diurnal amplitudes and times of maximum intensity have been determined. This thesis presents the results of such a study, using the data collected during the period from February to November 1963.

CHAPTER II

EXPERIMENTAL TECHNIQUES

The daily variation experiments on the cosmic ray photons have been carried out in the Cosmic Ray Laboratory which is located on the roof of the Allen Building at the University of Manitoba, geographic latitude 49.9° N, longitude 97.2° W, and elevation 236 meters above sea level. The laboratory was built with construction materials which would keep the transition effects of cosmic rays through matter to a minimum (roof thickness about 2.3 gm cm^{-2}). An air conditioning system was installed to maintain the room temperature at 70 $\pm$ 2° F all the time so that instability of the electronics due to drastic thermal variation could be eliminated. Studies on the time variation of the photon component were performed with a large NaI (Tl) crystal total absorption spectrometer as the detector, a conventional arrangement of electronics as the events recorder and a 400 channel pulse height analyser as the energy sorter. Data were collected in terms of differential energy spectra.

A. The Total Absorption Spectrometer and the Recording Units

It has been established that the cosmic radiation near the sea level is composed of charged and neutral particles. The present total absorption spectrometer has been primarily designed to separate the neutral component from the total cosmic radiation. Functionally speaking, the whole experimental arrangement consists of two systems; namely, the signal system which produces signal pulses upon detecting charged or uncharged particles, and the anticoincidence system which provides

anticoincidence pulses for the cancellation of the charged or not totally absorbed particles. Detailed information about the total absorption spectrometer and the recording electronics can be found in the reports of Standil et al. (1959) and Bukata (1958, 1960) while the characteristics of the whole apparatus in cosmic ray detection have been investigated by Chin (1961). A general description is given below.

The signal system contains a NaI (thallium activated) crystal with a cylindrical shape of 9-3/8 inches in diameter, 8-11/16 inches in height and a 45° bevel to a cone of 2-5/8 inches in diameter as shown in Fig. 2.1. When a cosmic ray particle, either charged or neutral, interacts with the crystal a flash of light of a decay time 0.25 micro-seconds is generated, the quantity of which is proportional to the amount of energy lost by the impinging particle in the crystal. Three photo-multipliers that view the bottom plane face of the crystal through a glass light pipe will pick up and convert the emitted light into electrical pulses which are electronically summed with a three channel mixer into a pulse designated as signal pulse. Being small in size, this pulse is further magnified by means of a linear amplifier before it is sorted into the proper channel of a 400 channel pulse height analyser (see Fig. 2.2).

As for the anticoincidence system, a cylindrical shield of plastic phosphor (type NE 102) has been constructed to envelope the NaI crystal entirely in terms of four sections: a circular top plate of 26 inches in diameter and 1 inch in thickness, two identical sections of hollow cylinder with an outer diameter of 26 inches and an inner diameter of 16 inches and a height of 11-1/2 inches, and a cylindrical bottom of 26 inches in diameter and 6 inches in thickness. Six photomultipliers were installed around the edge of the top plate, and five were placed

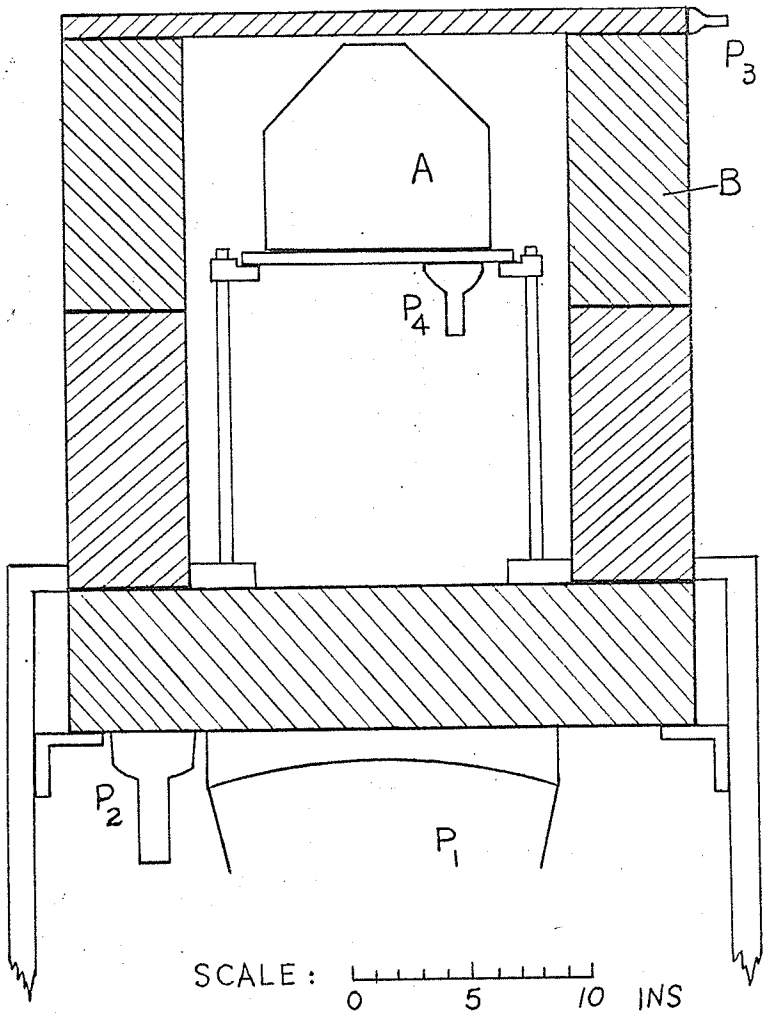

A	NaI (Tl) CRYSTAL
B	PLASTIC PHOSPHOR ANTICOINCIDENCE SHIELD
P_1	DU MONT K1328 PHOTOMULTIPLIER
P_2	ONE OF FOUR DU MONT 6364 PHOTOMULTIPLIERS
P_3	ONE OF SIX DU MONT 6292 PHOTOMULTIPLIERS
P_4	ONE OF THREE DU MONT 6364 PHOTOMULTIPLIERS

FIG. 2.1 TOTAL ABSORPTION SPECTROMETER

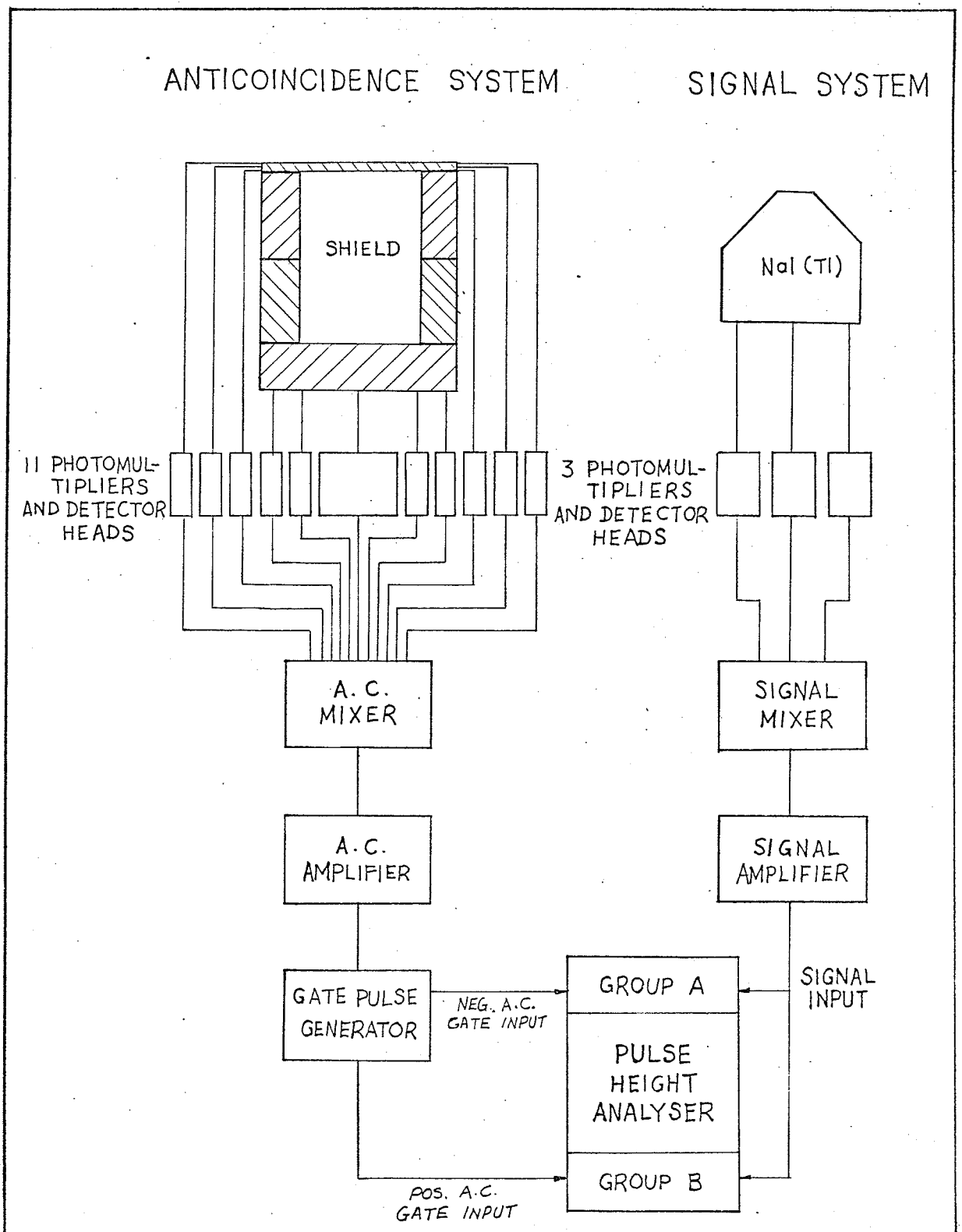

FIG. 2.2 BLOCK DIAGRAM OF THE SIGNAL AND ANTICOINCIDENCE SYSTEMS

directly under the bottom section. These eleven photomultipliers collect the light emitted in the anticoincidence shield due to an interaction between the cosmic radiation and the plastic phosphor, and convert it into electrical pulses which are added together in an eleven channel mixer as a single pulse called the a.c. pulse. Having been amplified by a linear amplifier, this a.c. pulse, if its size is above the bias setting of the gate pulse generator, will trigger the generator to produce a negative and a positive output pulse, each of 5 volts amplitude, which are fed into the 400 channel pulse height analyser as gating pulses.

In the present experiments, only two hundred channels of the pulse height analyser have been used. These two hundred channels have been subdivided into two separate and independent groups (one hundred channels for each) with their own signal input and anticoincidence input circuits. A signal pulse from the signal system is simultaneously fed into these two groups (designated as A and B) while the negative and the positive output pulses from the gate pulse generator in the anticoincidence system are transmitted to the coincidence and the anticoincidence gating input circuits of groups A and B respectively. A signal pulse accompanied with an anticoincidence pulse will be sorted into the proper chanel of group A while in the absence of an a.c. pulse, the signal pulse will be analysed and stored in the group B.

As a result, events in the signal system unaccompanied by events in the anticoincidence system (as recorded in group B) are ascribed to the neutral particles which are totally absorbed by the crystal, while the charged events are recorded in group A if events happen simultaneously in the anticoincidence system. The total absorption spectrometer which consists of the NaI crystal and the shield, and the block diagram of the whole experimental arrangement are shown in Fig. 2.1 and Fig. 2.2.

B. Function as a Total Absorption Spectrometer for the Neutral Component

To clarify the foregoing description, let us discuss the characteristics of the instrument. The NaI crystal, by itself alone, can detect charged and uncharged particles coming from all directions. The pulse height thus produced in the signal system is proportional to the energy lost by these particles in the crystal. In the case of an incident vertically moving charged particle, it suffers, practically without exception, from ionization loss or bremsstrahlung loss in the plastic phosphor shield of 1 inch thickness before it hits the crystal. Then, it may pass through the NaI crystal after transferring another part of its energy to the crystal or it may be totally absorbed by the crystal. The energy loss in the plastic shield will initiate an a.c. pulse which through the gate pulse generator will close group B of the pulse height analyser and allow group A to accept the signal pulse from the NaI crystal. Therefore, the differential spectrum as registered in group A is not an energy spectrum of the charged particles in an absolute sense because the energy loss in the crystal does not necessarily identify the entire energy possessed by the particles detected.

In the absence of an a.c. pulse, the particle detected by the NaI crystal will be recorded in group B of the pulse height analyser and is regarded as a neutral one. To understand the nature of the differential energy spectrum as recorded in group B, let us follow the events after a neutral particle is incident on the shield. This particle either has an intact passage or interacts with the plastic phosphor. In the latter case, there are two possibilities. Either the secondary particles produced in the interaction are totally stopped in the plastic phosphor, thus eliminating the possibility of its being detected by the NaI crystal; or some of the secondary particles impinge on the crystal and hence initiate

a pulse in the signal system. However, such secondary particles which are produced in the interaction between a neutral primary particle and the shield always contain at least one ionizing particle (except the case of (n, gamma ray) but this process is negligibly small for a neutron with energy greater than 10 MeV). This ionizing particle will generate an a.c. pulse in the anticoincidence system; thus, this event will be registered in group A as a charged particle. Therefore, the probability for a neutral particle, interacting with the shield, to be recorded in group B is negligibly small. In the former case (i.e. a neutral particle passing through but not interacting with the shield) three possibilities must be considered. First, this neutral particle is not detected simply because of its missing the crystal or because of its penetrating through the crystal again without any interaction. Second, it interacts with the crystal but some of the secondary particles of the interaction are picked up by the shield; hence, in terms of the above reasoning, it will not be recorded in group B. Third, both the primary neutral and its secondary particles are entirely stopped in the crystal, and this event is thus registered in group B in terms of its true energy and is said to be totally absorbed. With the combined operation of the NaI and the anti-coincidence shield, the spectrometer can select and record the totally absorbed neutral particles among all the cosmic ray particles. As a result, the differential spectrum as registered in group B represents the true energy spectrum of the totally absorbed neutral particles.

The efficiency of the plastic shield in detecting a charged particle has been estimated by an experiment (Chin, 1961) in which two differential spectra were determined separately. One spectrum was obtained without the operation of the plastic shield so that it represented the distribution due to both the charged and the neutral particles. The other

spectrum obtained with the operation of the plastic shield contained in principle only totally absorbed neutral particles. Assuming no neutral particles in the cosmic radiation, the differential spectrum obtained without anticoincidence can be regarded as the spectrum due to the pure charged component and the differential spectrum obtained with anticoincidence as the spectrum of those charged particles which escape the anticoincidence cancellation. For different energy loss ranges, the percentage elimination of the charged component was worked out with the above two spectra. As a result, it was determined that the shield can detect much greater than 68% of the charged particles which lose 12 to 50 MeV of their energies in the crystal. For charged particles with energy loss above 50 MeV, at least 96% are detected by the shield. Since the cosmic radiation does contain neutral particles, the above experimental values are merely lower limits for the "rejection efficiency".

C. Function as a Photon Monitor

For the purpose of investigating the nature of the neutral cosmic radiation observed by the present apparatus, a lead absorption experiment was performed to determine the absorption curve of the neutral component (Chin, 1961). In the experiment, lead of different thicknesses was placed above and close to the top of the anticoincidence shield, thus reducing the transition effect in the air between the lead and the detector. Experimental data were collected in terms of differential energy spectra of the totally absorbed neutral component.

Four energy ranges (10-12 MeV, 20-40 MeV, 40-60 MeV, and 100-270 MeV) were selected for analysis. These four experimental absorption curves had common qualitative features: the intensity decreased with increasing thickness and tended to reach a constant value at large absorber

thicknesses. The analysis of each of these four curves followed the same procedure.

First, the constant value of the intensity at large thickness was recognized as the back ground intensity which was not affected by any amount of lead thickness. Second, a new curve was constructed by subtracting the background intensity from the original experimental curve. This new curve appeared to be approximately a straight line (for all four energy ranges); hence, it implied that the neutral component detected is essentially composed of a single kind of particle. Third, comparison was made between the slope of this straight line (observed linear absorption coefficient) and the absorption coefficients for photons and neutrons in lead. Thus, it was concluded that the four observed straight lines were the absorption curves of photons primarily.

To assess the amount of neutrons possibly detected in the neutral component for a certain energy range a theoretical absorption curve for 2% neutrons and 98% photons was constructed and compared with the experimental absorption curve. Similar attempts were also made for the assumptions of 5% and 10% neutrons. In general, for all four energy ranges considered, the curves of 5% and 10% neutrons agreed poorly with the experimental curve. The zero % neutrons curve gave the best fit and the 2% neutron curve was the second best.

Even though the lead absorption experiment did not conclusively establish the exact nature of the detected neutrals, the analysis did show that the assumption of greater than or equal to 98% photons and less than or equal to 2% neutrons was quite consistent with the experimental observations.

D. Calibration and Data Collection

In the present experiments on the time variation of the photon component, data were accumulated every hour in the form of differential energy spectra. The experimental procedures involved (a) alignment of groups A and B of the analyser, the signal system and the anticoincidence system, (b) determination of the differential energy spectrum, and (c) a stability check of the whole apparatus.

A gamma ray of energy 1.12 MeV emitted by Zn^{65} was used as a calibration source. The resolution of the spectrometer was found to be 16.8% at this low energy. First, groups A and B of the pulse height analyser were lined up with a constant pulse from a pulse generator through the signal mixer and amplifier. By adjusting the lower level position of one of the groups, this constant pulse was stored in the same channel in both groups. (If we desire a particular channel in both groups for this constant pulse, we simply turn the common zero dial of the analyser.) The channel number corresponding to zero energy can be determined by the positions of two constant pulses of known sizes in group A or B. Second, to ensure an equal functioning of the three signal photomultipliers viewing the NaI crystal, their plate voltages were adjusted individually such that each of them, when operated alone, gave the 1.12 MeV gamma ray peak in the same channel of group A of the analyser. Third, the eleven a.c. photomultipliers observing the shield were aligned as follows: That phototube which views the central region of the shield bottom was taken as the "standard" and operated alone in the anticoincidence system. A differential spectrum of the background as seen by this phototube was collected in group A and then transferred to group B. With the Zn source near this phototube, another spectrum (for the same time interval) was obtained in group A. Then, these two spectra were overlapped

on a screen display and the channel number where they intersected each other was determined. For the rest of the phototubes, the same procedure was followed and each high voltage was adjusted so that all anticoincidence phototube gave the same intersection channel number. Thus all eleven phototubes had about the same output for a given light flash in the scintillator.

The differential energy spectrum for the photon component is determined by further adjustment of the signal and anticoincidence systems such that the energy range of interest is included in the spectrum and an effective separation of the neutral from the charged particles is attained. Together with a suitable choice in the output gains of the signal mixer and amplifier, the plate voltages of the three signal phototubes can be adjusted to obtain the energy range desired for the differential spectrum being investigated. A study in the high energy range required low plate voltages for the signal phototubes, and low gains for the mixer and the amplifier; the reverse would lead to a low energy range. Through the calibration of the 1.12 MeV gamma ray peak position, the energy range of the cosmic ray spectrum could be determined. (Assuming that the energy E_x required in the differential spectrum should appear in channel x with the mixer gain at b and the amplifier gain at a, and that the calibration spectrum of the gamma ray is to be done with the mixer gain at B and the amplifier gain at A, the 1.12 MeV peak position must be located at channel y from the following formula,

$$y = x \frac{A}{a} \frac{B}{b} \frac{1.12}{E_x}$$

If the zero channel does not coincide with the zero energy, x should be replaced by (x - d) where d is the actual channel position of the zero energy. Hence, the plate voltages of the three signal phototubes can be increased or decreased by an equal amount until the gamma ray peak is

observed in channel y.)

An effective separation of the neutral component from the charged was achieved by proper adjustment of the bias on the a.c. pulses from the anticoincidence system. After alignment of the eleven a.c. phototubes, we could control the a.c. counting rate by regulating the gain of the a.c. amplifier and the bias of the gate pulse generator. To begin with, we operated the signal system only,which gave a differential energy loss spectrum due to the charged and the neutral particles in group A of the analyser. The spectrum was left undisturbed in group A after its contents had been printed out. Then, we connected both the signal and the anticoincidence systems to group B of the analyser. Recording the a.c. counting rate at the output of the gate pulse generator, a differential spectrum of the neutral component was thus obtained for the same time interval in group B. On screen display, these two spectra were overlapped, and the effect of the elimination of the charged component on the neutral spectrum was examined. If the muon peak (Chin 1961) which appeared in the spectrum of the total cosmic radiation (registered in group A) could be seen in the neutral component spectrum (in group B), the cancellation was not satisfactory. Then, we erased the neutral spectrum in group B and obtained another neutral spectrum after a proper increase in the a.c. counting rate (i.e. a decrease in bias on the a.c. side). By so doing, any residue of the muon peak was found to vanish after a certain a.c. counting rate was reached. A number of neutral differential spectra were thus accumulated with different values of the a.c. counting rate until a further increase in a.c. counting rate gave a perceptible decrease in the neutral differential spectrum as a result of the abnormally large accidental cancellations. All these neutral differential spectra obtained with different a.c. counting rates were printed and plotted along with the

spectrum of the total component. By comparison, we determined the best value of the a.c. counting rate (1200 cts/sec) for an effective separation of the neutral from the charged component. Having assembled the whole apparatus as shown in Fig. 2.2, we accumulated a run with the chosen a.c. counting rate. This gave a differential spectrum of the neutral component in group B and one due to the charged particles in group A. Comparison of these two spectra with the previously obtained spectra assured us that a correct separation of the neutral from the charged component had been achieved.

In the present experiments, we are interested in the variations of the low energy cosmic ray photons. The whole system was adjusted so that the differential spectrum in group B covered photon energies from 3.8 to 183 MeV. We thus eliminated any gammas due to natural emitters in the surroundings. The differential energy loss spectrum of charged particles as registered in group A is not the point of interest in the present thesis. The time control system in the pulse height analyser was set at 52 minutes for a run. At the end of a run, the analyser was read out in destructive mode and the data printed out by an accounting machine. It took 8 minutes to complete the 200 channels tabulation together with the subtotal for every five channels, and then the analyser returned to the accumulation mode for data collection.

Calibration of the whole system was performed once every day. Hence, data collection was randomly interrupted for an hour in each day. For the signal system, the 1.12 MeV gamma ray peak position was checked with three signal phototubes operating. Whenever the gamma ray peak was found to drift away from channel 55, each of the signal phototubes was calibrated individually and appropriate adjustment was made on its plate voltage so as to properly line up the three signal phototubes again.

Then, the gamma ray peak was moved back to the designated position by a fine adjustment on the mixer unit. As for the anticoincidence system, the a.c. pulses were continuously monitored by a ratemeter connected to the output of the gate pulse generator. The a.c. counting rate was restored to the designated value during the calibration hour by adjusting the input bias voltage level so as to compensate for any slight shift of the electronics involved. Routine monitoring was also made on the output voltages of the power supply units every week. The functions of the mixers, amplifiers and gate pulse generator were calibrated regularly during the time of the calibration hour. The re-alignments of the signal and anticoincidence system were done whenever excessive individual adjustments seemed to be required. The performance of the above stability checking was aimed at keeping the whole system in operation under conditions as close to the original as possible.

The intensities of the neutral and of the charged in the first 20 channels of the spectra were summed up and plotted on an hourly basis for a final check on possible troubles in connection with the electronics and experimental environments. Along with the plotting of the atmospheric pressure and the ground temperature (supplied by the Department of Transport, Winnipeg), they have also served for the correlation study purposes. Any suspected data were thus discarded. Data were punched onto cards for processing with the IBM 1620 computer. The averaged differential energy spectrum (after pressure correction) for the photon component is illustrated in Fig. 2.3.

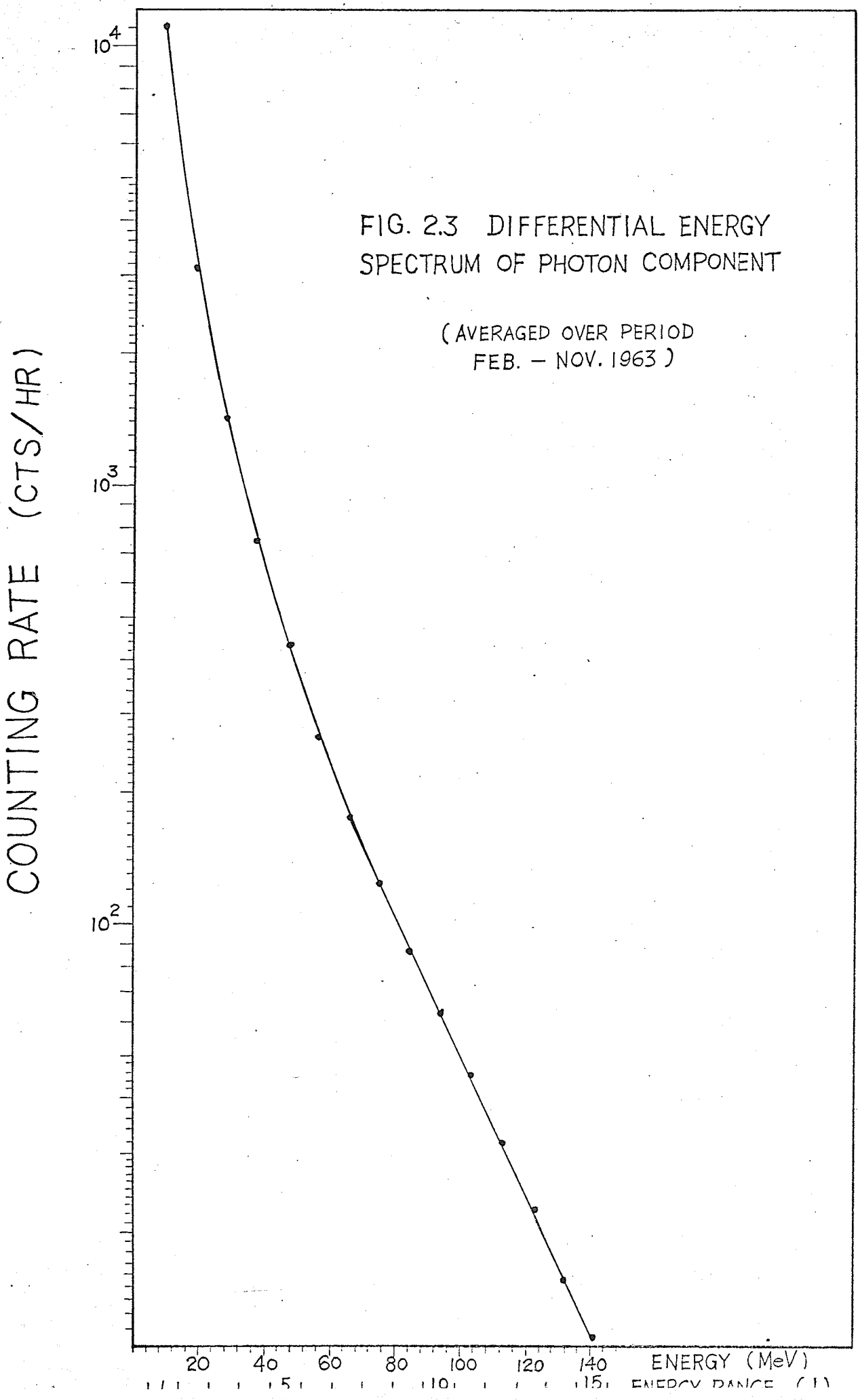

FIG. 2.3 DIFFERENTIAL ENERGY SPECTRUM OF PHOTON COMPONENT

(AVERAGED OVER PERIOD FEB. – NOV. 1963)

CHAPTER III

BAROMETRIC COEFFICIENTS

In the course of investigating periodic variations of the secondary cosmic radiation component deep in the atmosphere, meteorological effects have imposed a very complicated problem which has not been satisfactorily solved. Part of the variation of the secondary component originates in the change of atmospheric properties through the alteration of the multiplicity factor which couples the secondary to the primary radiation. During the process of multiplication, if all forebearers of the secondary component are stable particles, the meteorological effect can be determined only by the amount of matter traversed; if some unstable particles appear in the genetic line, the process will depend on the mass distribution along the path of the particles. For the former case, a barometric effect can be sufficient to represent the atmospheric effect. The latter requires a knowledge of the temperature distribution throughout the whole atmosphere above the station. As a rule, meteorological influences must be eliminated from the data especially when their magnitude and phase are comparable with those of the periodic variation under investigation.

Generally speaking, the secondary component data shows at least two types of time variation, meteorological and extra-atmospheric. Up to the present time, no completely satisfactory method has been discovered to effect a separation of these two so that either of them can be studied more reliably. Some workers, in their studies of the meteorological effects on the meson component, have utilized the pressure-

corrected nucleonic intensity to represent the secular variations of the primaries. However, the procedure to obtain the barometric coefficient of the nucleonic component has not taken completely into account variations in the primaries. More seriously, the neutron monitor does not respond to the same energy region of the primary spectrum as the meson detector.

Since the discovery of the pressure effect by Myssowsky et al. (1926), a great deal of work has been done on the meteorological effects on various secondary components such as messons, total ionizing particles, soft particles and neutrons. Empirical methods for the determination of the meteorological factors and theoretical formulations of the problem are referred to in the works of Blackett (1938), Duperier (1948, 1949), Maeda (1953, 1960), Simpson et al. (1953), Olbert (1953), Trefall (1953, 1955), Rose (1951), Dorman (1957), Wada (1957, 1960, 1961), Mathews (1959), Lindgren (1962), Lapointe et al. (1962), Carmichael et al. (1963, 1965), Bercovitch et al. (1963), Bercovitch et al. (1965), Drying et al. (1965), Kaminer et al. (1965), Mori et al. (1965) and Bercovitch (1966). However, no publication similar to the present study has been noted concerning the atmospheric effects on the cosmic ray photon component, except that of Bukata et al. (1962) which reported results for the pressure coefficients of photons with energies above 7 and above 35 MeV.

A knowledge of the processes giving rise to the photons near sea level is useful for the comprehension of the meteorological factors on the photon component. The well known ones with important bearings in the present problem are the decay of neutral pions and the bremsstrahlung of electrons produced in muon decay and in muon knock-on processes. The decay of neutral pions, occurring mainly near the top of atmosphere, initiates a cascade of electrons and photons, i.e. an air shower. The

number of shower particles reaches a maximum around the 200 mb level and then declines with atmospheric depth on account of absorption. The life time of a neutral pion is so short that it decomposes into photons practically at the same place where it is formed in the collision of the primary and the air nucleus. Hence, at sea level the meteorological effect on photons of neutral pion origin is purely barometric in character. Photons originating in electron-photon cascades generated by decay and knock-on electrons are, through the intermediate muon, traced back to the charged pion as their source. The competition between decay and capture processes of the charged pion, and the decay of muon are sensitive to the distribution of the air mass between the production level of the meson and the resulting photon. As a result, a temperature effect will play a role in the meteorological effect on these photons as observed at the bottom of the atmosphere. Because of the long life of the muon, decay electrons prevail in number at lower atmospheric depths and knock-on processes become more important near sea level where the matter is dense. Consequently, at the point of observation, the age of a shower initiated by an electron of muon origin depends on the place of birth and the energy of the electron; it may be old beyond its maximum of development or it may be still young enough for further cascading. In the old shower, most of the particles have an energy below the critical energy of an electron in air. The electrons will lose energy primarily by ionization (rather than radiation) while Compton scattering will be important for the photons. Therefore, the number of photons in the old shower will decrease with an increase in air pressure. In the crude model proposed by Heitler (1954), the particles in a young shower, if they are simultaneously observed, belong to the same generation with approximately same energy. Each of them is twice as energetic as that of the next generation. For an electron-

initiated shower, the population of electrons is greater than that of the photons by a factor of two in every generation except the first one. Since the constituents of the young shower have a strong power of particle procreation, a change in atmospheric pressure will introduce a different phenomenon. For a simple visulization, let us assume a layer of air with thickness less than one radiation length (about 37 mb) being added underneath the shower particles. The probability for a multiplication process will be enhanced. An original shower photon may disappear through materization while a new photon of lower energy may be emitted by a shower electron. Considering the facts that a photon has a longer radiation length and that electrons are greater in number, the overall effect of an increase in air pressure will lead to an increase in the number of photons with low energy and a decrease in photons of high energy. Observing a single young shower, or a large number of them with the same initial energies and origin, one would expect a positive barometer coefficient for the low energy photons and a negative barometer coefficient for those of high energy.

The present work has been concerned with a correlation of cosmic ray photon intensity and atmospheric pressure only. The deficiency of aerological data concerning the daily variation of the temperature distribution throughout the atmosphere in the vicinity of our station denies any meaningful attempt to study a temperature effect. (Ground temperature, regarded as a poor parameter for such studies, has been correlated with photon data on an hourly basis, but no apparent significant relationship has been found; if any, it can be connected to pressure as well.) Dawton et al. (1953) and Chasson (1954) have provided some experimental evidence on the temperature effect for the soft component (essentially electrons of muon origin). An effective total temperature

coefficient (of negative and positive temperature effects) is negligibly small, and the soft intensity fluctuations most strongly reflect barometric pressure changes alone. With these facts in mind, we therefore assume that a simple barometric correction on the raw data of the photon component gives an adequate elimination of the meteorological influence.

For the purpose of minimizing the effect of the primary secular variation, data for short time periods in which large changes in pressure appeared together with large variations in photon intensity were selected for a determination of barometric coefficients. Barometric coefficients were also been calculated for continuous data over longer periods so as to effect a comparison.

A. Determination of Barometric Coefficients

In what follows we have assumed, as is usual (Janossy et al. 1944, Duperier 1949, and Chasson 1954), a linear relationship between photon intensity variation (dI) and barometric pressure variation (dP). Thus,

$$dI = bdP \tag{1}$$

where b is a constant called the barometric coefficient. In the present analysis, hourly readings of intensity and pressure are used to obtain a barometric coefficient. For the ith hour, the relationship between the variations of intensity I_i and pressure P_i can be written as

$$\frac{I_i - I_m}{I_m} = B(P_i - P_m) \tag{2}$$

where I_m and P_m denote the mean values of intensity and pressure for the time period being considered, and B (which is b/I_m) is the barometric coefficient expressed as a percentage change of intensity per unit pressure change (%/mb). Letting $Y_i = I_i - I_m$, $X_i = P_i - P_m$, equation (2) can be simplied as

$$Y_i = BI_mX_i \tag{3}$$

which shows a standard linear correlational dependence that can be expressed by a straight regression line. A least-squares fit of the regression line through N pairs of I_i and P_i yields the statistical formulae for the barometric coefficient, the standard deviation of the barometric coefficient (D) and the correlation coefficient (C) for the time period in which N pairs of measurements have been taken.

$$B = \frac{1}{I_m} \frac{S(X_iY_i)}{S(X_i^2)} \tag{4}$$

$$D = \sqrt{\frac{S(Y_i - BI_mX_i)^2}{(N-1)S(X_i^2)}} \tag{5}$$

$$C = \frac{S(X_iY_i)}{\sqrt{S(X_i^2)S(Y_i^2)}} \tag{6}$$

All the summations (designated by S) are performed from i = 1 to i = N.

For the purpose of energy dependence studies, the differential spectrum of the photon component which covers energies from 3.8 to 183 MeV was divided into sixteen energy ranges numbered from 1 to 16. As a matter of convenience, J is used to denote the number of the energy range hereafter. Also, the entire differential spectrum has been treated as a single energy range numbered as 17. In fact, energy range 17 can be regarded as the integral number of counts per hour for photons with energy greater than 3.8 MeV since the intensity of photons with energy beyond 183 MeV is practically zero. The energy values for these seventeen ranges are given in Table 3.1.

The determination of barometric coefficients together with their standard deviations and correlation coefficients was made for the seventeen energy ranges using data of the 10-month period from February

to November 1963, according to the following grouping scheme: (1) data collection periods of one week, (2) data collection periods of one month, and (3) random short data collection periods (from 7 to 27 hours) when the pressure varied rapidly (changes from 6 to 47 mb) with apparently well correlated changes of photon intensity. Therefore, for each energy range we have three kinds of B, D, and C which are subscripted with W, M and R respectively. For a comparison among the values of the barometric coefficients obtained from the three kinds of data collection periods, weighted average barometric coefficients over the same long period of time were calculated and designated as BW_W, BW_M, and BW_R.

Table 3.1 presents the values of barometric coefficients (B_M), their standard errors (D_M), and correlation coefficients (C_M) for seventeen energy ranges in each of ten months. Without any sign before its numerical value, B_M is understood to be negative; the same is true for C_M which has the same sign as its corresponding B_M. For a positive value, a positive sign will be indicated. However, proper signs are indicated in all diagrams. All D_M are positive as expected. The monthly mean (hourly recorded) intensity and the monthly mean hourly pressure (P_M) are also given in the table.

TABLE 3.1

Feb. 1963 : P_M = 990.32 mb

J	Energy (MeV)	B_M (%/mb)	D_M (%/mb)	C_M	I_M (cts/hr)
1	3.8- 13.2	.508	.012	.854	10043
2	13.2- 22.6	.495	.015	.803	2917
3	22.6- 32.1	.526	.020	.719	1283
4	32.1- 41.5	.569	.024	.678	654
5	41.5- 50.9	.549	.032	.566	372
6	50.9- 60.4	.640	.039	.548	228
7	60.4- 69.8	.620	.047	.467	146
8	69.8- 79.2	.730	.054	.470	98
9	79.2- 88.7	.672	.064	.384	67
10	88.7- 98.1	.713	.077	.345	47
11	98.1-107.5	.707	.091	.294	33
12	107.5-116.9	.808	.106	.291	24
13	116.9-126.4	.522	.126	.162	17
14	126.4-135.8	.856	.151	.220	12
15	135.8-145.3	.650	.174	.147	9
16	145.3-183.0	.828	.139	.230	15
17	3.8-183.0	.517	.013	.852	15964

Mar. 1963 : P_M = 983.04 mb

J	Energy (MeV)	B_M (%/mb)	D_M (%/mb)	C_M	I_M (cts/hr)
1	3.8- 13.2	.486	.012	.895	10299
2	13.2- 22.6	.457	.014	.842	3031
3	22.6- 32.1	.433	.016	.787	1366
4	32.1- 41.5	.407	.022	.664	712
5	41.5- 50.9	.390	.026	.588	414
6	50.9- 60.4	.476	.033	.568	257
7	60.4- 69.8	.412	.042	.426	170
8	69.8- 79.2	.449	.052	.390	117
9	79.2- 88.7	.332	.060	.259	83
10	88.7- 98.1	.520	.074	.321	60
11	98.1-107.5	.562	.084	.310	44
12	107.5-116.9	.469	.097	.230	30
13	116.9-126.4	.439	.107	.195	22
14	126.4-135.8	.519	.136	.182	16
15	135.8-145.3	.340	.151	.109	11
16	145.3-183.0	.537	.118	.216	20
17	3.8-183.0	.469	.011	.905	16653

TABLE 3.1 (cont.)

Apr. 1963 : P_M = 984.60 mb

J	Energy (MeV)	B_M (%/mb)	D_M (%/mb)	C_M	I_M (cts/hr)
1	3.8- 13.2	.455	.008	.928	10256
2	13.2- 22.6	.440	.009	.894	2990
3	22.6- 32.1	.448	.013	.814	1351
4	32.1- 41.5	.448	.017	.741	708
5	41.5- 50.9	.506	.023	.679	411
6	50.9- 60.4	.521	.027	.621	258
7	60.4- 69.8	.480	.033	.517	172
8	69.8- 79.2	.504	.040	.466	121
9	79.2- 88.7	.522	.047	.421	87
10	88.7- 98.1	.488	.053	.357	65
11	98.1-107.5	.522	.064	.320	46
12	107.5-116.9	.617	.074	.325	33
13	116.9-126.4	.703	.086	.320	23
14	126.4-135.8	.532	.102	.212	16
15	135.8-145.3	.642	.124	.210	12
16	145.3-183.0	.854	.089	.369	22
17	3.8-183.0	.456	.007	.940	16570

May 1963 : P_M = 986.32 mb

J	Energy (MeV)	B_M (%/mb)	D_M (%/mb)	C_M	I_M (cts/hr)
1	3.8- 13.2	.526	.009	.912	10325
2	13.2- 22.6	.502	.011	.866	3000
3	22.6- 32.1	.555	.021	.721	1358
4	32.1- 41.5	.580	.020	.749	710
5	41.5- 50.9	.595	.026	.658	413
6	50.9- 60.4	.581	.033	.565	259
7	60.4- 69.8	.563	.039	.490	174
8	69.8- 79.2	.581	.044	.455	122
9	79.2- 88.7	.589	.051	.408	88
10	88.7- 98.1	.606	.064	.345	65
11	98.1-107.5	.570	.078	.275	47
12	107.5-116.9	.581	.084	.260	33
13	116.9-126.4	.729	.105	.261	23
14	126.4-135.8	.740	.116	.242	16
15	135.8-145.3	.778	.144	.206	12
16	145.3-183.0	.740	.113	.248	22
17	3.8-183.0	.532	.009	.921	16667

TABLE 3.1 (cont.)

Jun. 1963 : P_M = 982.98 mb

J	Energy (MeV)	B_M (%/mb)	D_M (%/mb)	C_M	I_M (cts/hr)
1	3.8- 13.2	.362	.032	.447	10893
2	13.2- 22.6	.387	.024	.572	3146
3	22.6- 32.1	.423	.033	.492	1426
4	32.1- 41.5	.452	.042	.425	760
5	41.5- 50.9	.547	.053	.409	443
6	50.9- 60.4	.421	.064	.275	280
7	60.4- 69.8	.581	.075	.322	189
8	69.8- 79.2	.594	.093	.270	134
9	79.2- 88.7	.624	.114	.233	97
10	88.7- 98.1	.805	.135	.253	72
11	98.1-107.5	.922	.143	.272	53
12	107.5-116.9	.796	.171	.200	36
13	116.9-126.4	.624	.190	.142	25
14	126.4-135.8	.649	.222	.127	17
15	135.8-145.3	.697	.274	.111	12
16	145.3-183.0	1.403	.220	.269	21
17	3.8-183.0	.393	.028	.522	17605

Jul. 1963 : P_M = 983.01 mb

J	Energy (MeV)	B_M (%/mb)	D_M (%/mb)	C_M	I_M (cts/hr)
1	3.8- 13.2	.733	.032	.745	11090
2	13.2- 22.6	.585	.030	.697	3251
3	22.6- 32.1	.531	.043	.515	1477
4	32.1- 41.5	.568	.059	.430	778
5	41.5- 50.9	.559	.078	.331	454
6	50.9- 60.4	.449	.095	.226	286
7	60.4- 69.8	.644	.107	.285	191
8	69.8- 79.2	.979	.143	.320	134
9	79.2- 88.7	.411	.160	.126	97
10	88.7- 98.1	.552	.190	.142	71
11	98.1-107.5	.489	.222	.108	51
12	107.5-116.9	.243	.256	.047	34
13	116.9-126.4	.215	.299	.035	24
14	126.4-135.8	.332	.371	.044	16
15	135.8-145.3	±.468	.464	±.050	11
16	145.3-183.0	±.591	.359	±.081	20
17	3.8-183.0	.667	.024	.808	17986

TABLE 3.1 (cont.)

Aug. 1963 : P_M = 987.07 mb

J	Energy (MeV)	B_M (%/mb)	D_M (%/mb)	C_M	I_M (cts/hr)
1	3.8- 13.2	.559	.015	.856	11520
2	13.2- 22.6	.573	.021	.777	3247
3	22.6- 32.1	.604	.030	.672	1465
4	32.1- 41.5	.624	.042	.562	772
5	41.5- 50.9	.720	.051	.550	446
6	50.9- 60.4	.677	.070	.407	277
7	60.4- 69.8	.601	.080	.325	181
8	69.8- 79.2	.776	.096	.347	123
9	79.2- 88.7	.576	.123	.210	87
10	88.7- 98.1	.748	.141	.235	62
11	98.1-107.5	.704	.168	.189	44
12	107.5-116.9	.672	.199	.153	31
13	116.9-126.4	.945	.231	.184	22
14	126.4-135.8	.787	.297	.120	15
15	135.8-145.3	.809	.324	.114	11
16	145.3-183.0	.618	.259	.109	17
17	3.8-183.0	.578	.014	.883	18322

Sep. 1963 : P_M = 988.20 mb

J	Energy (MeV)	B_M (%/mb)	D_M (%/mb)	C_M	I_M (cts/hr)
1	3.8- 13.2	.526	.012	.886	11532
2	13.2- 22.6	.503	.015	.833	3233
3	22.6- 32.1	.537	.021	.758	1457
4	32.1- 41.5	.551	.029	.642	767
5	41.5- 50.9	.518	.035	.553	444
6	50.9- 60.4	.564	.041	.517	276
7	60.4- 69.8	.596	.051	.461	181
8	69.8- 79.2	.475	.063	.317	124
9	79.2- 88.7	.408	.075	.235	86
10	88.7- 98.1	.401	.081	.215	62
11	98.1-107.5	.680	.100	.290	44
12	107.5-116.9	.480	.117	.179	31
13	116.9-126.4	.461	.137	.148	23
14	126.4-135.8	.795	.163	.211	16
15	135.8-145.3	.726	.209	.152	11
16	145.3-183.0	.253	.163	.069	18
17	3.8-183.0	.524	.011	.898	18306

TABLE 3.1 (cont.)

Oct. 1963 : P_M = 985.47 mb

J	Energy (MeV)	B_M (%/mb)	D_M (%/mb)	C_M	I_M (cts/hr)
1	3.8- 13.2	.506	.010	.884	11546
2	13.2- 22.6	.458	.016	.734	3250
3	22.6- 32.1	.479	.019	.691	1467
4	32.1- 41.5	.506	.025	.612	776
5	41.5- 50.9	.516	.031	.542	451
6	50.9- 60.4	.529	.041	.449	280
7	60.4- 69.8	.552	.049	.400	184
8	69.8- 79.2	.490	.055	.326	126
9	79.2- 88.7	.507	.068	.277	88
10	88.7- 98.1	.653	.075	.320	62
11	98.1-107.5	.592	.092	.241	45
12	107.5-116.9	.498	.100	.188	32
13	116.9-126.4	.358	.123	.112	22
14	126.4-135.8	.523	.149	.134	15
15	135.8-145.3	.748	.175	.163	11
16	145.3-183.0	.775	.141	.208	17
17	3.8-183.0	.498	.011	.869	18373

Nov. 1963 : P_M = 985.98 mb

J	Energy (MeV)	B_M (%/mb)	D_M (%/mb)	C_M	I_M (cts/hr)
1	3.8- 13.2	.588	.011	.907	11000
2	13.2- 22.6	.547	.013	.874	3122
3	22.6- 32.1	.578	.016	.840	1417
4	32.1- 41.5	.603	.021	.762	749
5	41.5- 50.9	.659	.029	.688	433
6	50.9- 60.4	.722	.033	.675	270
7	60.4- 69.8	.654	.041	.555	179
8	69.8- 79.2	.743	.051	.524	120
9	79.2- 88.7	.723	.057	.466	84
10	88.7- 98.1	.633	.065	.379	61
11	98.1-107.5	.880	.083	.408	44
12	107.5-116.9	.639	.094	.274	31
13	116.9-126.4	.599	.118	.209	22
14	126.4-135.8	.806	.134	.244	16
15	135.8-145.3	.841	.158	.218	11
16	145.3-183.0	.669	.125	.219	19
17	3.8-183.0	.588	.010	.928	17580

On account of the enormous volume of results, B_W, C_W, B_R and C_R are not tabulated. However, their distributions are plotted in the form of histograms for every energy range J as shown in Fig. 3.1 and Fig. 3.2 respectively. Numerical values of barometric coefficients and correlation coefficients are divided into intervals of width 0.2 along the abscissa and their numbers within the intervals are indicated by the ordinate. Histograms of B_M and C_M for every energy range are also given in Fig. 3.3. The characteristics of the barometric coefficients and correlation coefficients are summarized as follows. It should be noted that the energy range 17 reflects the behavior of the low energy ranges instead of the high ones.

1. There is no obvious relationship between the barometric coefficient and the correlation coefficient for any particular energy range.

2. Barometric coefficients are more or less normally distributed for every energy range. The histograms for B_W and B_R bear a close resemblance in the high energy ranges. For B_M, some energy ranges (Fig. 3.3; J = 6, 7, 8, 11) show skewness.

3. Dispersion in the distribution of barometric coefficients is greater for the higher energy ranges. The extent of spread is much smaller for B_M.

4. The distributions of correlation coefficients are skew at the low energy ranges (J = 1, 2). With increasing J, they tend to show the shape of a normal distribution and the mode moves from high numerical value to a low one. In general, the majority of the correlation coefficients have a numerical value greater than 0.8 for energy ranges 1 and 2. They spread out widely in values with the mode down to 0.2 for energy ranges beyond 13.

5. Skewness of the C_M distribution are conspicious in a large number of energy ranges (J = 2, 4, 7, 8, 10, 12, 13, 16; Fig. 3.3).

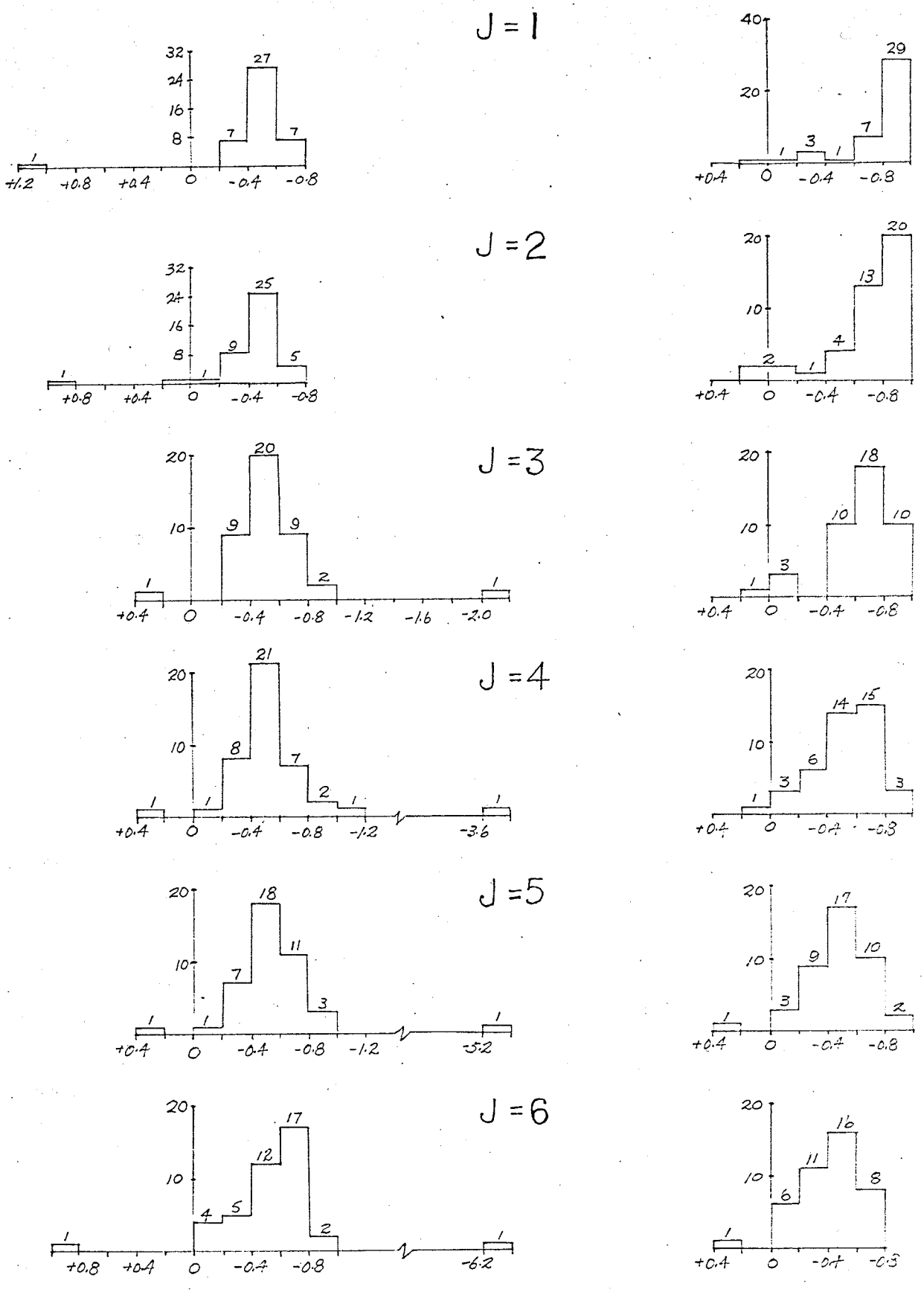

FIG. 3.1A NUMBER DISTRIBUTIONS OF B_W AND C_W

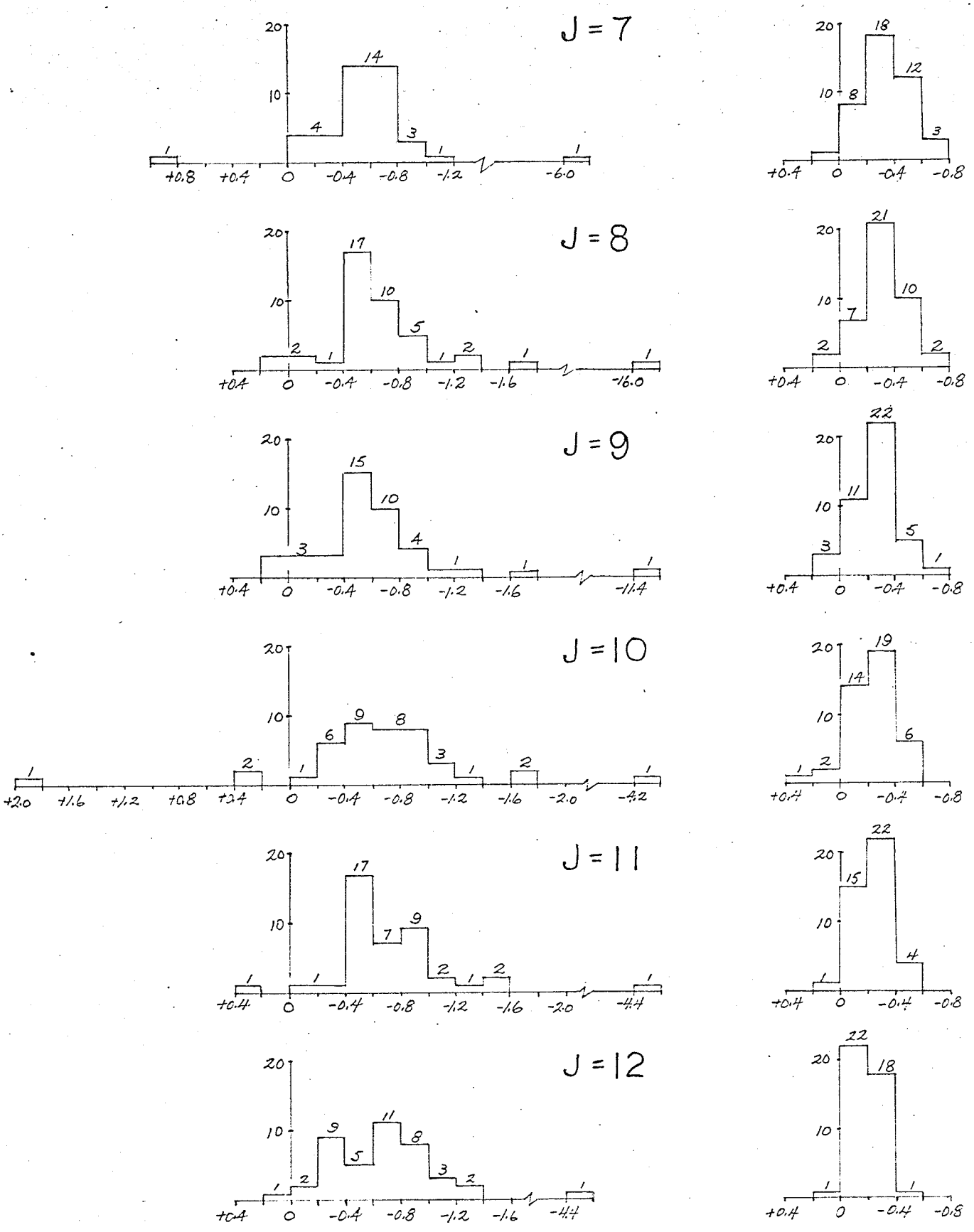

FIG. 3.1B NUMBER DISTRIBUTIONS OF B_W AND C_W

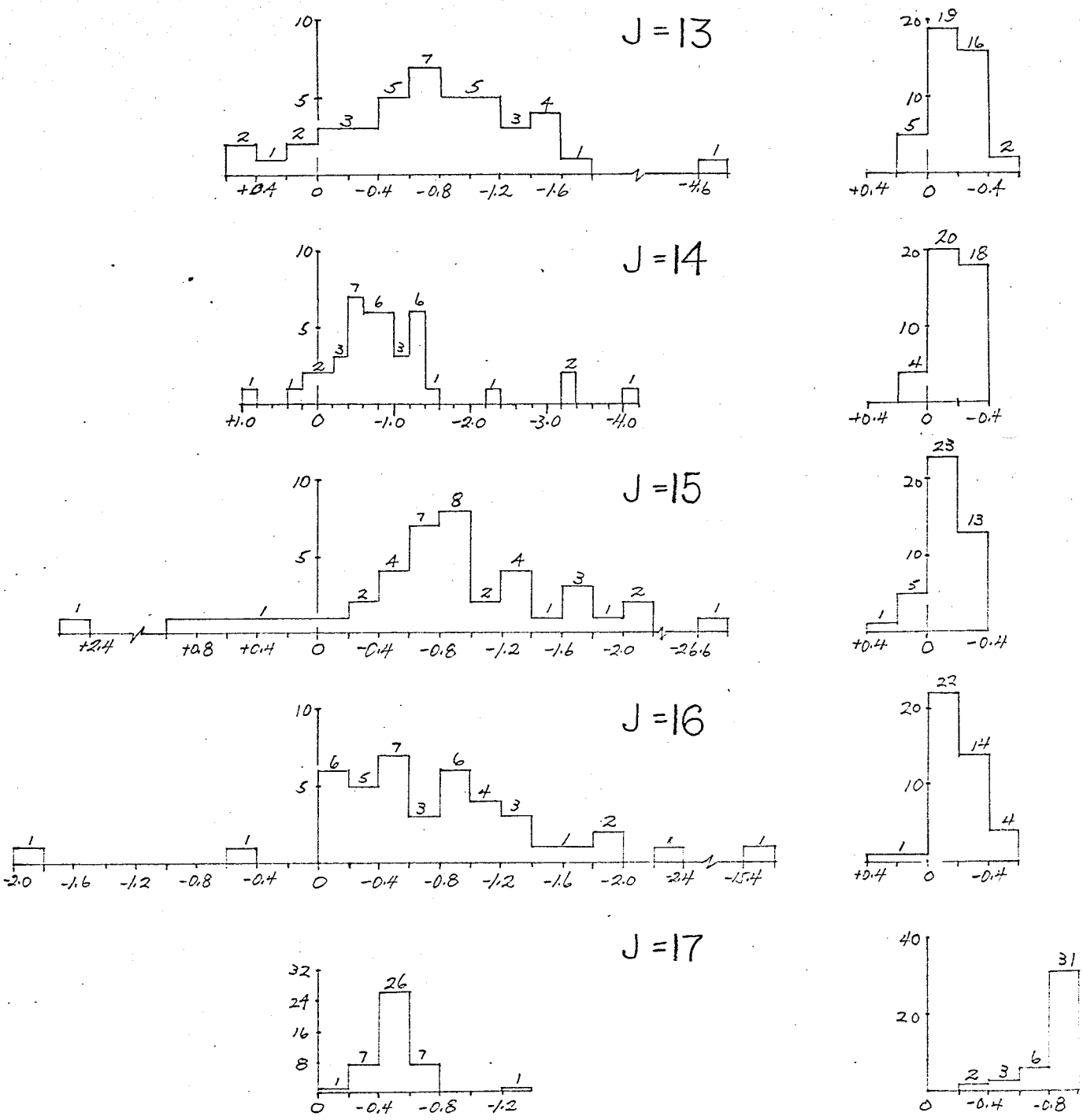

(42 PAIRS OF B_W AND C_W FOR EACH J)

FIG. 3.1C NUMBER DISTRIBUTIONS OF B_W AND C_W

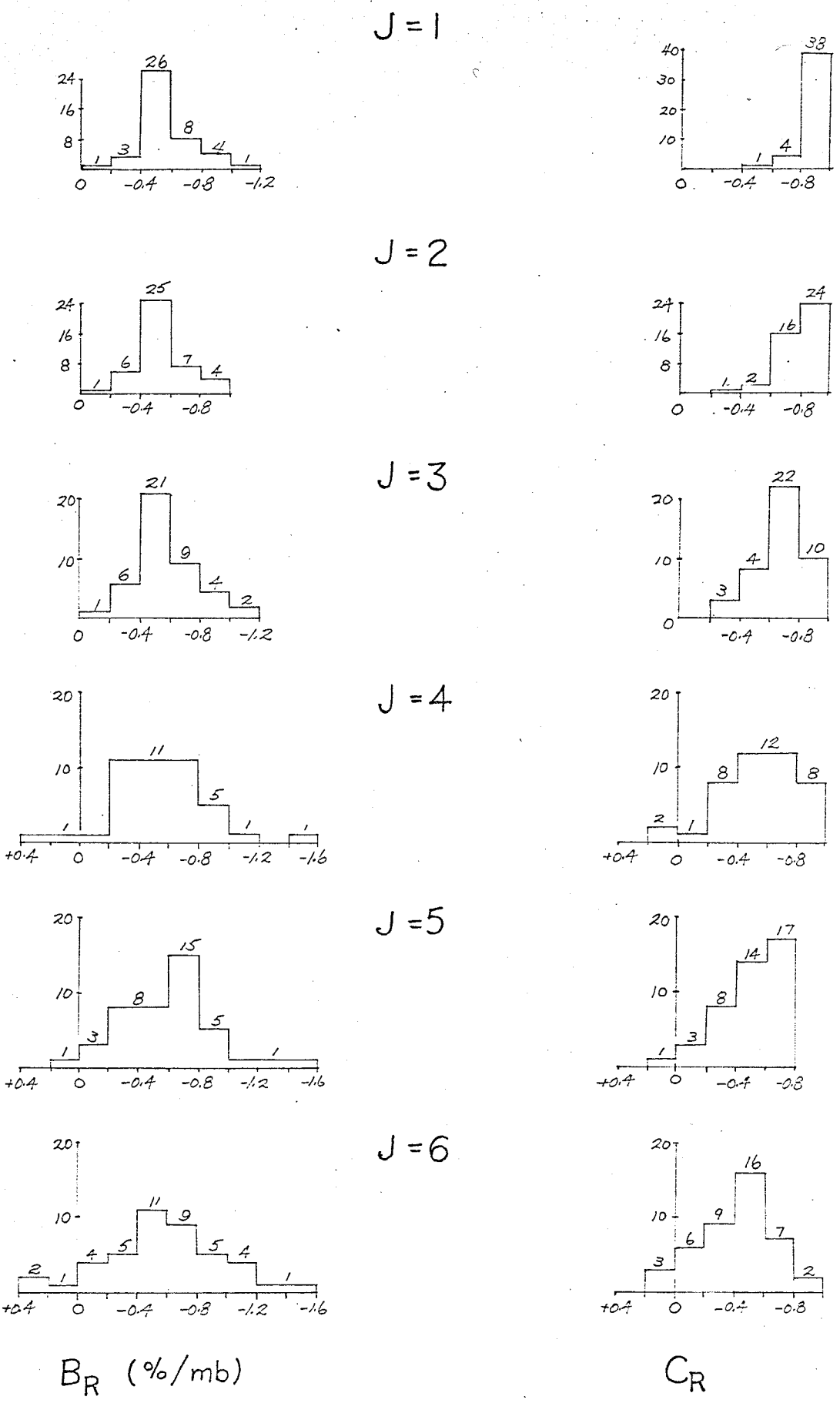

FIG. 3.2A NUMBER DISTRIBUTIONS OF B_R AND C_R

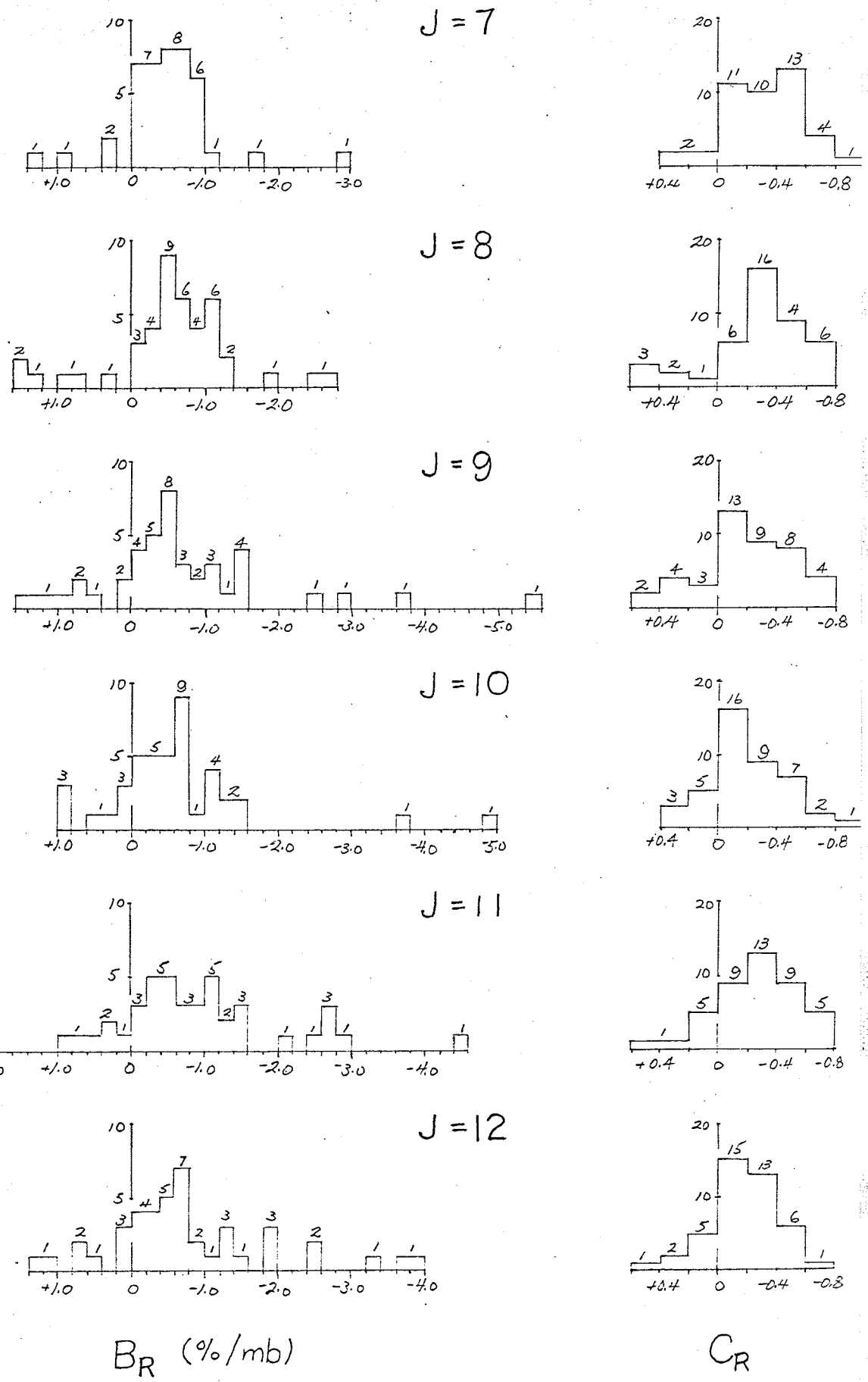

FIG. 3.2B NUMBER DISTRIBUTIONS OF B_R AND C_R

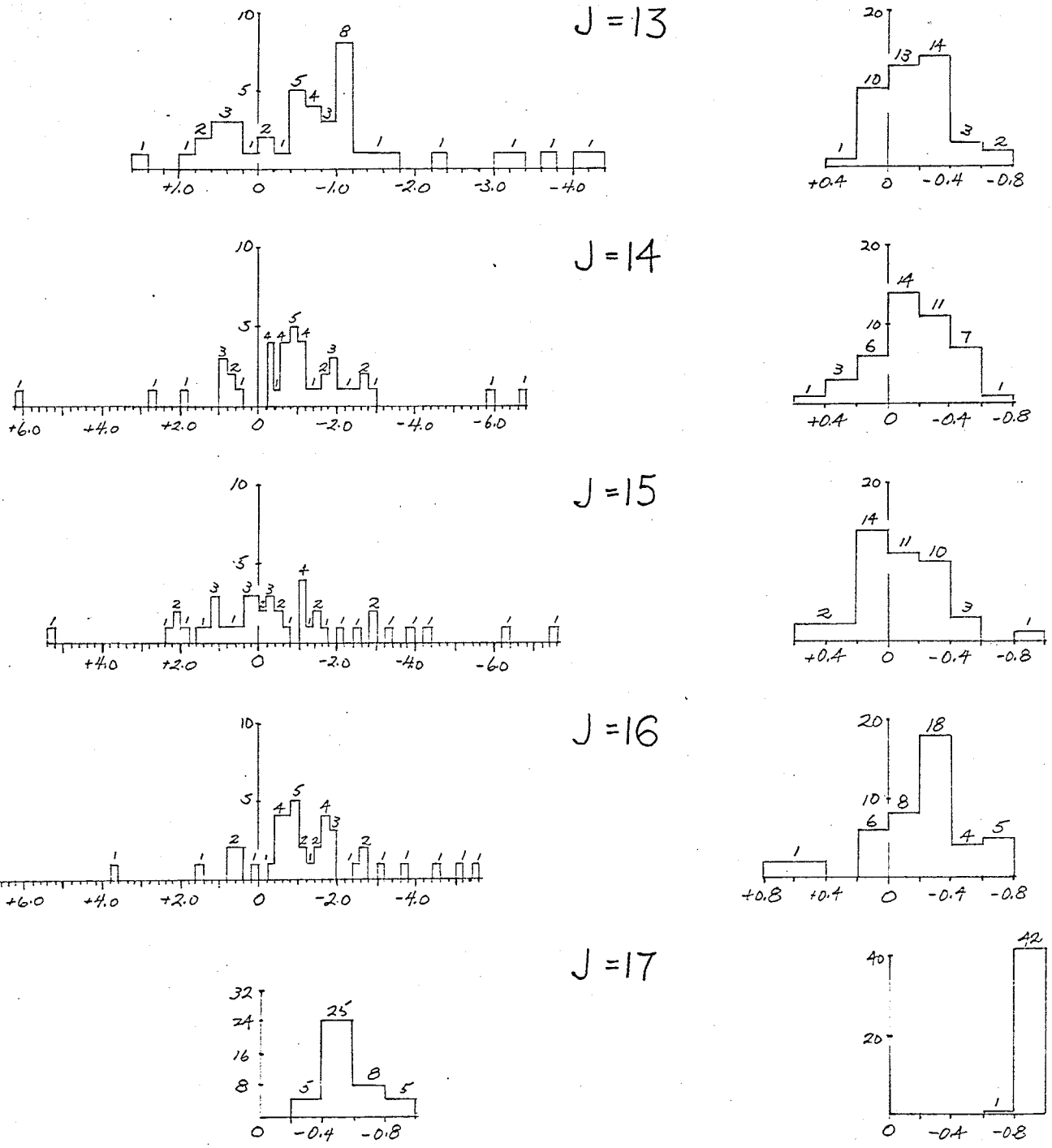

(43 PAIRS OF B_R AND C_R FOR EACH J)

FIG. 3.2C NUMBER DISTRIBUTIONS OF B_R AND C_R

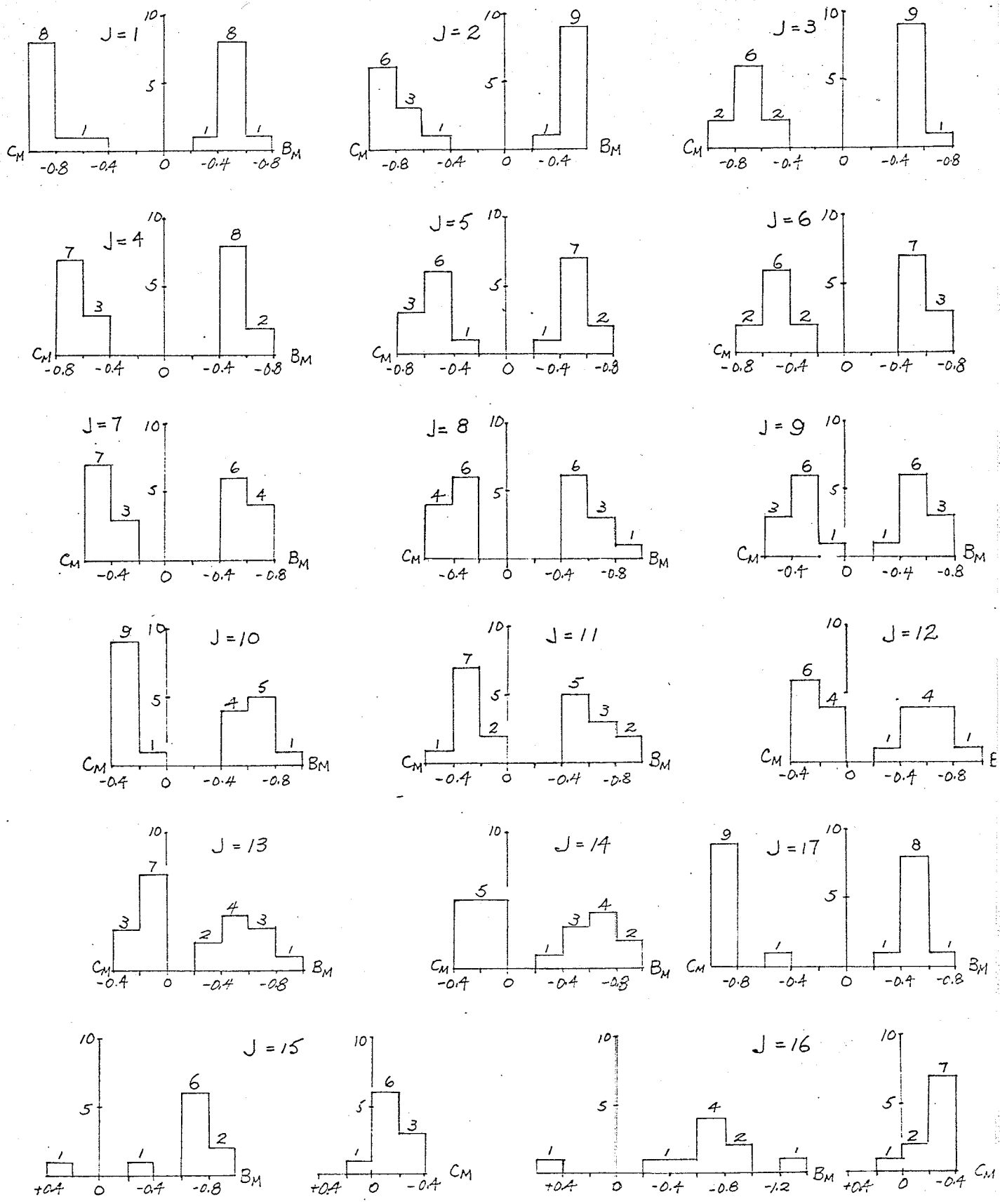

(10 PAIRS OF B_M AND C_M FOR EACH J)

FIG. 3.3 NUMBER DISTRIBUTIONS OF B_M (%/mb) AND C_M

6. All B_M are negative except for two positive cases: one in the energy range 15 and the other in 16. Both have a correlation coefficient less than 0.1.

7. A positive B_W exists in every energy range. Their frequency of occurrence is small for energy ranges below J = 13. The overwhelming majority of the positive B_W are accompanied by a correlation coefficient less than 0.2. Only one of the total of 35 cases has a value equal to 0.56.

8. Beyond energy range 3, a positive B_R appears in every energy range and the number of such events increases with the higher energy ranges. Usually most of the positive B_R have a small correlation coefficient which is less than 0.4. Out of a total of 95 positive B_R in all energy ranges, 11 possess correlation coefficients between 0.4 and 0.6; only one has a value of 0.64.

9. The existence of negative barometric coefficients with large numerical value deserves our attention. Barometric coefficients belonging to this category are defined as those which stand distinctly outside the bulk in the histogram. Practically speaking, there is none of this kind in the B_M distributions. Twenty two cases (out of 714 positive and negative B_W) of large negative B_W occur in all energy ranges; twenty of them have a correlation coefficient less than 0.56. However, in the B_R distributions, thirty cases (out of 731 positive and negative B_R) can be found with correlation coefficients larger than 0.5. A list of these events is provided in Table 3.2. For comparison, the modes of B_R and C_R corresponding to their energy groups are also tabulated. The date of the event and the number of intensity-pressure pairs used in the calculation are also listed for reference.

TABLE 3.2

J	Energy (MeV)	Large Negative Coefficients B_R (%/mb)	Large Negative Coefficients C_R	Modes B_R (%/mb)	Modes C_R	Date Day	Date Mon. (1963)	Number of Data
4	32.1- 41.5	1.454	.866	.5	.5	7	3	7
7	60.4- 69.8	2.845	.786	.5	.3	25	2	13
		1.648	.783			5	9	13
8	69.8- 79.2	1.918	.699	.5	.2	16	9	13
		2.491	.735			3	10	8
		2.689	.670			20	10	18
9	79.2- 88.7	2.953	.554	.7	.2	25	2	13
		3.648	.766			7	3	7
		2.523	.614			8	5	12
10	88.7- 98.1	4.916	.881	.7	.2	27	2	16
		3.790	.678			7	3	9
11	98.1-107.5	2.134	.673	.9	.3	20	2	22
		2.593	.684			21	2	17
		2.720	.562			8	5	12
		4.424	.745			3	10	8
		2.654	.741			10	10	25
12	107.5-116.9	3.389	.552	.7	.2	21	2	17
		3.871	.662			7	3	9
13	116.9-126.4	3.665	.517	1.1	.3	21	2	17
		4.011	.601			19	4	16
14	126.4-135.8	6.620	.728	.9	.1	7	3	9
		6.000	.551			7	3	7
15	135.8-145.3	2.113	.581	1.1	.1	3	4	15
		6.280	.523			3	8	17
		7.437	.947			12	8	10
16	145.3-183.0	4.324	.684	.9	.3	21	2	17
		5.493	.723			7	3	7
		3.029	.618			24	3	18
		3.800	.622			8	5	12
		5.041	.773			12	8	10

For a general discussion, let us examine the nature of data sampling in connection with the determination of B_R, B_W, and B_M. As expected, the barometric coefficients and correlation coefficients, determined by the method of the least-squares fitting of a linear regression line, should have a normal distribution because each set of experimental points from which a barometric coefficient and a correlation coefficient are calculated is independent of each other, and can be regarded to be

randomly chosen among its own category. B_R have been determined from a group of particularly selected intensity-pressure pairs according to the best visual correlation. The use of all available intensity-pressure data without any discrimination in the evaluation of B_W and B_M for continuous periods of a week and of a month is equivalent to a random sampling procedure. We might expect some differences in the distribution histograms among these three groups. Since the photon intensity has a correlational dependence on many parameters besides pressure, the distributions of B_R and C_R should show the smallest dispersion among the three groups and most of C_R should center at a high numerical value. However, for low energy ranges ($J = 1, 2, 3$) B_R and C_R do not show these advantages distinctly over the other two groups. Beyond energy range 4, their distributions behave even worse (i.e. show greater dispersion). Therefore, the choice of such short periods of rapid-pressure-change does not seem to be particularly advantageous in the present experiment. Apparently, there are no basic differences in the histograms of the barometric coefficients and correlation coefficients for these three groups except for slight differences in the positions of the modes and the extent of dispersion of the distributions. Upon visual examination, B_M and C_M have the smoothest distribution histograms with the least spread in values. It is highly probable that during the time periods considered, the pressure effect is the main factor responsible for the gross variation of photon intensities.

For all three grouping schemes, photon intensities in the low energy region ($J = 1, 2$) exhibit a very good correlation with pressure. The absolute values of the correlation coefficients fall off towards the higher energy region, that is to say, high energy photons are poorly correlated with pressure. For photon energy ranges beyond number 6,

correlation coefficients become less than or equal to 0.5. There are two ways of looking at this result. Physically, over the same period of time, if intensities of low energy photons can be well correlated with pressure while those of high energy exhibit a poor relationship with pressure, there may be some process other than pressure change in the atmosphere which is operative only on the high energy photons. Another and more likely possibility is simply statistical. In our present experimental data, counting rates fall off with increasing energy (see Table 3.1). For example, photons in energy range 6 are only 200 to 300 counts per hour. This amounts to a statistical fluction of at least 5%. Taking 0.54%/mb for the barometric coefficient of such photons (from Table 3.3), the effect due to a change of 9 mb in pressure can be entirely nullified by the statistical fluctuation in counting rate. Our pressure data shows that a large variation in pressure (such as 20 mb) is not very frequent. It is natural that the fluctuation of counting rate will greatly reduce the correlational dependence of the high energy photon intensities with the pressure. We should expect that such a masking effect becomes more severe for photons of energy ranges higher than 6.

Most of the positive B_R are present with a correlation coefficient less than 0.4. They constitute the tail end of the normal distribution in their own energy range. When data of a week or of a month are employed in the calculation, their numbers of occurrence are diminished drastically and their accompanying correlation coefficients are further reduced to 0.2. Apparently, statistical fluctuation are the main cause for the existence of such positive coefficients. (Another possible explanation lies in a consideration of the pressure effect on young showers. A large increase in air mass within a relatively short period of time may enhance the production of shower particles. If they

contribute a number of new photons which can outnumber those photons of the same energy undergoing the absorption process, the barometric coefficient pertaining to such an energy range will become positive instead of negative. Since the overall balance of the photon intensity depends solely on pressure, a high correlation coefficient should be expected. In view of the poor values of correlation coefficients for these positive B_R, this is almost certainly not the case.) Only two cases of positive values have been found for B_M; they occurred with very low correlation coefficients in energy ranges 15 and 16 during July 1963. As compared with other months, July shows a small pressure variation most of the time and the correlation coefficients of all energy ranges for this month are also very low. Most likely, photon intensities in July are influenced more by some factors other than pressure. On the other hand, the masking effect of fluctuations in counting rates at high energy ranges can provide a statisfactory explanation.

The appearance of large negative B_R with high value of C_R (say, greater than 0.5) is interesting (see Table 3.2) but not understood. Similar to the behavior of the positive barometric coefficient, B_W with large negative values possess only very small C_W and their frequency is much smaller than the case of short periods of rapid-pressure change. They disappear when a month's data are used. Hence, such phenomena gradually vanish in calculations with a large amount of observed data. However, a high correlation coefficient does imply the genuineness of the relationship of such events with pressure even though their frequency is negligible at energy ranges below 6, and small for energy ranges higher than 7.

In view of the above facts and discussions, barometric coefficients over a short period of time have a great variabiltiy. They

may be positive or negative, they may have abnormally large numerical value, they may result in either a good or poor correlation with pressure. However, the large statistical uncertainty inherent in the present counting rates prohibits any definite conclusion on the rare events. Nevertheless, the barometric coefficients determined over a period of a month do show regularity in their distributions which is especially good in the low energy region. Negative barometric coefficients with abnormally large values disappear entirely. Positive barometric coefficients occur only twice at the high energy end with negligible correlation coefficients. Excluding the energetic photons of energy ranges above 5 from our consideration due to their large statistical uncertainty, the majority of B_M values for the same energy can be grouped into an interval of width 0.2%/mb. Such B_M values are accompanied by high correlation coefficients. Hence, it can be concluded that the pressure effect on the low energy photons remains fairly constant.

B. Energy Dependence of Barometric Coefficients

The weighted average barometric coefficients, BW_R, BW_W and BW_M for each energy range are calculated from the populations of B_R, B_W and B_M respectively. Results are tabulated in Table 3.3 together with their standard deviations DW_R, DW_W and DW_M, and also plotted in Fig. 3.4. All weighted average barometric coefficients are negative.

TABLE 3.3

J	Energy (MeV)	Weighted Average Barometric Coefficients (%/mb) BW_R	DW_R	BW_W	DW_W	BW_M	DW_M
1	3.8- 13.2	.504	.005	.487	.003	.490	.003
2	13.2- 22.6	.510	.008	.474	.004	.470	.004
3	22.6- 32.1	.540	.012	.490	.005	.489	.006
4	32.1- 41.5	.563	.017	.502	.006	.492	.007
5	41.5- 50.9	.542	.021	.510	.008	.511	.009
6	50.9- 60.4	.629	.026	.548	.010	.541	.011
7	60.4- 69.8	.602	.032	.540	.012	.522	.013
8	69.8- 79.2	.673	.042	.544	.015	.528	.016
9	79.2- 88.7	.526	.048	.524	.018	.519	.019
10	88.7- 98.1	.625	.056	.547	.022	.537	.022
11	98.1-107.5	.745	.065	.605	.026	.595	.026
12	107.5-116.9	.538	.079	.560	.030	.531	.030
13	116.9-126.4	.728	.091	.571	.035	.558	.036
14	126.4-135.8	.677	.109	.618	.042	.591	.043
15	135.8-145.3	.473	.130	.615	.051	.584	.051
16	145.3-183.0	.684	.105	.616	.039	.563	.040
17	3.8-183.0	.511	.004	.496	.002	.488	.003

An examination of the energy dependence of the barometric coefficients for these three categories reveals:

1. In each of the energy ranges, BW_W agrees with BW_M within statistical error. However, beyond energy range 1, the numerical values of BW_W are systematically somewhat higher than those of BW_M.

2. In the low energy region (J less than 8), BW_R have the largest numerical values among the three. Above energy range 9, more than half of BW_R have values in agreement with BW_W and BW_M (within one standard deviation).

3. On the whole, from energy range 2 upward, the absolute values of the barometric coefficients (BW_R, BW_M, and BW_R) tend to increase with photon energies.

The energy dependence of barometric coefficients may serve as a key to the understanding of the atmospheric effects on the photon

component. Bukata et al. (1962) have explained the barometric coefficients of photons above 7 MeV in terms of a simple absorption model. The present experimental results in the form of differential spectra make possible a more detailed study of such a hypothesis. Before introducing the model, some numerical relationships have been found between the total mass absorption coefficients of photons in air (designated as T) given by Davisson (1965) and the experimental barometric coefficients of the photon component as shown in Table 3.3. Table 3.4 presents the values of T and the calculated values of RW_M and XW_M for energies up to 100 MeV, where $RW_M = -T/BW_M$ and $XW_M = -BW_M/T$. All RW_M and XW_M are positive and their corresponding standard deviations are denoted by SR_M and SX_M. The effective value of photon energy for a particular energy range is assumed to be the middle one of the range in connection with the choice of its corresponding T value. This assumption slightly overestimates the effective energy since the photons inside the range are distributed in a larger number at the low energy end.

TABLE 3.4

Energy J	T (cm^2/gm)	RW_M	SR_M	XW_M	SX_M
1	.0160	3.32	.02	.300	.002
2	.0146	3.16	.03	.315	.003
3	.0147	3.05	.03	.328	.004
4	.0148	3.05	.04	.328	.004
5	.0151	2.99	.05	.334	.006
6	.0153	2.88	.05	.348	.007
7	.0156	3.02	.07	.331	.008
8	.0158	3.04	.09	.327	.010
9	.0161	3.18	.11	.314	.011
10	.0163	3.12	.12	.321	.013

The energy dependence of T is also plotted in Fig. 3.4. It can be seen that the T curve has a minimum around 20 MeV (or energy range 2)

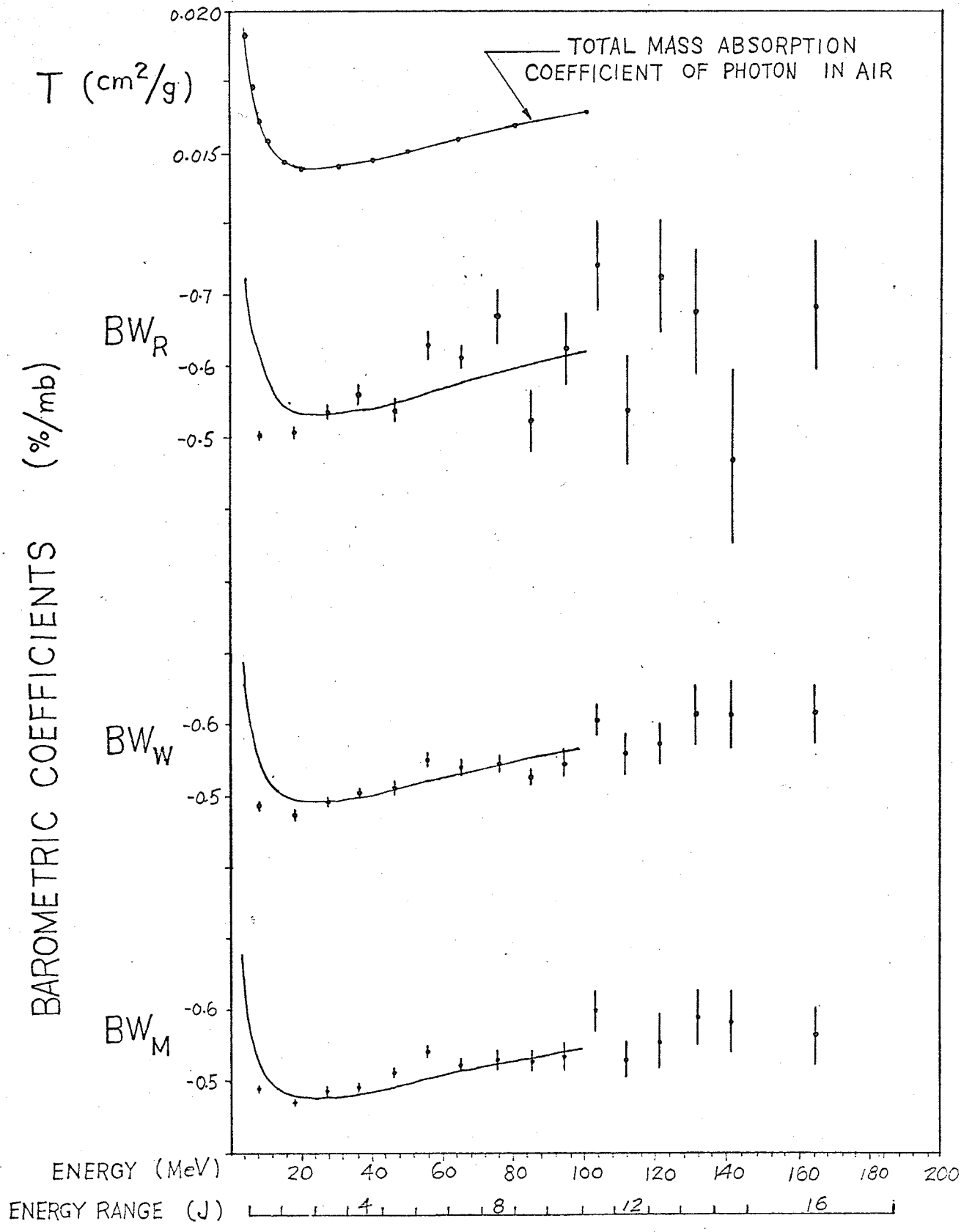

FIG. 3.4 ENERGY DEPENDENCE OF BAROMETRIC COEFFICIENTS

where the minimum of BW_M occurs. Table 3.4 shows that RW_M has a value near 3 for all the energy ranges. (The average of RW_M over all energy ranges is 3.09.) This means that on the whole the barometric coefficient reflects an absorption process as the essential nature of the pressure effect on the observed photon componment. In order to understand the meaning of the ratio between the total mass absorption coefficient and the barometric coefficient, we introduce at present the simple absorption model. Using a very crude approximation to represent the overall effect of the complicated processes involved in the development of the photon component through the entire atmosphere, let us assume that the photon intensity of a specified energy has reached its maximum I_o at the atmospheric depth $(1 - X)P$ and then undergoes solely the absorption process through the rest of the atmosphere XP. P is the thickness of the whole atmosphere above the point of observation (indicated by the pressure reading) and X is the fraction of the atmosphere participating in the absorption process. The intensity of the surviving photons I, as observed at the station, will obey the law

$$I = I_o \, e^{-XPT} \tag{7}$$

where I, I_o, X and T are energy dependent. Differentiating equation (7) with respect to pressure, we obtain

$$\frac{dI}{dP} = -IXT \tag{8}$$

By definition, the barometric coefficient

$$B = \frac{1}{I} \frac{dI}{dP} \tag{9}$$

Substituting equation (8) into (9),

$$B = -XT \tag{10}$$

Therefore,

$$X = -B/T \tag{11}$$

and recalling that R is the negative ratio of T to B, we get

$$R = 1/X \tag{12}$$

The interpretation of the experimental results for the barometric coefficients BW_M in terms of the simple absorption model will yield some physical implications concerning the meaning of the barometric coefficient, the development of the photon component in the atmosphere and the origin of the observed photons.

1. From equation (11), the barometric coefficient has one more physical meaning than its original definition. Since T is a constant for photons of a specified energy, the barometric coefficient for such photons can determine the "effective" level of their maximum intensity. The time variation of the barometric coefficient will simply mirror the fluctuation of such a level with time.

2. Even though the photons observed at the station have gone through various processes at various atmospheric depths and have been influenced by various factors due to the variation of the atmosphere structure, the overall effect of pressure variation during a long period of time is such that the upper 2/3 of the atmosphere serves as the medium for the full development of the photons while the lower 1/3 simply acts as the absorber. Such an implication agrees with the work of Bukata et al. (1962) and is reasonably consistent with the general picture of the development of the photon component in the atmosphere.

3. The "effective" levels of generation for photons of energy from 4 to 100 MeV are found within a narrow band of the atmospheric column about 1/3 of one atmosphere above the point of observation. The width of this narrow band is about 5% of one atmosphere.

4. The majority of the electron-photon showers which are responsible

for the observed photons have reached an old age at these "effective" levels. As the decay electrons and the knock-on electrons of muon origin only become important in the lower atmosphere, this implies that young showers initiated by them do not in fact play an important role in the observed photon component (energy below 100 MeV). If this is the case, the temperature effect on these photons will not be significant. In other words, most of the photons as observed in our experiments are the end product of old showers.

The energy dependence of XW_M as shown in Table 3.4 seems to suggest the influence of photons of young shower origin. Starting at the low energy end, the value of XW_M increases with energy, passes through a maximum near energy range 6 and then declines slowly. Considering the general nature of the development of old showers in the atmosphere, the photon component becomes softer with increasing atmospheric depth, and in the frame of the simple absorption model photons of higher energy will reach their maximum at a higher level with respect to the ground. That is to say, X, which indicates the height of the level of maximum intensity, should increase with photon energy. Values of XW_M from energy ranges 1 to 6 do agree with such a conjecture. The slow decline in the values of XW_M from energy ranges 6 to 10 requires another explanation. As already mentioned, a young shower has a genetic relationship back to the muon. Inside the atmosphere, the muon component is hardened in its average energy as it penetrates deeper in the atmosphere. As a result, the photons will also be hardened with atmospheric depth. For energy ranges above 6, if the photons detected include an increasing relative number of photons produced in young showers this could then explain the slow decrease of XW_M with increasing energy.

A theoretical curve for the simple absorption process is

constructed to fit the experimental points of BW_M within the 100 MeV range. Assuming that the ratio of T to BW_M is constant over the energies concerned, the theoretical barometric coefficients in each energy range can be calculated by dividing T (for each energy range) by this ratio. The average of RW_M, 3.09, is chosen for such a ratio and the results are represented by the solid line as shown in Fig. 3.4. For photons with energy above 100 MeV, the statistics are poorer. However, between 100 to 200 MeV, T increases slowly with energy as predicted by Heitler (1954); hence, the energy dependence of the experimental barometric coefficients agrees at least qualitatively with the above over-simplified absorption model.

As for the energy dependence of BW_W, it can be taken practically the same as that of BW_M since their values agree very well. Also, no fundamentally different physical meaning can be deduced from the energy dependence of BW_R. This sampling method only leads to an implication that in the frame of the simple absorption model the levels of generation of photons will be situated in a wider band (about 10% of the entire thickness of the atmosphere) and somewhat higher up. The theoretical absorption curves for both BW_W and BW_R have been drawn (Fig. 3.4) according to the same method of analysis as for BW_M. The adopted ratios are 3.05 and 2.78 respectively.

C. Seasonal Variation of Barometric Coefficients

Since the barometric coefficients of the photon component are determined from selected data by means of the correlation method, their values are subject to statistical fluctuations as has been briefly discussed in section A of this chapter. However, the present experimental barometric coefficients were determined by a single correlation with pressure, regardless of any other factors operating in the atmosphere. They are total pressure

coefficients in character which serve at most as a first approximation in reflecting the meteorological effect. Since the atmospheric structure undergoes changes from time to time, the barometric coefficients, over a long period of time, may be subject to changes related to seasonal variations of the atmosphere. A study was thus carried out on the variability of the barometric coefficients of the photon component during the period between February and November 1963.

Fig. 3.5 provides some information on the variation of some of the barometric coefficients as obtained in long periods and short periods of time. The values of B_R fluctuate irregularly and tremendously even within the period of a month. In spite of poor statistics, their large variability appears to be real. As soon as longer periods of data are involved, the dispersion of these values for the coefficients tends to be smaller as shown by the behavior of B_W and B_M. Undoubtedly, this is a result of the improved statistics but it also indicates that the pressure effect on the photons, averaged over a longer period of time, becomes more regular and less fluctuating. Although the seasonal variations of B_R, B_W, and B_M (illustrated in Fig. 3.5) mirror the behavior of photons of energy range 1, similar phenomena can be observed for those of energy ranges from 2 to 16.

The seasonal variation of barometric coefficients for photons of energy ranges from 1 to 17 together with their correlation coefficients C_M are shown in Fig. 3.6. The dotted lines are simply employed to connect the same series of experimental points for an easy inspection in all the diagrams hereafter. Their particulars can be summarized as follows:

1. On the whole, there is no definite relationship between the values of B_M and C_M since their variations do not track at all well.

2. In the months of June and July, correlation coefficients for all

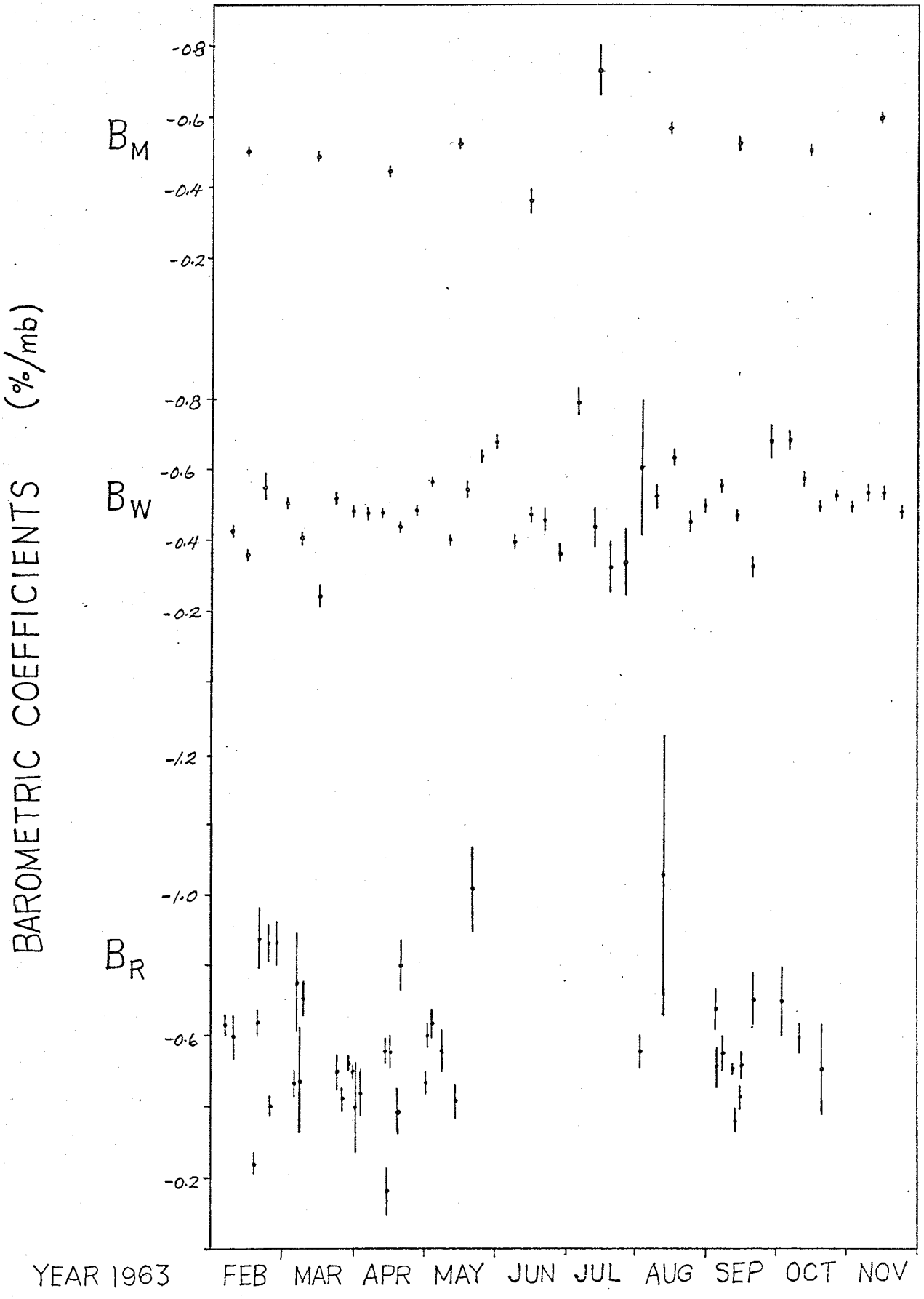

FIG. 3.5 SEASONAL VARIATIONS OF B_M, B_W, B_R OF PHOTONS ($J=1$, 3.8 - 13.2 MeV)

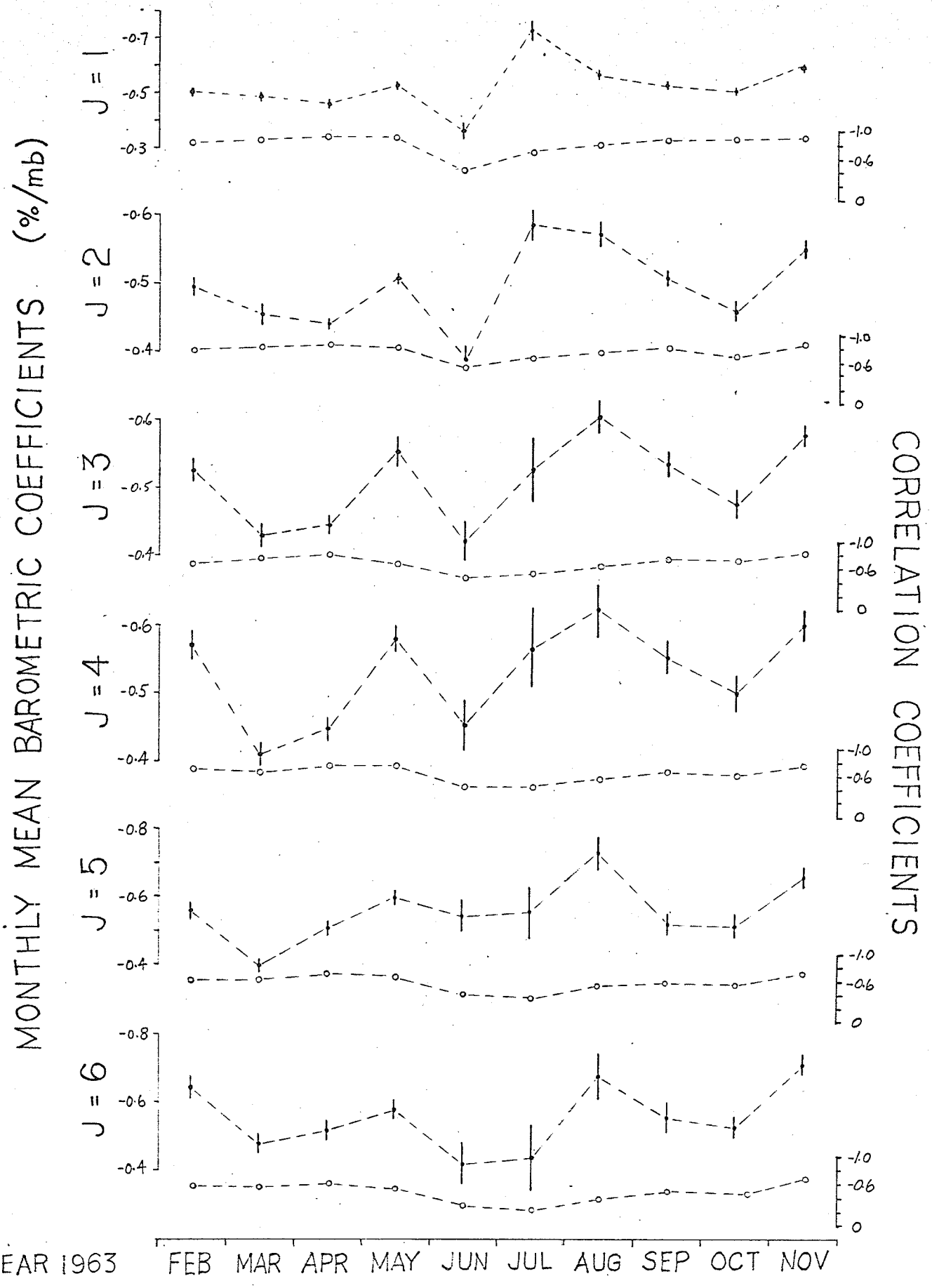

FIG. 3.6A SEASONAL VARIATIONS OF MONTHLY MEAN BAROMETRIC COEFFICIENTS B_M

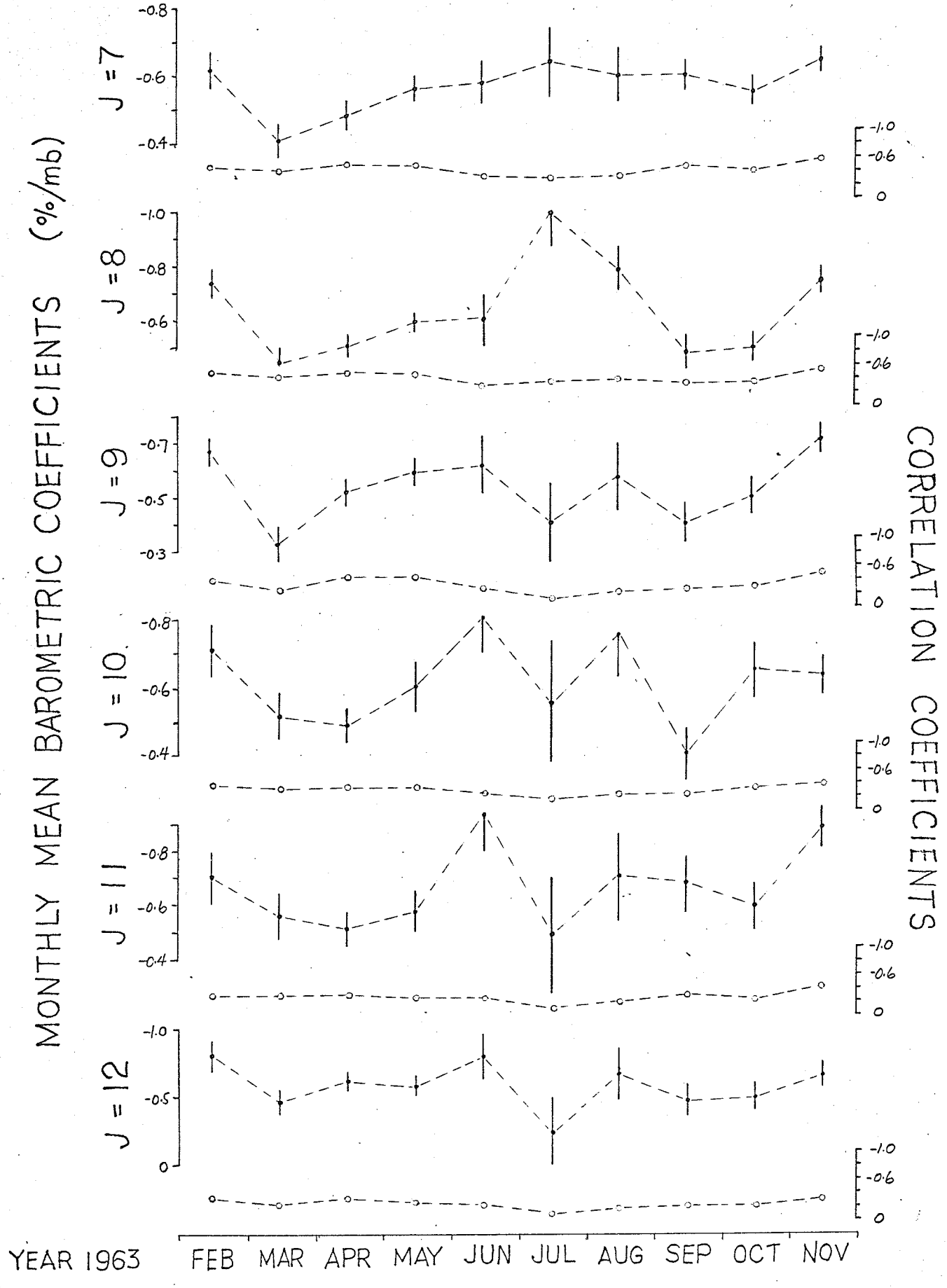

FIG. 3.6B SEASONAL VARIATIONS OF MONTHLY MEAN BAROMETRIC COEFFICIENTS B_M

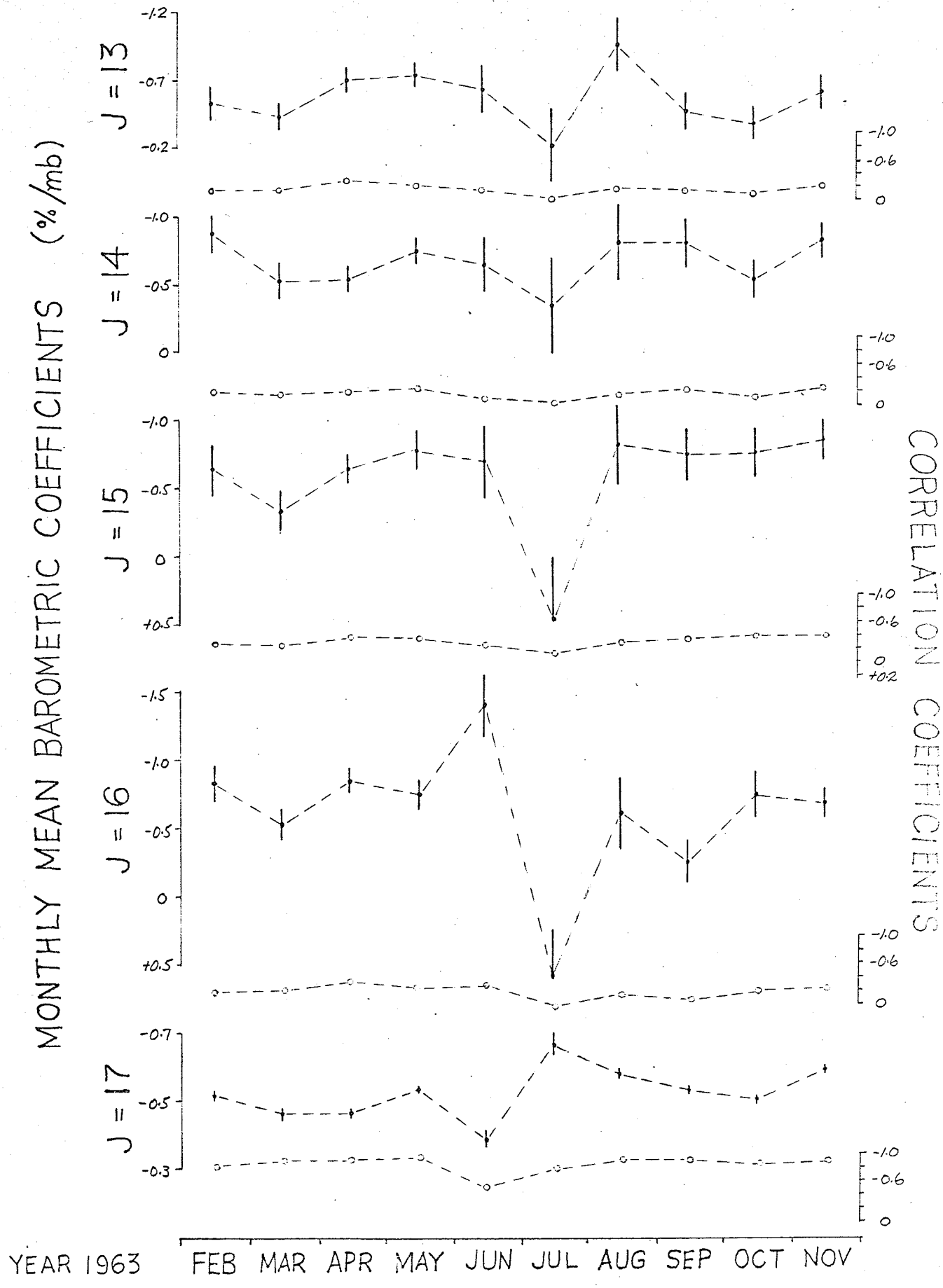

FIG. 3.6C SEASONAL VARIATIONS OF MONTHLY MEAN BAROMETRIC COEFFICIENTS B_M

energy ranges are generally poor as compared with the rest of the months.

3. For energy range 1, the values of the barometric coefficient in June and July deviate obviously from those of other months. However, this becomes less obvious for higher energy ranges.

4. For energy ranges above 6, the correlation coefficients are in general less than 0.5; therefore, it seems that nothing definite can be concluded here.

5. For photons with energy ranges below 6, the barometric coefficients in the period from July to November are on the average somewhat higher than those from February to June. This seems to show the existence of a seasonal difference in the barometric coefficients of photons.

D. Pressure Correction in the Study of Solar Diurnal Variation

As we have a number of barometric coefficients and they undergo some seasonal variation, there is a problem in choosing the barometric correction before any study of the solar diurnal variation can be conducted. At present, five kinds of barometric coefficients are available; namely, BW_R, BW_W, BW_M, B_M, and B_W. The pressure effect is eliminated from the photon intensity of the ith hour (I_i) by using the following formula:

$$I^{corr.} = I_i - B(P_i - P_M)I_M \qquad (13)$$

where $I^{corr.}$ is the pressure corrected photon intensity in the ith hour, P_i is the pressure reading in the ith hour, B is the barometric coefficient, P_M and I_M are respectively the average hourly pressure reading and photon intensity over a certain time period being considered.

BW_R, BW_M, and BW_W, being the weighted average barometric coefficients over the same long duration of time, are basically the same in nature except that their values are somewhat different (see Table 3.3).

B_M and B_W belong to their particular month and week; hence, their values vary with time. To eliminate some of the five kinds of barometric coefficients, a short period of two weeks data were utilized to test the individual effect of each coefficient in the pressure correction of photon intensity. Using equation (13) with P_M and I_M as the mean hourly pressure and intensity within a week, every hour's intensity within such a week was then corrected. The corrected hourly intensity readings of the week were summed up for a 24 hour daily variation. Such a method was applied to photon intensities for energy ranges 1 to 17. Fig. 3.7 illustrates the results of the pressure corrections for four kinds of barometric coefficients (BW_R, BW_W, B_W and B_M) when the photon intensity data of energy range 17 over one week (Oct. 2 to Oct. 8, 1963) was employed. The same shape is maintained for each of these four kinds of pressure-corrected daily variations. There are only slight differences in the values for the corrected counting rates. Such results are similar for all energy ranges and for the data of the next week (Oct. 9 to 15, 1963). Thus, any one of these barometric coefficients yields about the same daily variation of photon component.

Following the same procedures, a further test was made on the effect of corrections using BW_R, BW_M and B_M on data obtained during a long period of five months. P_M and I_M were the values taken from each month's averages while B_M belonged to the same month. The conclusion reached was the same as that given above, i.e. the resulting solar daily variation is quite insensitive to the actual coefficient used.

During the study of the solar durinal variation, pressure corrections were applied with both BW_R and B_M to photon data which were grouped into eleven periods of time (the grouping scheme will be described in Chapter IV). The pressure-corrected daily variation curves for the

photon component were plotted for comparison and again, these two extreme kinds of barometric coefficients lead to essentially the same results. Fig. 3.8 is an example of these two types of variation curve after pressure correction; they are practically identical. The only exception occurred in the time period 6 in which the counting rates of photon energy ranges 1 and 17 corrected by BW_R gave a perceptible difference from those corrected by B_M (Fig. 3.9). As for energy ranges higher than 2, such differences are masked by the large statistical fluctuations of the counting rates. However, such a difference might influence the results of a harmonic analysis on the daily variation. Nevertheless, the amplitudes and times of maximum intensity obtained from these two kinds of pressure-corrected curves in time period 6 by a harmonic analysis agreed well within one standard deviation through all energy ranges (Fig. 3.10). We therefore conclude that for our present experimental data any one of the determined barometric coefficients is suitable for use in a pressure correction prior to a diurnal variation study.

E. Summary

A variety of barometric coefficients has been determined in this experiment and their relative effects compared in the correction of raw data. In general, the low counting rates of the total absorption spectrometer make it difficult to draw definite conclusions for photons of high energies. The barometric coefficients determined from data acquired over a short period of time (as represented by B_R) show the greatest dispersion in their values and the occurrences of rare events such as positive barometric coefficients and negative coefficients with abnormally high values. The former appears to be the consequence of large statistical fluctuations but the latter seems real on account of high

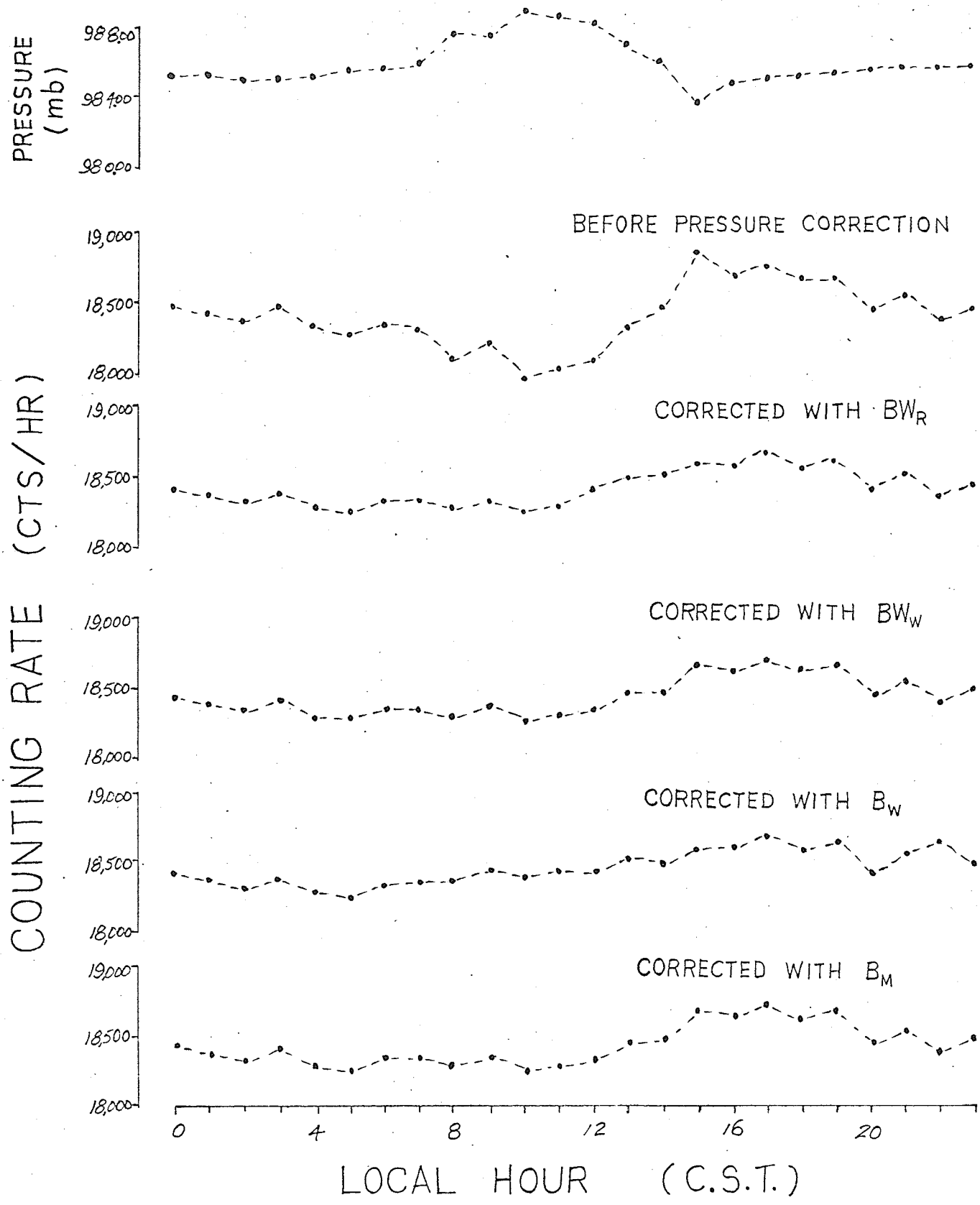

FIG. 3.7 FOUR KINDS OF PRESSURE CORRECTED DAILY VARIATIONS OF PHOTONS J = 17
(AVERAGED OVER PERIOD OCT. 2 – 8, 1963)

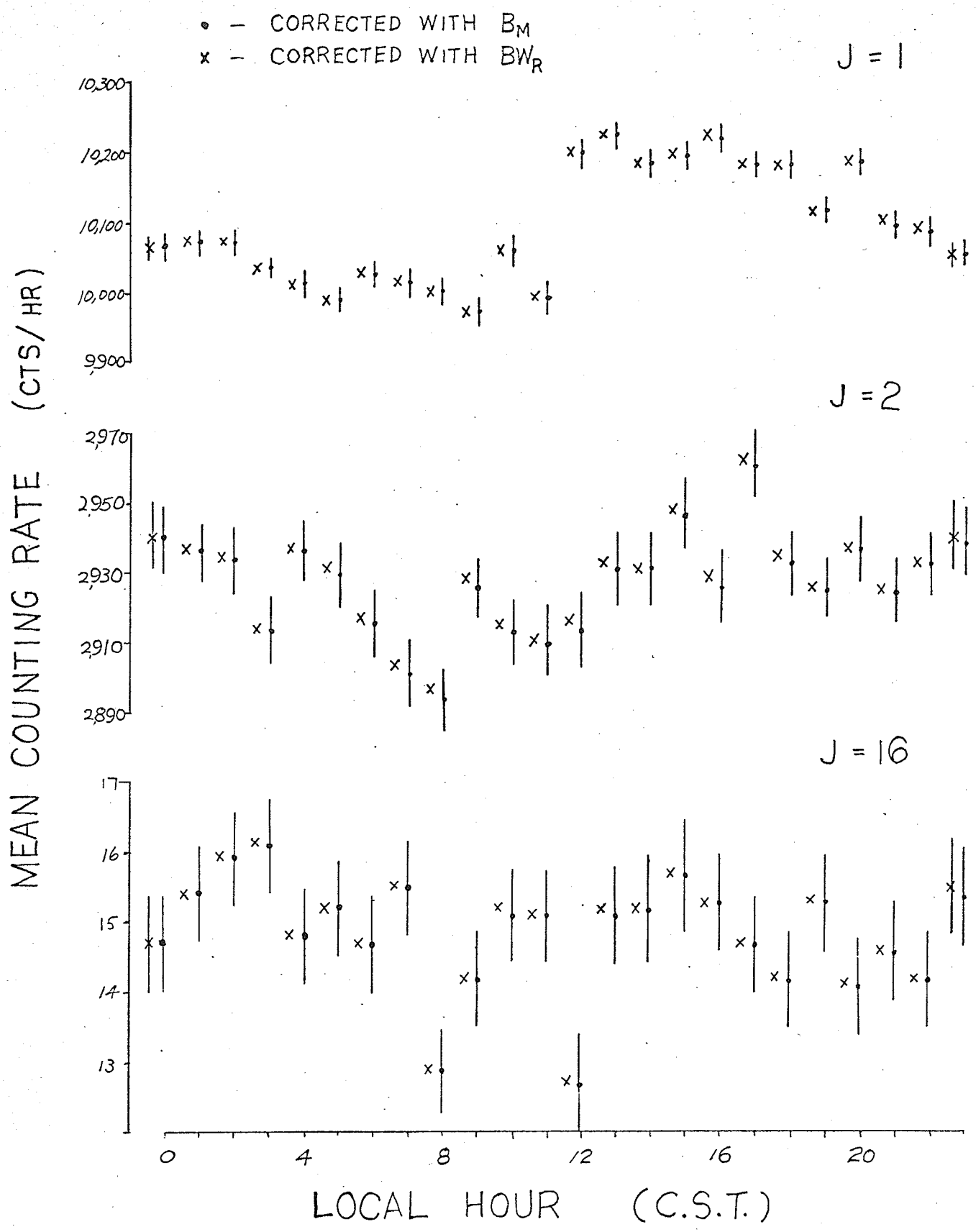

FIG. 3.8 PRESSURE CORRECTED MEAN DAILY VARIATIONS (WITH B_M, BW_R) OF VARIOUS PHOTON ENERGIES
(FOR PERIOD #1, FEB. 6 – MAR. 5, 1963)

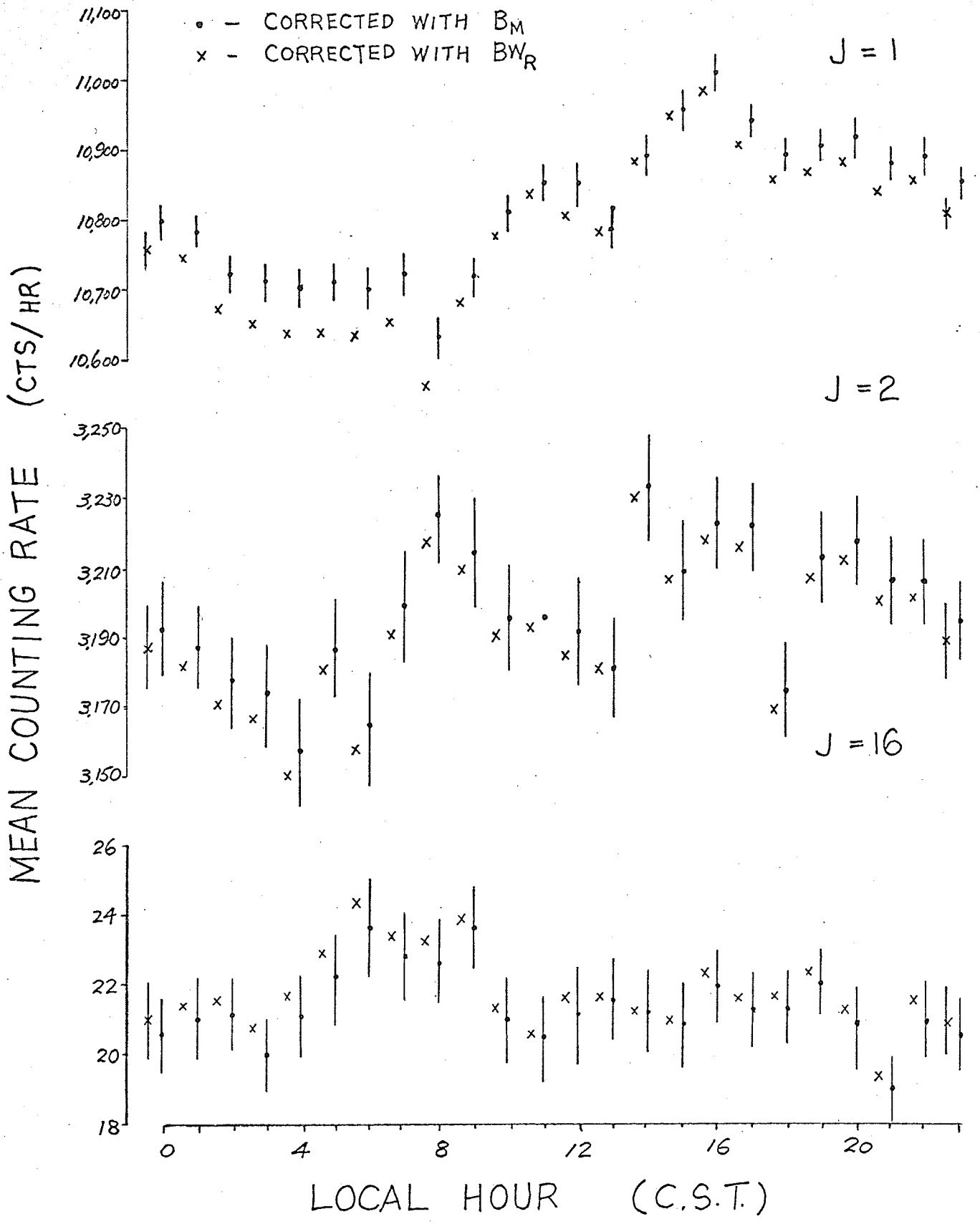

FIG. 3.9 PRESSURE CORRECTED MEAN DAILY VARIATIONS (WITH B_M, BW_R) OF VARIOUS PHOTON ENERGIES (FOR PERIOD #6, JUN. 21 - JUL. 17, 1963)

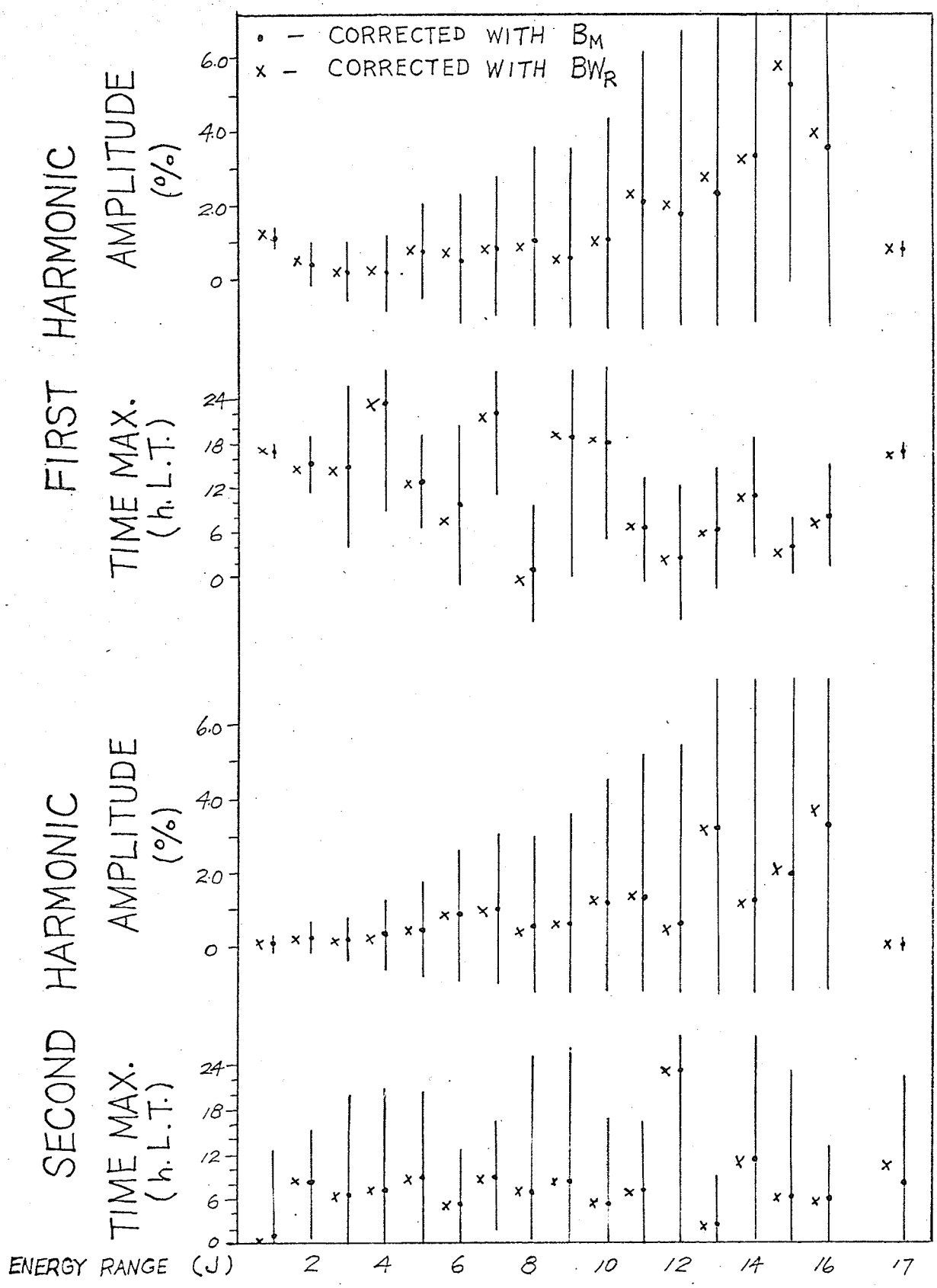

FIG. 3.10 HARMONIC RESULTS OF DAILY VARIATIONS CORRECTED WITH B_M, BW_R FOR PERIOD #6

(JUN. 21 - JUL. 17, 1963)

correlation coefficients. For a short period of time, on the order of about 20 hours, the atmospheric effect reflected by B_R seems to be quite complicated and beyond explanation in terms of a simple absorption process. However, statistically, over a period of a month the atmospheric effect becomes more regular and simplified. Monthly barometric coefficients (B_M) exhibit the elimination of all rare events and a narrow distribution of their values. This suggests that in the long run, the averaged atmospheric effect on photons is essentially barometric in nature. For a duration of many months, the energy dependence of photon barometric coefficients suggests strongly that a simple absorption process is the main meteorological influence on the photon component observed near sea level.

In terms of this simple absorption model, the barometric coefficient indicates the position of the "effective" level of generation of the observed photons as a function of energy. The overall effect of the lower 1/3 of atmosphere on the photon component is predominently absorption. Young showers of muon origin do not seem to play an important role in the photons observed near sea level; this seems particularly true for the low energy photons. The seasonal variation in the barometric coefficients of the photon component is quite large. In the frame of the simple absorption model, this implies a seasonal fluctuation in the height of the "effective" level of generation.

CHAPTER IV

SOLAR DIURNAL VARIATION

Since time variation studies of cosmic radiation began, the 24 hour daily variation of cosmic radiation has become one of the interesting topics which has attracted a great deal of effort from many research workers in an attempt to find an understanding of its real nature. Conventionally, a harmonic analysis is applied to the daily variation and the amplitude and the phase of the harmonic components are deduced as the physical quantities characterizing the variation. Up to the present time, the solar diurnal variation still remains an active subject in time variation studies of the cosmic radiation. Its nature has been gradually disclosed as a consequence of the solar modulation of the galactic cosmic radiation. This chapter will present the first study (to the best of our knowledge) on the solar diurnal variation of the photon component near sea level. Our main purpose is to experimentally establish the nature and energy dependence of the solar diurnal amplitude and of the time of maximum intensity for cosmic ray photons deep in the atmosphere. Also, the significance of the higher harmonics will be discussed, and the seasonal variation of the solar diurnal effects will be investigated. Before the presentation of our experimental results and comments, the general nature of the solar diurnal variation will be introduced through a review of previous work.

A. Review of Previous Work

In 1928, Lindholm reported a cosmic ray variation (ionization chamber data) with local time. Its amplitude was less than 0.5% and the

intensity reached its maximum near noon. Similarly, Compton et al. (1937) found a consistent variation about 0.2% above the mean around noon with a minimum shortly after midnight. Later, more and more workers confirmed the existence of such a kind of cosmic ray time variation.

Early speculation on the origin of this small variation led to the consideration of meteorological factors. Duperier (1946), Lange et al. (1948) and Hogg (1949) applied corrections on the hard component either for pressure or for temperature, or for both, but the solar diurnal variation did not disappear. However, temperature-corrected results of the hard component are usually contradictory. Duperier (1946) and Dorman et al. (1954) obtained a greater amplitude and a shift of the time of maximum while Dolbear et al. (1951) found the amplitude diminished to half of its original value. Studying the meteorological effects on the hard component, Glokova et al. (1958), Glokova (1960) and Kuzmin (1960) came to the conclusion that there is a constant component of seasonal variation of atmospheric origin and the temperature effect is very important in long period variations of cosmic radiation. Comparing the meson and the neutron diurnal variations at Deep River, Bercovitch et al. (1963) derived a vector to show the contribution of atmospheric variation in the diurnal variation of the hard component. This atmospheric vector has an amplitude 0.033% in summer with the time of maximum at about 7 h L.T. while in winter the corresponding values are 0.016% and 5 h; these amplitudes are very small as compared with 0.2% as estimated by Dorman (1957) and 0.11% by Quenby et al. (1960). Using the meson data at Deep River, Bercovitch (1966) established a linear correlation between the atmospheric temperature contribution to the diurnal variation of the meson intensity and the diurnal variations of the ground air temperature and the barometric pressure. The atmospheric effect has also been considered as the origin

of the semi-diurnal variation. Katzman et al. (1960) ascribed the semi-diurnal component of the nucleonic data to the semi-diurnal fluctuation of the atmospheric pressure.

The latitude dependence of the solar diurnal variation of the nucleonic component has been studied by many workers. Firor et al. (1954) did not find a significant change of the amplitude with latitude; it increases somewhat from about 0.45% at the equator to about 0.6% at 48° latitude. Meanwhile, the hard component showed an amplitude decrease on transition from latitude 50° (about 0.3%) to 80° (about 0.1%) as found by Dorman (1957). Using neutron data from sixteen stations, Katzman et al. (1960) found a significant geomagnetic latitude dependence of the phase. The time of maximum shifts toward evening hours from the pole (about 13 h L.T.) to the equator (about 17 h). Kane et al. (1960), working on IGY neutron data, arrived at the conclusions that the diurnal amplitude increases somewhat from the equator (about 0.25%) to medium latitudes (about 0.35%) but diminishes at high latitudes (about 0.15%), and that the amplitude and phase are different for stations situated at corresponding latitudes in the Northern and Southern hemispheres and for stations at close latitudes. Schwacheim's (1960) analysis of IGY neutron data produced similar conclusions with additional remarks that the mean monthly values of the diurnal amplitude show a good correlation among closely situated stations but poor for distant stations, and that the semi-diurnal amplitude diminishes with increasing latitude while its time of maximum remains constant at all latitudes. By means of neutron data from thirty stations for periods free from magnetic disturbance, Dorman et al. (1963) reported a shift of the time of maximum for the first harmonic towards earlier hours with increasing cutoff energy. Having studied the latitude effect of mean solar diurnal variation of the neutron

component (IGY data), Kitamura (1965) reported that the amplitude observed at 50° to 60° geomagnetic latitude is larger than that at other latitude and the time of maximum at sea level is earlier by about one hour than that at mountain altitude in the equatorial region. In order to investigate the variation of latitude dependence of the diurnal variation, Murakami et al. (1965) studied the phase difference and the ratio of amplitudes of diurnal variation between high and low latitude stations, using the neutron data observed at Zugspitze, Norikura and Sulphur Mountain. They concluded that a fluctuation exists in the latitude dependence on account of the variation in the primary rigidity spectrum of diurnal variation.

Alfven et al. (1943) were among the earliest workers to study the directional dependence of the solar diurnal variation. Directing their telescope at an zenith angle 30° in the north and in the south during alternative hours, they discovered a similar magnitude in the diurnal amplitude but a difference in phase of about 6 hours for these two directions, and hence concluded that the diurnal variation depends definitely on the direction of arrival of particles. To interpret the above results, Malmfors (1948) ascribed an anisotropy to the high energy primary cosmic radiation. This view was further supported by Elliot et al. (1950, 1951) who performed similar experiments with directional counter arrays to record simultaneously particles coming from the north and the south at zenith angles 45°. They concluded that particles of rather high energies (on the order of tens of BeV) are involved in the diurnal variation. Sekido, Kodama and Yagi (1950) and Sarabhai et al. (1955) observed that the diurnal amplitude increases with decreasing semiangle of the telescope in the east-west plane. Using counter telescopes to look at different angles with respect to the earth's equatorial plane, Sandström et al. (1960), assuming an effective rigidity of about 25 BeV/c

for the detected particles, inferred that the diurnal amplitude diminishes with increasing angle between the asymptotic direction of the primary flux and the equatorial plane.

Sekido and Yoshida (1950) published their observations of research on the solar diurnal variation during the time of a magnetic storm. In general, the more intense the storm, the greater will be the decrease in the cosmic ray intensity and the wider the fluctuation in the diurnal results. Applying the method of superposition of epochs to the total ionizing component data during eleven storms, they found that the diurnal amplitude on the day of storm onset is almost doubled. A few days after the storm, the amplitude is still greater than that before the storm and the time of maximum advances towards the earlier hours. Elliot et al. (1951) obtained similar results for the diurnal variation of the difference between the north and south pointing telescopes. Studying the influence of the twenty five effective magnetic storms on the diurnal variation, Glokova et al. (1955) came to the same conclusion as above for both the first and the second harmonics. Comparing the diurnal variations between the high energy component (90 cm lead shield) and the general component (no shield) recorded by the vertical telescopes during the storms, Yagi et al. (1956) demonstrated that the general component has a greater increase in diurnal amplitude and a shift in the time of maximum towards earlier hours than the high energy component. Kuzmin et al. (1958), from shielded ion chamber data corrected for atmospheric effects, discovered a particular kind of magnetic storm which causes a rise in the diurnal amplitude without altering the time of maximum. Mori et al. (1963) have analysed the IGY data in periods of cosmic ray storms by means of the "three points method" (that is to say, 3 stations separated in geomagnetic longitude by about 120°) and a spherical harmonic analysis

so as to separate the diurnal variation at a moment from the worldwide time variation. With the development of the storm, the time of maximum usually moves towards noon and sometime towards midnight. Such events can be classified into three types according to the position of the responsible flare with respect to the central meridian plane.

Correlation between geomagnetic activity and solar diurnal variation has been made for days with high K_p (geomagnetic planetary three-hour range index) by a number of workers such as Ehmert et al. (1951), Trumpy (1953), Firor et al. (1954). They reached the general conclusion that during days of high K_p the diurnal amplitude increases, and the time of maximum moves to earlier hours. Narrow angle telescopes show greater effects than instruments with wide directional sensitivity. However, Sekido et al. (1951) found a reduced amplitude for the semi-diurnal component on days with high K_p. Grouping data of crossed telescopes directed at the vertical, north and south according to five grades of K_p values, Sandström (1955) noted that with increasing K_p the diurnal amplitude increases and the time of maximum shifts regularly towards the earlier hours. This effect is most pronounced for the vertical and the south directions but less for the north direction. Some work has also been done for the correlation of the diurnal variation and the local geomagnetic index K. Elliot et al. (1951) found a greater fluctuation in the diurnal variation of the difference between the south and the north for days with K greater than or equal to 18. Kuzmin et al. (1958) reported that the diurnal variation as recorded by a counter telescope at 60 m.w.e. underground has an increase of 0.10% in amplitude for days with K greater than 17. Using a counter telescope with 10 cm lead, Barton et al. (1958) observed that as the daily sum of K increases from 10 to 40, the amplitude increases from 0.1% to 0.6% and the time of maximum shifts more than six

hours; the semi-diurnal amplitude also increases four times. As for the neutron component, Firor et al. (1954) found a close relationship between the diurnal variation and the K index; the diurnal amplitude is high for a high level of K value. Statistical analysis of the crossed telescope data at Moscow and geomagnetic field disturbance data at the equator by Inozemtseva (1964) showed the appearance of a local source of cosmic ray daily variation during a change of 100 gammas in the geomagnetic field strength.

In a study of the hard component data from 1936 to 1946, Yoshida et al. (1954) drew some conclusions on the 27-day recurrence tendency of the diurnal variation. This tendency is rather stable throughout several rotations of the sun. On average, the diurnal amplitude increases with decreasing cosmic ray intensity. Employing the method of superposition of epochs on data of 115 storms with the day of onset of storm as the zero day, they found that the stability of the 27-day recurrence for diurnal amplitude last for about three cycles. Glokova et al. (1955) and Grigorov (1955) did not see any perceptible tendency of a 27-day recurrence of the diurnal variation near the minimum of the solar activity. However, Kuzmin et al. (1958) reported the existence of 27-day recurrence for the diurnal variation during the year of decline in solar activity (1951) and in years of minimum solar activity (1953-1954). In addition, the maximum of 27-day variation of the diurnal variation coincides with the maximum of the 27-day variation in solar activity, and the recurrence of the diurnal variation has no close relationship with magnetic activity. Mori et al. (1964) noticed that during 1962 and 1963, the solar diurnal variation of the cosmic radiation showed a strong 27-day recurrence tendency and was strongly correlated with K_p value.

The diurnal variation of the hard component, uncorrected for

meteorological factors, shows an increase in amplitude with increasing solar activity and a shift in the time of maximum towards a later hour (Glokova, 1952). Having analysed the hard component data (1946 - 1953), Sarabhai et al. (1954) discovered a relationship between the time of maximum of the diurnal variation and the intensity of the coronal line of wave length 5303 Å but a weak correlation with the sunspot number. Magnetic and solar activity exert an influence on the semi-diurnal variation to different extents for high and low latitudes. Using the method of moving averages to eliminate the effects of seasonal variation, Glokova et al. (1955) and Glokova et al. (1957) correlated the successive mean annual values of the first harmonic, K, C (preliminary international character figure of geomagnetic activity), and R (relative sunspot number). It was noted that the time of maximum shifted towards earlier hours in the year 1953 but started to reverse this trend to later hours in the year 1954. This reversal coincided with the minima of the K, C, R curves well within the accuracy of one season. Investigating the relation between the world-wide distribution of neutron diurnal variations and the relative sunspot number, Kanno (1963) and Kanno et al. (1965) observed that the time of maximum moved with increasing solar activity towards the late hours at a rate which was higher for low and middle latitudes than for the polar region. Correlating the nucleonic component data at Deep River and Yakutsk with the solar flare index during IGY, Sastry (1964) found an apparent increase in the diurnal amplitude on days following a high flare index day. The solar daily variations recorded during the period 1958 - 1964 by the east and west pointing directional telescopes at Mt. Chacaltaya showed that the diurnal amplitude (for both directions) was lower in 1964 (minimum solar activity) as compared with its value in 1958 (maximum solar activity) and the time of maximum in the two directions had same value in these two

years (Ahluwalia et al. 1965). From an analysis of the world-wide neutron data obtained during 1957 - 1965, Kolomeets et al. (1965) came to conclusions that the diurnal amplitude increases as solar activity decreases for high latitude stations but decreases at middle and low latitudes, that the seasonal effect of solar diurnal amplitude with either one or two maxima was detected for different years of solar activity,and that no time variation in semi-diurnal amplitude and phase was observed.

Mariner II measurements of the solar wind velocity during August to December, 1962 did not show any relationship between it and the amplitude and the time of maximum of the cosmic ray diurnal variation as observed by the neutron monitor at Deep River (Snyder et al. 1963).

In a seasonal variation study of diurnal variation by means of hard component data, Glokova (1952) concluded that such a variation is most pronounced during the time of maximum solar activity. However, Kuzmin (1955 a, b) observed that if the temperature effect is considered, seasonal variation of the diurnal effect of the hard component will be eliminated. Again, Glokova (1956) reported a conspicuous variation in the mean diurnal amplitude and phase of the hard component during the winter and the summer of the period 1951 - 1952. Using the moving average method, Glokova et al. (1957) deduced a regular seasonal fluctuation of diurnal variation for the meson component, and thought that it was due to the world-wide variation of the diurnal effect in connection with the solar activity. Firor et al. (1954) observed that the seasonal variations of the diurnal variation of the neutron component resembled each other in the equator and the middle latitude regions, and considered them as of non-atmospheric origin.

The long term fluctuation of the solar diurnal variation of cosmic radiation has been investigated. Thambyaphillai et al. (1953),

after an analysis on the hard component data from many stations, remarked that the diurnal phase shift is systematic and of world-wide character. From 1933 to 1942, the time of maximum gradually moved to a later hour, but shifted in the opposite direction during 1942 to 1952. It was suggested that the secular variation of the diurnal effect may follow a 22 year cycle of solar activity. This view was supported by Steinmauer et al. (1955). Sandström (1955) studied the secular phase shifts of the particles coming from the vertical, the north and the south during 1948 - 1950, and stated that such a shift is practically independent of the direction of arrival. On the basis of results presented by Lange et al. (1948), Sarabhai et al. (1953) and Sarabhai et al. (1955), Dorman (1957) reviewed the secular fluctuations of the diurnal effect. The mean annual diurnal variation (Huancayo data, equator) demonstrated that during 1939 - 1941, the diurnal waves had a maximum around noon with a gradual addition of a new component whose time of maximum was in the night hours. From 1946 to 1948, the diurnal wave became a double peaked curve and by 1952, the time of maximum appeared at night. The duration of a complete cycle of fluctuation seems to be about 22 years. At Abmadabad (14° N), three months' mean diurnal variation showed a similar fluctuation. In June 1951, the 24 hour wave had a maximum around 11 h, but on account of the appearance of a night component with a maximum around 3 h, the time of maximum gradually shifted towards earlier hours until the end of 1952. However, Cheltenham data (middle latitude) of 1938 - 1952 and Moscow data (middle latitude) of 1953 - 1956 exhibited a different type of fluctuation for the mean annual diurnal variation. There is no clearly defined existence of two components. However, a shift in the time of maximum towards morning hours was evident. From their analysis of ion chamber data of Huancayo, Cheltenham, Christchurch

and Tokyo, Venkatesan et al. (1959) came to the conclusion that the diurnal amplitude is positively correlated with solar and magnetic activities. The direction of anisotropy, after correction for the influence of the geomagnetic field on the particle's trajectories, tends to move towards morning hours during the minimum solar activity and occurs at 7 h during the lowest minimum (June - July 1954). Later, Forbush et al. (1960) continued the above work up to year 1959. The deviation of the mean annual vector from the mean vector over 23 years shows a systematic variation in phase with a 22 years period.

Working on the results of the directional dependence of the diurnal variation obtained by Elliot et al. (1950), Brunberg et al. (1954) determined that the particles responsible for such a diurnal effect had an effective rigidity of about 21 BeV/c and came from an angle 65° to the east of the earth-sun line. With the experimental data for the ionizing component, neutron component and hard component recorded at different latitudes, Dorman (1957) applied the method of coupling constants to ascertain the energy spectrum of the primary diurnal variation (Appendix A). To attain an agreement between the calculated amplitudes and the experimental ones, he found the values for all parameters of the spectrum of the primary variation which had been assumed to have the form AE^r. E is the primary energy; A, being the power of the source of the diurnal variation, has a value of 0.14; r, the exponent, has a value of -1; and the lower bound of the primary energy is 6.6 BeV. Considering the geomagnetic effect on the particle's path and using the concept of effective direction, Dorman estimated that the source of diurnal variation had an averaged azimuthal position at 82° to the east of the earth-sun line during the period of 1937 - 1951. However, the calculated asymptotic latitude of the diurnal source shows remarkably different values for different cosmic ray secondary components recorded at different locations. For a better

agreement between the theoretical and experimental values of the amplitudes and the source position, Dorman suggested that A is dependent on the asymptotic latitude of the source and that the lower bound of the primary energy responsible is around 7.5 BeV. Having analysed the directional measurement of cosmic radiation at Mawson, Quenby et al. (1960) found that the primaries responsible for the diurnal variation had a mean rigidity of 10 - 20 GeV/c and the direction of the primary source was at 70° to the east of the earth-sun line. Using the data of neutron monitors, ion chambers and counter telescopes at various depths underground at Yakutsk during 1957 - 1958, Kuzmin (1960) determined the energy spectrum of the primary diurnal variation as $0.155E^{-1}$ with a lower bound energy of 10 - 15 GeV. Rao et al. (1963) developed a method to calculate the diurnal amplitude and phase, using the concept of asymptotic cones of acceptance. Results do not show any simple relationship between the phase and the longitude and latitude. The theoretical calculations agree well with the mean diurnal variation experimentally observed by 22 neutron monitors during IGY. It was thus concluded that during this time, the diurnal anisotropy is independent of rigidity in the range 1 - 200 BV, varies as a cosine function of the asymptotic latitude, has a maximum amplitude of 4×10^{-3} times the average cosmic ray flux, and a maximum intensity in the direction of 85° to the east of the earth-sun line. Later, the zero exponent was confirmed by Kane (1964) who analysed the IGY neutron data, and such characteristics of the diurnal anisotropy remain practically invariant up to the year 1965 as reported by Faller et al. (1965) and McCracken et al. (1965). Employing the world-wide neutron data for the year 1958, Dorman et al. (1963) deduced that the exponent of the primary variation spectrum changes from -0.3 to -0.6 and there is no clear dependence of the exponent on the sunspot number except for a few months. Kuzmin et al. (1963) assembled data on the meson

component at various depths underground together with hard and nucleonic components data. They found that in 1958 - 1959 the exponent had a value of -0.5 and the lower bound primary energy was 7 BeV while in 1960 - 1962 the respective values were -1.0 and 7 BeV. Utilizing the model proposed by Rao et al. (1963), Jacklyn et al. (1965) developed a method of determining the upper limiting rigidity for the solar diurnal variation in free space. He estimated that the mean value in 1958 was 95 GV with an error about 10 - 20 GV, and decreased by about 20 - 40 GV over the period of 1958 - 1962. Using data from 14 stations, Ables et al. (1965) investigated the semi-diurnal anisotropy during the period 1953 - 1965 by means of the numerical filter techniques. The phase and amplitude distribution histograms for each station and year, when fully corrected for geomagnetic effects on primary trajectories, indicate a consistent semi-diurnal anisotropy having an amplitude of about 0.1% and maxima along a line 60° west of the earth-sun line. They also remarked that such an anisotropy might be energy dependent.

Day-to-day changes of the solar diurnal variation have been studied with the achievement of high counting rates in cosmic ray monitors. Firor et al. (1954) discovered a high variability from day to day in the diurnal variation of the nucleonic component. The time of maximum appears in day time as well as in night time. Some of the days do not show any appreciable diurnal variation. Using ion chamber data, Sittkus (1955) observed an association of large amplitude and time of maximum near noon for some groups of days with a 27-day recurrence tendency. From the analysis of the data collected in 1954 with telescopes directed in the east-west plane, Sarabhai et al. (1958) attempted a phenomenological classification of daily variations into three types: namely, days with a maximum during the day time (designated as d-type), days with a maximum

at night time (n-type), and days with two maximum (s-type). The majority of days showed a maximum either at 12 h or at 3 h L.T. For each type, peak to peak amplitudes were as large as 2%, and the 27-day recurrence appears especially pronounced for the d-type. With data supplied by Huancayo and Churchill, Sarabhai et al. (1963 a) studied the diurnal variation for the period 1958 - 1962 by means of a statistical distribution of day-to-day amplitudes, times of maximum, and times of minimum. Conclusions were drawn as follows. The time of maximum shifts to earlier hours only at the equatorial station but not at high latitude. The peak-to-peak amplitude decreases appreciably for Huancayo neutrons, decreases less for Churchill mesons, but remains unchanged for Churchill neutrons. The majority of the days show the exponent of the anisotropy spectrum to be from -0.8 to -1.0. Using the same data as above and applying a correction for the geomagnetic effect, Sarabhai et al. (1963 b) derived the exponent of the anisotropy spectrum on a daily basis. The percentage frequency for zero exponent is always less than for positive and negative exponents. The frequency of days with positive exponent increased from 26% in year 1958 to 56% in 1961, while the frequency of days with negative exponent decrease from 1958 to 1961. In year 1962, almost all days had a negative exponent. In the study of IGY neutron data, Kane (1963) compared the diurnal variation with solar and terrestrial phenomena on a daily basis, but did not find any one-to-one correspondence with any phenomenon. Large diurnal amplitudes may follow type IV solar bursts and precede cosmic ray storms and geomagnetic storms. There exists a (29 ± 1) days recurrence tendency and a minor 8-days recurrence tendency. Vladimirsky et al. (1965) applied the method of construction of the directional intensity (Stepanyan 1962) to the neutron data for the period 1957 - 1958 and obtained continuous values of diurnal amplitude and phase for each day.

In addition to the main afternoon's maximum, another region of the relatively stable phases was revealed in 02 - 06 h L.T. Large diurnal amplitudes are connected mainly with two types of sudden commencement magnetic storms. For the first type, the maximum amplitude occurs before the sudden commencement while for the second type it occurs after the sudden commencement. The type IV radio bursts not followed by sudden commencement magnetic storms influence the diurnal amplitude.

Along with the large number of experimental investigations on the diurnal variation as outlined above, there have been many theoretical attempts at explaining the origin of the diurnal variation. Janossy (1937) proposed an east-west asymmetric effect of primary cosmic rays near the earth on account of the sun's magnetic dipole field in order to explain the excess of cosmic ray particles on the evening side of the earth. This hypothesis was further modified by Alfven (1947), Treimen (1954), and Elliot (1960, 1962) in terms of trapped orbits and solar absorption mechanism. However, Stern (1964) pointed out that this model cannot explain the effect of the reversal of the solar dipole field on the direction of the cosmic ray anisotropy.

For the explanation of the diurnal variation component which is directed at 90° to the east of the earth-sun line, Brunberg et al. (1954) suggested a mechanism of co-rotation of cosmic radiation with the sun. The rotating magnetic dipole field of the sun induces an electric field, and the particles will drift in a direction perpendicular to the solar magnetic field and the induced electric field. According to Compton and Getting effect, this drift velocity produces a diurnal amplitude of about 0.4%.

In order to account for the radial component of the diurnal variation, the time of maximum of which is at 12 h L.T. in the free space,

Alfven (1954) put forth the hypothesis of the solar origin of cosmic radiation. Particles of low energy will be accelerated to high energies about 10^{14} eV by the corpuscular stream. Colliding with the magnetic field inhomogeneities, particles will diffuse away from the region of their origin, resulting in an anisotropic flux in the direction of the sun. However, this theory can hardly be justified on account of too many arbitrary parameters in the evaluation of the amplitude of the radial component.

Many workers (for example, Alfven 1951, Swann 1954, Dorman 1955) have studied the modulation mechanism of the solar corpuscular stream on the charged particle. An electric field is induced in the moving corpuscular stream by the general magnetic field of the sun. Cosmic ray particles, crossing the corpuscular stream, will be either accelerated or decelerated. The integral effect of the solar corpuscular streams will be such that the diurnal anisotropy is located at 90° to the left of the earth-sun line. Such a mechanism also gives rise to a power law for the energy spectrum of the primary diurnal variation.

In 1958, Parker predicted theoretically an Archimedean spiral structure for the interplanetary magnetic field as the direct result of the solar wind streams. Such a configuration has been found experimentally consistent with the studies of the arrival directions of solar proton (McCracken 1962) and the direct measurements in space by Pioneer V (Coleman et al. 1960, Greenstadt 1965), Mariner II (Smith 1964), and IMP-I (Ness et al. 1964). As a result, this new discovery has to be considered in any solar diurnal variation theory whenever the interplanetary magnetic field is involved.

Ahluwalia et al. (1962) advanced a theory to account for the diurnal variation. In the Archimedes spiral magnetic field as produced

under the combined effects of the solar wind and the rotation of the sun, an electric field is induced in the interplanetary space. Cosmic ray particles of low energy, trapped in the spiral, will drift across the induced electric field under the guiding center approximation. The relative motion between the frame of reference moving with drift velocity, in which the cosmic radiation is isotropic, and the earth will cause an anisotropy on account of the Compton-Getting effect. As a consequence, the energy spectrum of the primary variation and hence the observed diurnal amplitude can be related to the anisotropy direction which is determined by the solar wind velocity and the angular velocity of the solar rotation. However, this theory meets with difficulties. First, this theory implies that the time of maximum of the anisotropy in free space must be within 90° to the east of the earth-sun line. Bercovitch (1963), using the day-to-day diurnal variation of the neutron component and taking into account the smearing effect of the geomagnetic field, showed that about half of the experimental points give anisotropy directions lying beyond 90°. Secondly, experimental evidence as presented by Snyder et al. (1963) indicates that no correlation can be found between solar wind velocity and the diurnal amplitude and the time of maximum. Thirdly, Stern (1964) argued from the theoretical point of view that no anisotropy will arise from a conservative electric field since this field will also produce a density gradient effect which cancels entirely the drift effect as suggested by Ahluwalia's model.

Recently, Parker (1964) discussed the conditions of the interplanetary magnetic field in which a net streaming of cosmic radiation can exist. In the general interplanetary magnetic field, either stationary or time varying, cancellation between the density gradient effect and the electric drift effect will lead to a failure in explaining any observable

anisotropy of cosmic rays. The presence of irregularities in the general magnetic field will cause particle diffusion. A suitable variation of the diffusion coefficient with space coordinates can result in an azimuthal and a radial streaming of cosmic radiation. To explain the origin of the diurnal variation, the interplanetary magnetic field at the earth's orbit must be sufficient regular so that the cosmic ray particles tend to move along the magnetic lines of force. Beyond the earth's orbit, sufficient irregularities must be present to eliminate the density gradient so that the electric drift effect can cause an appreciable net streaming of cosmic rays. Assuming the absence of a net radial streaming of cosmic radiation, the azimuthal flux at earth will have a velocity of rigid rotation with the sun.

As a modification of Ahluwalia's model, Axford (1965) treated the cosmic ray particles as a gas with a distribution function satisfying the Boltzman equation with a collision term. This collision term is used to represent the scattering effect of the cosmic ray particles due to the irregular component in the garden hose configuration of the interplanetary magnetic field. Equations of continuity and of momentum conservation are also set up to describe the state of the cosmic ray gas. Assuming a plane configuration equivalent to the model of the interplanetary magnetic field which has a spiral form within the solar wind cavity surrounded by a boundary region of magnetic turbulence, the velocity of the cosmic ray anisotropy is solved with the boundary condition that the radial velocity of cosmic ray gas vanishes at the solar surface and at the border of the turbulence. For the case without scattering in the solar wind cavity, the cosmic ray gas streams in a direction parallel to the orbital motion of the earth about the sun with a velocity due to the co-rotation of the gas with the sun. The fractional amplitude of this anisotropy, according to

the Compton-Getting formula, will be about 0.7% for the diurnal variation as observed in the free space.

Using orientation histograms to study on a day-to-day basis the distributions of the time of maximum and the time of minimum for the neutron component along with the distribution of the direction of the average interplanetary field as measured by satellite, Sarabhai et al. (1965) suggested a virtual sink for the galactic cosmic radiation towards the sun along the spiralling interplanetary magnetic field for those days with a difference of 6 - 9 h between the time of maximum and the time of minimum. Cosmic ray particles moving along the magnetic spiral will be scattered by the irregularities close to the sun, resulting in a deficiency in cosmic ray intensity as observed at the earth in the morning hours. This phenomenon has also been investigated by Mercer and Wilson (1965) who proposed an absorption mechanism for the removal of the cosmic ray particles. The primary particles, isotropically distributed, will mirror between the sun and the earth. Those with small pitch angles will mirror closer to the sun and thus be absorbed. Considering the absorption effect and the co-rotation of the cosmic radiation as the causes of the daily variation, they estimated the direction and the magnitude of the vector sum of these two effects which turns out to be in fair agreement with the observed variations as given by neutron data at Sulphur Mountain and Calgary.

B. Daily Variation

Since data for the photon component has been accumulated every hour in terms of a differential energy spectrum, a study on its solar diurnal variation can be carried out for each of the energy ranges covering the whole spectrum. In the present analysis, seventeen energy ranges were

selected according to the scheme described in Chapter III (see Table 3.1).

To make possible any analysis on the variation of extra-terrestrial origin, the meteorological effect must be removed from the observed data. In Chapter III, it was concluded that any one of the barometric coefficients will lead to similar results in the wave shape and in the harmonic analysis of the daily variation, and that such a barometric coefficient can be regarded, in the first approximation, as a total pressure coefficient which may eliminate sufficiently the meteorological effects. Hence, our data has been pressure corrected as described in Chapter III, using the weighted average rapid-pressure-change barometric coefficients (Table 3.3).

Considering the low counts per hour as recorded by the total absorption spectrometer, it is impossible to reach any statistically significant conclusions if the daily variation is analysed on a day-to-day basis. For example, the highest hourly counting rate for energy range 1 is of the order of 10^4 which has about 1% relative fluctuation error, a magnitude comparable to variations under investigation. To improve the statistical accuracy, 27 days are treated as a period, and the method of superposition of epochs is employed to produce a mean daily variation which consequently represents the average feature of the daily variation in such a period. The data collected from February 6 to November 29, 1963 is thus grouped into eleven periods. Furthermore, these eleven periods are taken as a single group (designated as period 12) for better statistics and hence more accuracy in studying the general features of the average daily variation.

To illustrate the effect of counting rates, the daily variation of period 1 and period 12 are given in Fig. 4.1A and Fig. 4.1B respectively. It can be seen that daily variations in period 12 are

better defined and show much smaller standard errors than the corresponding ones in period 1. Variations for energy ranges with high counting rates (J = 1, 17) preserve their shape in both periods while those with low counting rates (J = 6, 16) display inconsistent features. Therefore, whenever possible, conclusions should be drawn from the data of period 12, especially when the general properties of the variation are considered.

The investigation of the photon energy dependence of the daily variation wave forms leads to a distinction of two classes. The first class consists of waves for energy ranges from 1 to 5 (see Fig. 4.1B and Fig. 4.1C). Their common pattern of wave shape shows the general tendency: a decline from zero local hour to 9 or 10 h, then a rise up with a maximum around 16 and 17 h, and then a falling off until 23 h. This kind of wave form is on the whole similar to that of the nucleonic component registered at Deep River during the same period of time (Fig. 4.1E). However, the daily variations of the second class with energy ranges from 6 to 16 (Figures 4.1B, 4.1C and 4.1D) do not resemble the first class, nor do they show consistent features among themselves due to the wild scattering of points on each variation. In order to reduce these statistical fluctuations, we combined energy ranges from 6 to 9, from 10 to 16, and then from 6 to 16 (designated as J = 21, 22, and 23 respectively as shown in Fig. 4.1E). Here again, these three combined variations do not clearly fall into the wave pattern of the first class. In particular, the last one which covers all the energy ranges in the second class show another type of undulation, being fairly constant from 1 to 12 h and then rising up again. The existence of two different types of daily variation for different photon energies is interesting. Undoubtedly, daily variation of the first class (J = 1 to 5) are essentially solar diurnal in nature. However, the second class seems

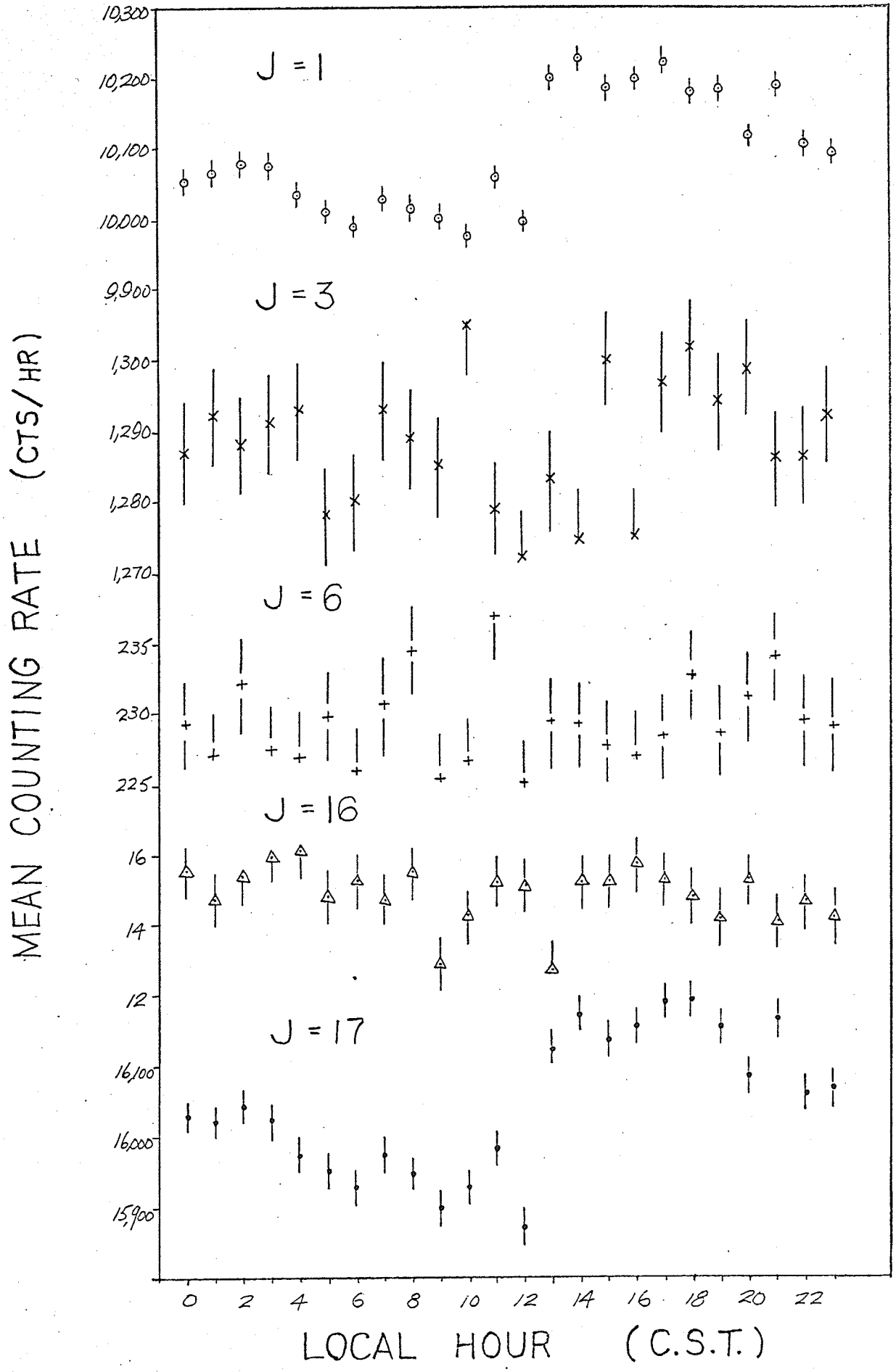

FIG. 4.1A MEAN DAILY VARIATIONS FOR PERIOD #1
(FEB. 6 - MAR. 5, 1963)

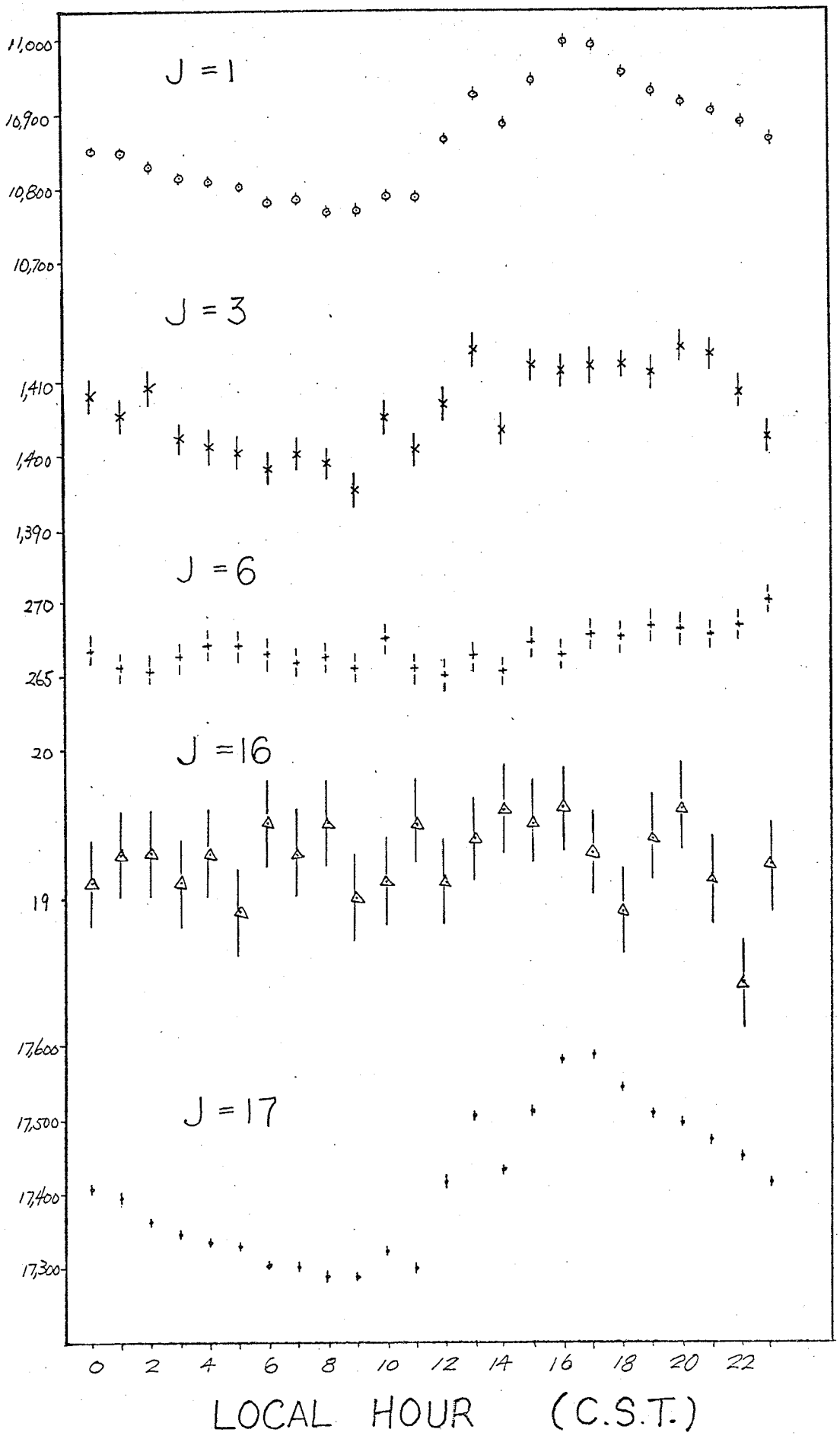

FIG. 4.1B MEAN DAILY VARIATIONS FOR PERIOD #12
(FEB. 6 - NOV. 29, 1963)

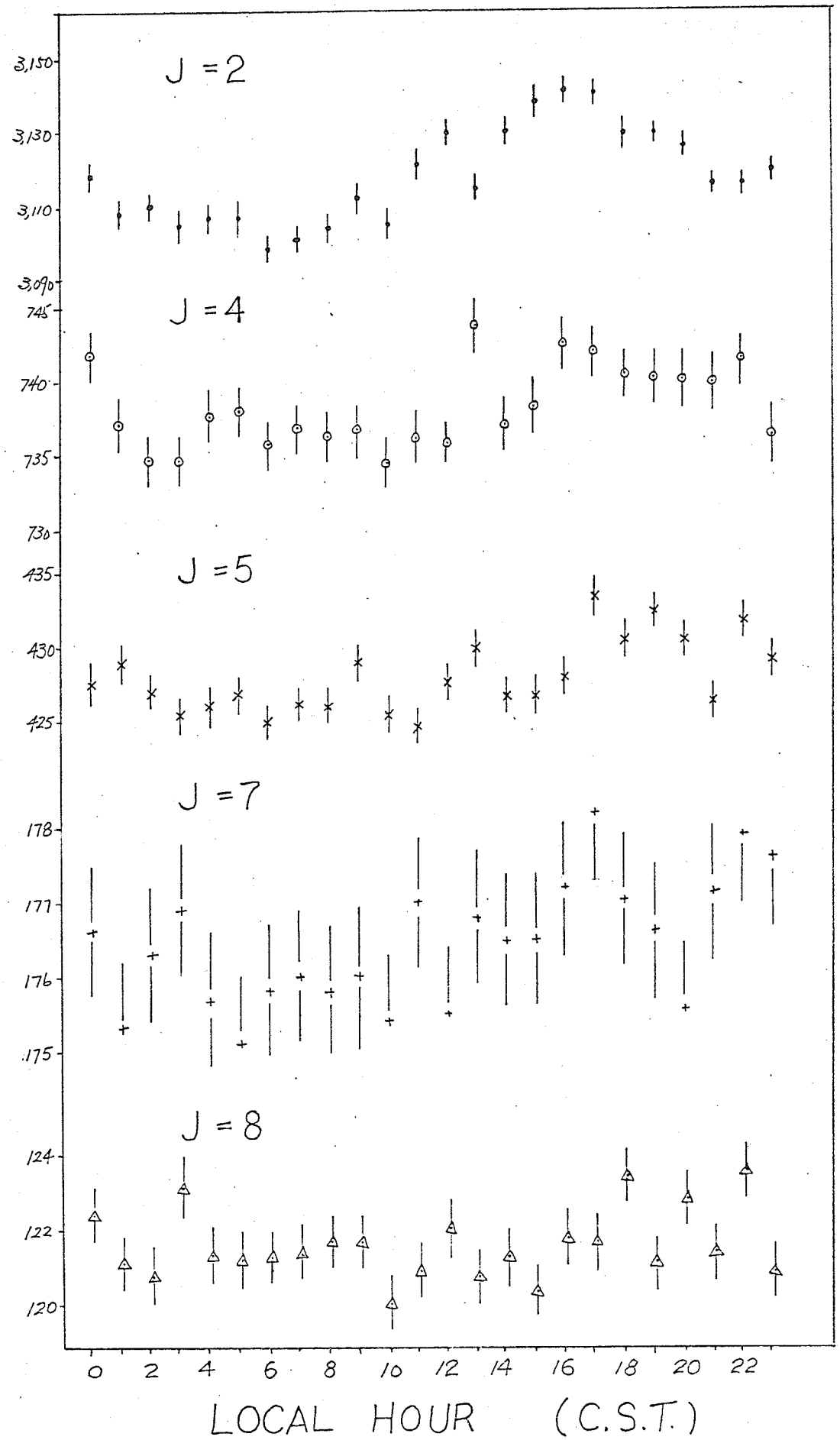

FIG. 4.1C MEAN DAILY VARIATIONS FOR PERIOD #12
(FEB. 6 - NOV. 29, 1963)

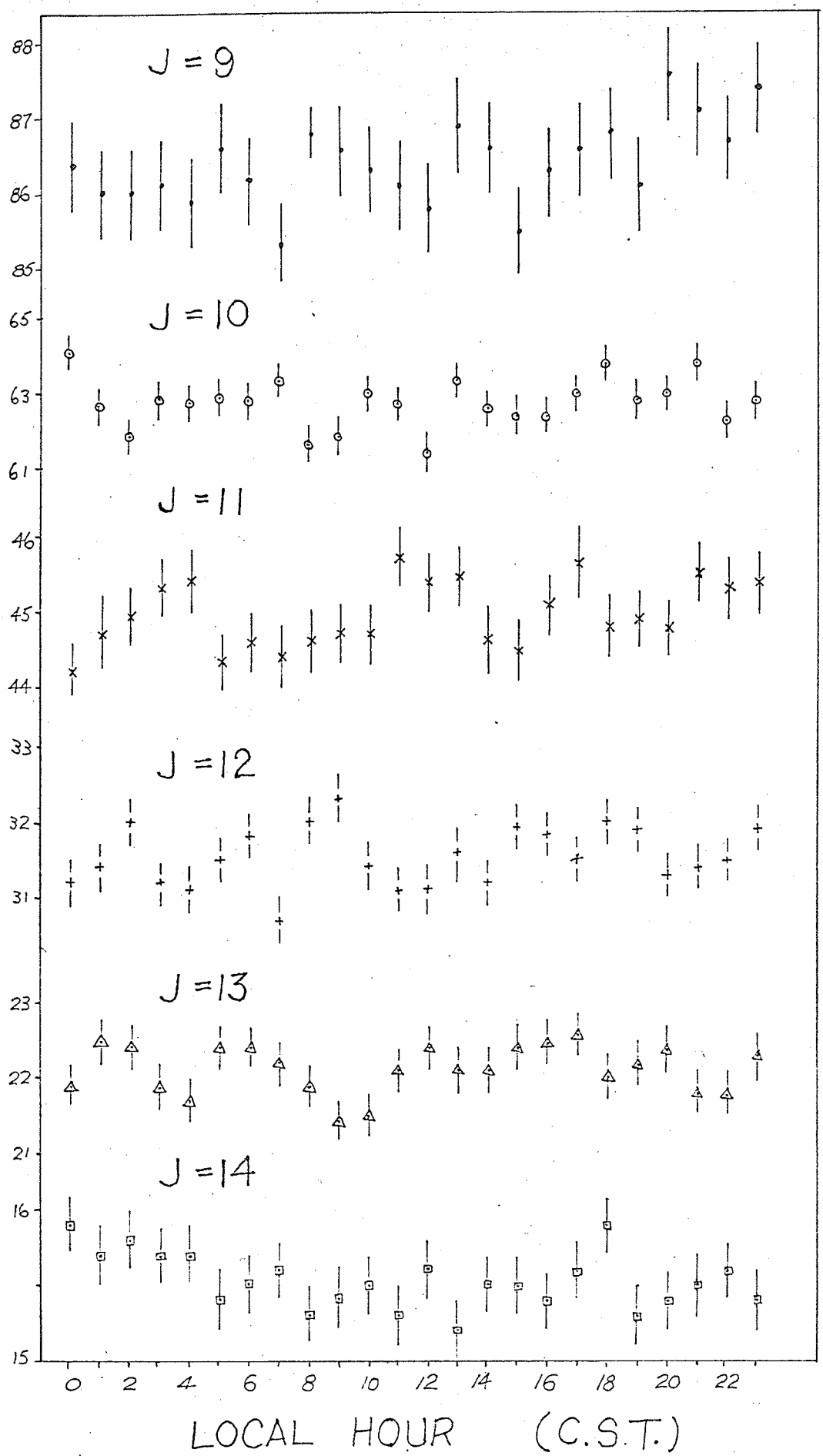

FIG. 4.1D MEAN DAILY VARIATIONS FOR PERIOD #12
(FEB. 6 - NOV. 29, 1963)

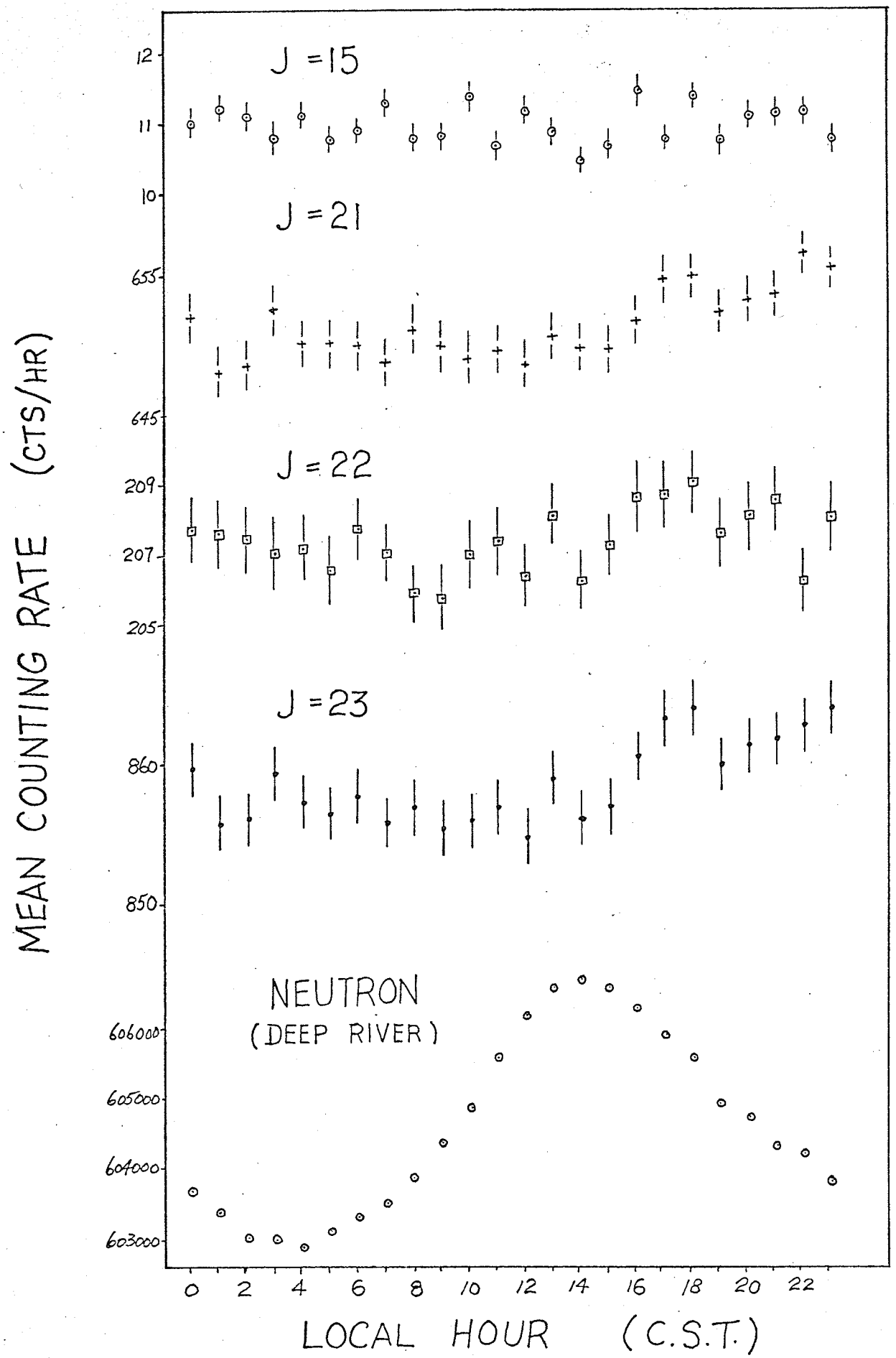

FIG. 4.1E MEAN DAILY VARIATIONS FOR PERIOD #12
(FEB. 6 - NOV. 29, 1963)

to deviate considerably from this diurnal nature. This implies that the primary cosmic radiation responsible does not participate strongly in the solar diurnal process. If this is the case, these primaries will have energies either higher than the upper limit or smaller than the lower limit of the solar diurnal modulation mechanism. Unfortunately, with the present relatively small sensitive volume of the spectrometer and resultant low counting rates, the existence of these two classes of daily variation cannot be conclusively established. As for the daily variations of the second class (J = 6 to 16), their nature will be discussed later in this Chapter.

C. Harmonic Analysis

For a separation of the daily variation into harmonics, a finite Fourier analysis has been applied to the pressure-corrected intensities for various photon energy ranges and for various periods, using a modified program from the IBM 1620 General Program Library. The mathematical method is outlined below:

Let f(t) represents the intensity of the experimental daily variation as a function of time t, and let it be represented by a Fourier series in the form

$$f(t) = \frac{a_o}{2} + S(a_p \cos \frac{2\pi p}{T} t + b_p \sin \frac{2\pi p}{T} t)$$

where p is the order of harmonic, T is the period of the first harmonic and S represent the summations taken from p = 1 to p = p'. If there are n experimental f(t) obtained at equal time interval (designated by h) in the period T, then T = nh, t = kh where k = 0, 1, 2, ..., n - 1, and p' will be less than or equal to n/2. Fourier coefficients, a_o, a_p, b_p, can be computed by the formulae:

$$a_o = \frac{2}{n} S(f(k))$$

$$a_p = \frac{2}{n} S(f(k) \cos \frac{2\pi p}{n} k)$$

$$b_p = \frac{2}{n} S(f(k) \sin \frac{2\pi p}{n} k)$$

where S represent the summations taken from k = 0 to k = n - 1. In the present case, n = 24 and T = 24 hours. The amplitude A_p, phase C_p and the time of maximum intensity M_p for the p th harmonic are given by

$$A_p = (a_p^2 + b_p^2)^{1/2}$$

$$C_p = \arctan \frac{a_p}{b_p}$$

$$M_p = \frac{1}{p} \frac{T}{2\pi} \arctan \frac{b_p}{a_p}$$

As all the twenty four values of f(k) do not differ considerably from their average $a_o/2$, their standard deviations can be taken as

$$D_{f(k)} = \left(\frac{a_o}{2} \right)^{1/2}$$

Hence, standard deviations for A_p, C_p are given by

$$D_{A_p} = D_{f(k)} \left(\frac{2}{n} \right)^{1/2}$$

$$D_{C_p} = \frac{D_{f(k)}}{A_p} \left(\frac{2}{n} \right)^{1/2}$$

The final results of the Fourier analysis will be presented in the form of

amplitude of p th harmonic = $A_p(\%) \pm D_{A_p}(\%)$

time of maximum of p th harmonic = $M_p \pm D_{M_p}$ (local hour)

where

$$A_p(\%) = \frac{A_p}{a_o/2} 100\%$$

$$D_{A_p}(\%) = \frac{D_{A_p}}{a_o/2} 100\%$$

$$D_{M_p} = \frac{T}{2\pi} D_{C_p}$$

The present analysis on the daily variation was performed up to and including the third harmonic. The computed amplitudes, A, and times of maximum, M, together with their standard errors, D_A and D_C for the first, second and third harmonics are tabulated in Table 4.1 for each of the twelve time periods.

TABLE 4.1

Period 1 : Feb. 6 - Mar. 4, 1963

J	First Harmonic				Second Harmonic				Third Harmonic			
	A	D_A	M	D_C	A	D_A	M	D_C	A	D_A	M	D_C
	(%)	(%)	(hr)	(hr)	(%)	(%)	(hr)	(hr)	(%)	(%)	(hr)	(hr)
1	.97	.07	16.33	.28	.37	.07	2.11	.74	.13	.07	4.77	2.16
2	.44	.13	19.36	1.15	.26	.13	2.27	1.93	.08	.13	7.62	6.18
3	.29	.20	20.08	2.67	.28	.20	5.59	2.77	.40	.20	0.04	1.94
4	.50	.28	16.87	2.16	.28	.28	5.91	3.90	.22	.28	0.09	4.94
5	1.02	.37	21.02	1.40	.55	.37	6.08	2.58	.53	.37	5.86	2.70
6	.34	.48	20.28	5.43	.59	.48	6.78	3.07	.06	.48	0.61	29.72
7	.75	.60	23.17	3.05	.29	.60	8.08	7.89	.53	.60	4.92	4.30
8	1.72	.73	21.96	1.61	.44	.73	9.46	6.31	.32	.73	4.88	8.59
9	1.41	.88	11.98	2.38	1.77	.88	6.37	1.91	1.03	.88	3.31	3.28
10	1.19	1.05	20.86	3.38	.92	1.05	10.95	4.38	1.21	1.05	4.49	3.30
11	1.56	1.25	21.13	3.05	1.34	1.25	5.72	3.56	.47	1.25	4.49	10.06
12	1.76	1.48	19.71	3.21	.71	1.48	9.56	7.91	.92	1.48	5.55	6.16
13	3.61	1.74	20.83	1.84	2.42	1.74	4.11	2.75	3.21	1.74	6.26	2.07
14	5.64	2.08	23.81	1.41	2.60	2.08	4.76	3.06	4.91	2.08	7.10	1.62
15	4.89	2.47	21.61	1.93	2.35	2.47	4.46	4.02	1.09	2.47	2.93	8.67
16	1.88	1.87	24.07	3.80	3.78	1.87	2.32	1.89	.62	1.87	0.18	11.57
17	0.73	.06	17.07	.30	.26	.06	2.56	.83	.08	.06	5.62	2.89

TABLE 4.1 (cont.)

Period 2 : Mar. 5 - Mar. 31, 1963

J	First Harmonic				Second Harmonic				Third Harmonic			
	A	D_A	M	D_C	A	D_A	M	D_C	A	D_A	M	D_C
	(%)	(%)	(hr)	(hr)	(%)	(%)	(hr)	(hr)	(%)	(%)	(hr)	(hr)
1	.75	.07	16.61	.36	.36	.07	2.68	.76	.15	.07	5.25	1.80
2	.30	.13	15.46	1.69	.24	.13	2.35	2.07	.18	.13	7.67	2.85
3	.31	.19	22.38	2.38	.23	.19	6.71	3.18	.15	.19	5.84	5.02
4	.53	.27	21.62	1.98	.39	.27	4.28	2.65	.44	.27	5.48	2.33
5	.78	.36	18.49	1.75	.48	.35	7.42	2.81	.23	.35	1.60	5.77
6	.16	.45	4.72	10.65	.21	.45	4.74	8.18	.52	.45	2.26	3.32
7	.71	.55	12.10	3.00	1.18	.55	4.90	1.80	.65	.55	5.03	3.26
8	.96	.67	5.36	2.65	.63	.67	3.60	4.05	.69	.67	2.43	3.71
9	1.42	.79	19.59	2.14	1.26	.79	4.60	2.41	1.37	.79	6.55	2.21
10	1.05	.93	20.65	3.40	1.60	.93	6.81	2.23	2.38	.93	4.83	1.50
11	1.08	1.09	18.67	3.83	.18	1.09	2.98	22.87	.54	1.09	3.26	7.67
12	1.37	1.31	22.42	3.65	1.45	1.31	0.51	3.44	.17	1.31	2.35	29.55
13	1.51	1.55	4.96	3.93	1.37	1.55	11.05	4.35	2.01	1.55	4.54	2.95
14	2.42	1.83	2.50	2.89	2.59	1.83	2.37	2.70	1.03	1.83	0.24	6.78
15	1.49	2.16	20.36	5.54	2.20	2.16	10.62	3.76	5.14	2.16	0.03	1.61
16	3.10	1.61	3.74	1.99	1.67	1.61	1.63	3.68	3.48	1.61	5.62	1.77
17	.55	.06	16.96	.39	.27	.06	3.03	.79	.12	.06	5.57	1.74

Period 3 : Apr. 1 - Apr. 27, 1963

J	First Harmonic				Second Harmonic				Third Harmonic			
	A	D_A	M	D_C	A	D_A	M	D_C	A	D_A	M	D_C
	(%)	(%)	(hr)	(hr)	(%)	(%)	(hr)	(hr)	(%)	(%)	(hr)	(hr)
1	.56	.07	16.11	.48	.10	.07	11.58	2.67	.09	.07	4.91	3.00
2	.55	.13	16.49	.92	.33	.13	4.28	1.54	.11	.13	5.20	4.67
3	.30	.20	17.99	2.54	.07	.20	11.17	9.98	.26	.20	2.28	2.84
4	.09	.27	12.85	11.74	.09	.27	6.42	11.42	.54	.27	4.84	1.94
5	.48	.36	20.92	2.84	.21	.36	1.85	6.34	.44	.36	7.45	3.09
6	.54	.45	20.60	3.18	.64	.45	0.91	2.67	.33	.45	7.08	5.18
7	.92	.55	21.09	2.29	.95	.55	0.35	2.21	.12	.55	3.40	16.85
8	.69	.66	21.20	3.67	1.46	.66	4.33	1.72	.39	.66	6.25	6.50
9	.88	.77	19.12	3.35	.19	.77	1.73	15.74	1.20	.77	2.37	2.47
10	.67	.90	6.61	5.14	1.12	.90	9.34	3.07	1.03	.90	1.98	3.34
11	1.33	1.07	20.66	3.07	1.61	1.07	7.46	2.53	1.65	1.07	1.33	2.47
12	2.39	1.26	6.40	2.02	.29	1.26	6.49	16.83	2.42	1.26	5.43	1.99
13	1.82	1.51	3.89	3.16	1.23	1.51	1.47	4.68	1.20	1.51	5.64	4.79
14	3.48	1.81	16.23	1.99	2.47	1.81	11.00	2.80	3.29	1.81	3.76	2.10
15	2.30	2.10	4.52	3.49	1.91	2.10	10.38	4.20	3.30	2.10	7.20	2.43
16	1.60	1.53	6.10	3.64	2.58	1.53	8.09	2.26	1.83	1.53	7.55	3.18
17	.48	.06	16.54	.45	.06	.06	1.48	3.81	.08	.06	4.84	2.66

TABLE 4.1 (cont.)

Period 4 : Apr. 28 - May 24, 1963

J	First Harmonic				Second Harmonic				Third Harmonic			
	A	D_A	M	D_C	A	D_A	M	D_C	A	D_A	M	D_C
	(%)	(%)	(hr)	(hr)	(%)	(%)	(hr)	(hr)	(%)	(%)	(hr)	(hr)
1	.71	.07	16.27	.38	.38	.07	2.07	.70	.12	.07	5.04	2.34
2	.32	.13	14.12	1.55	.13	.13	2.96	4.03	.09	.13	6.73	5.47
3	.39	.20	14.55	1.92	.02	.20	11.10	30.24	.12	.20	1.58	6.34
4	.29	.27	10.49	3.59	.38	.27	2.18	2.74	.46	.27	4.91	2.25
5	.33	.36	10.34	4.06	.28	.36	0.62	4.78	.37	.36	1.32	3.62
6	.15	.45	5.29	11.73	.80	.45	6.22	2.14	.81	.45	3.83	2.11
7	.81	.55	10.07	2.57	.53	.55	3.92	3.92	.85	.55	5.18	2.47
8	.36	.65	14.47	6.92	.51	.65	8.88	4.88	.94	.65	2.26	2.65
9	.48	.77	13.15	6.09	1.05	.77	8.58	2.81	1.00	.77	6.16	2.95
10	1.19	.90	21.28	2.88	1.23	.90	9.99	2.78	.32	.90	0.70	10.66
11	.44	1.05	8.40	9.06	2.63	1.05	10.67	1.53	1.06	1.05	3.64	3.77
12	1.80	1.26	4.29	2.67	.51	1.26	5.69	9.49	2.65	1.26	6.84	1.81
13	1.33	1.51	15.57	4.35	1.09	1.51	6.52	5.30	1.20	1.51	3.57	4.82
14	2.05	1.79	18.44	3.34	1.86	1.79	5.70	3.67	.52	1.79	3.01	13.14
15	6.00	2.10	14.51	1.34	1.20	2.10	2.97	6.70	3.17	2.10	7.80	2.54
16	3.92	1.51	11.69	1.47	1.54	1.51	11.81	3.75	1.82	1.51	5.90	3.18
17	.54	.06	15.70	.40	.26	.06	2.12	.80	.09	.06	5.05	2.24

Period 5 : May 25 - Jun. 20, 1963

J	First Harmonic				Second Harmonic				Third Harmonic			
	A	D_A	M	D_C	A	D_A	M	D_C	A	D_A	M	D_C
	(%)	(%)	(hr)	(hr)	(%)	(%)	(hr)	(hr)	(%)	(%)	(hr)	(hr)
1	.86	.07	16.06	.31	.44	.07	2.76	.59	.19	.07	6.31	1.40
2	.32	.13	15.36	1.53	.14	.13	4.85	3.49	.14	.13	0.15	3.61
3	.26	.19	22.97	2.83	.29	.19	4.90	2.57	.37	.19	2.83	1.97
4	.22	.26	3.79	4.61	.40	.26	10.08	2.52	.17	.26	7.43	6.02
5	.27	.34	18.62	4.87	.63	.34	5.61	2.10	.27	.34	7.31	4.82
6	.89	.43	22.38	1.85	.91	.43	6.61	1.81	.31	.43	5.16	5.31
7	.41	.53	4.40	4.90	.18	.53	4.82	11.13	.57	.53	7.57	3.56
8	.46	.63	1.66	5.16	.58	.63	2.25	4.13	.76	.63	4.21	3.17
9	.48	.73	7.16	5.79	.82	.73	4.74	3.40	.46	.73	4.82	6.11
10	.56	.85	13.79	5.83	2.51	.85	4.22	1.30	1.54	.85	6.82	2.11
11	1.34	1.00	5.94	2.84	1.01	1.00	11.01	3.77	1.23	1.00	7.72	3.10
12	.08	1.21	12.46	56.25	1.26	1.21	6.59	3.66	1.34	1.21	7.78	3.44
13	1.10	1.45	11.88	5.02	2.48	1.45	10.32	2.24	3.69	1.45	2.06	1.50
14	2.18	1.75	4.98	3.08	2.84	1.75	9.34	2.36	1.18	1.75	2.97	5.67
15	1.39	2.06	22.40	5.66	2.07	2.06	7.02	3.81	2.09	2.06	2.66	3.76
16	3.10	1.56	10.50	1.93	1.05	1.56	10.78	5.67	2.18	1.56	6.25	2.73
17	.57	.05	16.21	.37	.30	.05	3.21	.70	.11	.05	6.58	1.81

TABLE 4.1 (cont.)

Period 6 : Jun. 21 - Jul. 17, 1963

J	First Harmonic				Second Harmonic				Third Harmonic			
	A	D_A	M	D_C	A	D_A	M	D_C	A	D_A	M	D_C
	(%)	(%)	(hr)	(hr)	(%)	(%)	(hr)	(hr)	(%)	(%)	(hr)	(hr)
1	1.37	.07	16.72	.19	.20	.07	.47	1.33	.07	.07	6.54	3.96
2	.55	.13	15.13	.89	.24	.13	8.50	2.05	.33	.13	7.12	1.47
3	.23	.19	14.49	3.19	.19	.19	6.52	3.84	.26	.19	5.95	2.76
4	.27	.26	23.40	3.66	.26	.26	7.22	3.78	.15	.26	5.74	6.46
5	.79	.34	12.88	1.64	.45	.34	8.99	2.85	.58	.34	2.71	2.25
6	.70	.43	7.76	2.32	.98	.43	5.32	1.68	.36	.43	7.33	4.57
7	.85	.52	21.88	2.35	1.04	.52	8.96	1.92	1.23	.52	7.67	1.63
8	.92	.63	23.96	2.60	.41	.63	7.15	5.79	.38	.63	4.09	6.36
9	.60	.74	19.20	4.74	.68	.74	8.54	4.18	1.84	.74	3.10	1.54
10	1.09	.86	18.42	3.03	1.27	.86	5.94	2.58	1.94	.86	2.90	1.69
11	2.30	1.00	6.31	1.67	1.41	1.00	7.01	2.72	.62	1.00	2.40	6.20
12	2.09	1.21	2.66	2.30	.49	1.21	1.02	9.43	.30	1.21	2.22	15.21
13	2.74	1.45	5.86	2.03	3.20	1.45	2.63	1.74	2.36	1.45	7.48	2.36
14	3.30	1.72	10.69	1.99	1.11	1.72	11.05	5.92	1.24	1.72	4.50	5.28
15	5.84	2.07	3.52	1.35	2.09	2.07	6.10	3.78	3.07	2.07	7.19	2.57
16	3.89	1.55	7.45	1.52	3.76	1.55	5.91	1.57	2.07	1.55	7.10	2.85
17	.94	.05	16.51	.22	.07	.05	10.69	2.95	.11	.05	6.79	1.94

Period 7 : Jul. 18 - Aug. 13, 1963

J	First Harmonic				Second Harmonic				Third Harmonic			
	A	D_A	M	D_C	A	D_A	M	D_C	A	D_A	M	D_C
	(%)	(%)	(hr)	(hr)	(%)	(%)	(hr)	(hr)	(%)	(%)	(hr)	(hr)
1	.82	.07	14.88	.32	.22	.07	1.79	1.19	.08	.07	4.70	1.89
2	.71	.13	14.95	.68	.03	.13	1.73	16.92	.08	.13	4.67	6.03
3	.96	.19	14.98	.75	.48	.19	.61	1.49	.04	.19	1.81	15.98
4	.79	.26	15.36	1.26	.56	.26	1.34	1.78	.36	.26	3.00	2.77
5	.45	.34	15.57	2.90	.43	.34	.29	3.00	.19	.34	4.97	6.75
6	.52	.43	17.98	3.18	.69	.43	10.32	2.40	.71	.43	4.38	2.33
7	.59	.53	13.42	3.42	.38	.53	4.56	5.31	.46	.53	2.66	4.36
8	.78	.63	3.18	3.09	.22	.63	10.57	10.92	.97	.63	1.72	2.48
9	.89	.74	20.91	3.17	1.00	.74	6.98	2.83	1.08	.74	6.96	2.64
10	2.16	.87	12.12	1.54	.91	.87	3.47	3.65	.37	.87	2.66	8.99
11	.37	1.04	14.51	10.78	.87	1.04	7.53	4.53	1.95	1.04	1.76	2.04
12	2.65	1.25	16.52	1.80	1.23	1.25	3.71	3.88	2.45	1.25	1.15	1.94
13	1.11	1.49	16.68	5.16	.70	1.49	3.09	8.17	1.74	1.49	7.26	3.27
14	2.56	1.83	21.19	2.72	.99	1.83	4.37	7.07	4.82	1.83	0.29	1.45
15	2.08	2.17	0.52	4.00	2.23	2.17	1.56	3.72	1.91	2.17	2.75	4.35
16	1.69	1.66	15.74	3.77	3.41	1.66	3.11	1.86	1.24	1.66	3.16	5.12
17	.78	.05	14.98	.26	.21	.05	1.50	.99	.07	.05	4.11	3.05

TABLE 4.1 (cont.)

Period 8 : Aug. 14 - Sept. 9, 1963

J	First Harmonic				Second Harmonic				Third Harmonic			
	A	D_A	M	D_C	A	D_A	M	D_C	A	D_A	M	D_C
	(%)	(%)	(hr)	(hr)	(%)	(%)	(hr)	(hr)	(%)	(%)	(hr)	(hr)
1	.71	.07	16.17	.36	.17	.07	1.75	1.53	.03	.07	0.33	8.40
2	.61	.13	15.11	.79	.15	.13	0.98	3.31	.19	.13	0.75	2.51
3	.85	.19	14.10	.85	.26	.19	11.71	2.81	.22	.19	5.07	3.19
4	.71	.26	15.48	1.39	.41	.26	8.73	2.40	.28	.26	7.49	3.57
5	.91	.34	13.34	1.43	.23	.34	6.61	5.72	.50	.34	7.39	2.59
6	.69	.43	15.15	2.39	.21	.43	7.46	8.00	.13	.43	3.91	12.80
7	.37	.54	14.45	5.45	.06	.54	6.68	33.32	.23	.54	6.23	8.83
8	.65	.65	17.09	3.80	.67	.65	10.52	3.69	.87	.65	0.55	2.85
9	.83	.77	0.25	3.56	1.49	.77	0.67	1.99	.87	.77	7.48	3.41
10	.77	.92	4.77	4.56	.35	.92	9.84	9.89	.40	.92	4.77	8.75
11	2.23	1.09	9.67	1.86	1.59	1.09	1.47	2.61	1.40	1.09	3.18	2.97
12	1.41	1.29	12.56	3.50	1.28	1.29	11.54	3.86	.25	1.30	2.14	20.06
13	1.36	1.54	14.58	4.32	2.77	1.54	2.02	2.12	1.63	1.54	3.68	3.61
14	3.15	1.83	23.11	2.22	3.57	1.83	0.59	1.95	.31	1.83	3.53	22.45
15	2.85	2.21	14.91	2.96	5.50	2.21	8.63	1.53	1.75	2.21	1.67	4.83
16	1.78	1.72	12.20	3.68	1.85	1.72	3.22	3.54	1.60	1.72	4.88	4.10
17	.68	.05	15.66	.30	.14	.05	1.14	1.48	.06	.05	0.02	3.58

Period 9 : Sept. 10 - Oct. 6, 1963

J	First Harmonic				Second Harmonic				Third Harmonic			
	A	D_A	M	D_C	A	D_A	M	D_C	A	D_A	M	D_C
	(%)	(%)	(hr)	(hr)	(%)	(%)	(hr)	(hr)	(%)	(%)	(hr)	(hr)
1	.76	.07	16.24	.34	.17	.07	3.05	1.52	.14	.07	6.46	1.77
2	.38	.13	16.45	1.26	.20	.13	1.05	2.44	.16	.13	2.61	3.12
3	.36	.19	17.90	2.00	.19	.19	1.75	6.07	.08	.19	5.25	8.46
4	.25	.26	1.62	3.97	.40	.26	4.46	2.46	.54	.26	4.83	1.85
5	.34	.34	14.04	3.80	.20	.34	9.65	6.51	.35	.34	7.16	3.74
6	.42	.43	10.12	3.90	.54	.43	3.99	3.08	.19	.43	5.08	8.62
7	.31	.54	18.52	6.54	.49	.54	11.35	4.16	.40	.54	7.62	5.16
8	.47	.65	13.93	5.32	2.06	.65	6.53	1.20	.66	.65	5.34	3.75
9	.74	.78	18.93	4.00	.97	.78	5.90	3.05	1.00	.78	2.90	2.96
10	.66	.92	22.22	5.32	1.04	.92	3.16	3.36	.12	.92	0.22	27.37
11	1.53	1.09	17.33	2.72	.90	1.09	4.61	4.63	.86	1.09	2.75	4.84
12	3.19	1.29	11.74	1.54	.98	1.29	3.62	5.02	1.30	1.29	5.03	3.80
13	1.08	1.53	20.43	5.44	2.26	1.53	4.15	2.58	2.60	1.53	4.98	2.25
14	1.99	1.84	23.29	3.54	1.20	1.84	4.44	5.86	1.77	1.84	7.46	3.97
15	2.63	2.22	6.44	3.22	1.75	2.22	8.30	4.86	2.01	2.22	2.53	4.22
16	2.59	1.73	21.54	2.56	1.33	1.73	0.56	4.98	4.00	1.73	1.93	1.65
17	.58	.05	16.36	.35	.15	.05	2.98	1.32	.09	.05	5.97	2.31

TABLE 4.1 (cont.)

Period 10 : Oct. 7 - Nov. 2, 1963

J	First Harmonic				Second Harmonic				Third Harmonic			
	A	D_A	M	D_C	A	D_A	M	D_C	A	D_A	M	D_C
	(%)	(%)	(hr)	(hr)	(%)	(%)	(hr)	(hr)	(%)	(%)	(hr)	(hr)
1	.75	.07	15.83	.34	.36	.07	2.04	.71	.05	.07	3.65	5.49
2	.39	.13	15.01	1.23	.27	.13	0.03	1.77	.16	.13	3.17	2.93
3	.66	.19	15.75	1.09	.15	.19	0.04	4.80	.34	.19	2.81	2.09
4	.51	.26	12.50	1.94	.47	.26	2.91	2.09	.17	.26	1.79	5.86
5	.53	.34	15.15	2.43	.33	.34	4.01	3.94	.23	.34	6.70	5.71
6	.29	.43	22.93	5.69	.69	.43	11.54	2.40	.36	.43	0.35	4.63
7	.88	.53	15.51	2.32	.64	.53	9.77	3.18	.19	.53	5.32	9.24
8	.57	.64	14.56	4.33	.43	.64	10.05	5.71	.33	.64	7.17	7.57
9	1.29	.77	9.84	2.28	1.27	.77	10.80	2.32	.52	.77	2.78	5.61
10	.91	.91	20.00	3.85	1.32	.91	10.96	2.64	.84	.91	0.40	4.17
11	1.73	1.08	12.53	2.39	1.06	1.08	11.47	3.90	.85	1.08	1.30	4.88
12	1.75	1.29	18.46	2.81	2.26	1.29	5.90	2.18	1.26	1.29	7.43	3.90
13	1.90	1.54	15.44	3.10	2.44	1.54	1.51	2.41	.44	1.54	4.72	13.41
14	1.07	1.85	4.33	6.62	3.60	1.85	2.44	1.96	3.58	1.85	7.56	1.97
15	.64	2.22	0.59	13.26	3.13	2.22	3.14	2.71	2.46	2.22	6.83	3.44
16	3.94	1.74	16.22	1.69	2.71	1.74	0.31	2.45	2.36	1.74	1.40	2.82
17	.65	.05	15.63	.31	.29	.05	1.62	.69	.07	.05	2.99	2.86

Period 11 : Nov. 3 - Nov. 29, 1963

J	First Harmonic				Second Harmonic				Third Harmonic			
	A	D_A	M	D_C	A	D_A	M	D_C	A	D_A	M	D_C
	(%)	(%)	(hr)	(hr)	(%)	(%)	(hr)	(hr)	(%)	(%)	(hr)	(hr)
1	.25	.07	18.46	1.07	.25	.07	2.15	1.04	.05	.07	5.05	5.68
2	.15	.13	17.05	3.38	.16	.13	3.40	3.10	.15	.13	7.64	3.27
3	.20	.19	21.69	3.62	.37	.19	0.50	1.99	.20	.19	1.45	3.63
4	.21	.26	16.01	4.79	.20	.26	8.22	5.00	.08	.26	3.87	12.81
5	.78	.35	20.57	1.70	.27	.35	5.90	4.95	.36	.35	3.19	2.18
6	.34	.44	23.18	4.99	.38	.44	7.04	4.39	.90	.44	5.78	1.85
7	.58	.54	11.93	3.55	.38	.54	0.48	5.46	.04	.54	5.59	57.45
8	.51	.66	12.52	4.98	.93	.66	3.43	2.70	.73	.66	6.85	3.44
9	1.34	.79	4.33	2.23	.42	.79	8.72	7.22	1.04	.79	5.11	2.90
10	1.12	.92	2.42	3.16	1.47	.92	3.69	2.40	.76	.92	4.55	4.62
11	1.43	1.09	15.22	2.92	1.39	1.09	1.03	2.98	.81	1.09	4.51	5.11
12	1.13	1.30	9.58	4.37	1.25	1.30	4.20	3.97	1.43	1.30	7.91	3.46
13	.90	1.54	13.39	6.56	.81	1.54	11.26	7.31	.50	1.54	7.16	11.69
14	2.81	1.82	9.14	2.48	1.33	1.82	7.58	5.23	1.19	1.82	4.05	5.86
15	.80	2.17	14.19	10.32	4.73	2.17	5.16	1.75	2.69	2.17	3.75	3.08
16	.30	1.67	1.89	21.01	2.40	1.67	4.98	2.66	2.40	1.67	3.44	2.65
17	.21	.05	18.54	1.00	.20	.05	2.28	1.04	.03	.05	5.73	6.22

TABLE 4.1 (cont.)

Period 12 : Feb. 6 - Nov. 29, 1963

J	First Harmonic				Second Harmonic				Third Harmonic			
	A	D_A	M	D_C	A	D_A	M	D_C	A	D_A	M	D_C
	(%)	(%)	(hr)	(hr)	(%)	(%)	(hr)	(hr)	(%)	(%)	(hr)	(hr)
1	.85	.02	16.45	.08	.27	.02	2.24	.26	.05	.02	5.56	1.30
2	.50	.03	16.39	.26	.13	.03	2.48	1.04	.06	.03	0.23	2.18
3	.46	.05	16.97	.42	.07	.05	1.23	2.72	.09	.05	2.09	2.20
4	.34	.07	16.86	.79	.07	.07	4.04	3.77	.11	.07	4.99	2.47
5	.56	.09	17.49	.64	.13	.09	5.98	2.67	.12	.09	7.88	2.92
6	.35	.12	19.46	1.29	.21	.12	6.26	2.11	.12	.12	4.90	3.81
7	.40	.14	17.30	1.40	.05	.14	11.18	11.64	.15	.14	6.14	3.79
8	.43	.17	20.31	1.53	.24	.17	5.69	2.81	.09	.17	1.86	7.61
9	.34	.21	18.53	2.31	.40	.21	7.53	2.00	.13	.21	4.07	5.87
10	.57	.24	19.75	1.63	.23	.24	5.26	4.10	.15	.24	3.73	6.33
11	.40	.29	15.95	2.75	.34	.29	10.47	3.25	.58	.29	2.16	1.88
12	.30	.34	16.29	4.39	.34	.34	5.23	3.82	.66	.34	7.13	1.98
13	.58	.41	17.32	2.70	.97	.41	2.10	1.61	.33	.41	5.57	4.76
14	.81	.49	22.86	2.29	.53	.49	1.23	3.55	.54	.49	7.88	3.48
15	.61	.58	20.60	3.64	.60	.58	6.65	3.72	.68	.58	0.24	3.30
16	.72	.44	11.26	2.31	.61	.44	2.29	2.75	.15	.44	6.28	11.17
17	.70	.01	16.56	.08	.20	.01	2.35	.28	.03	.01	5.88	1.96

With the results of Table 4.1, three problems can be studied: (a) the importance of the second and the third harmonics in the composition of the daily variation, (b) the energy dependence of solar diurnal amplitudes and times of maximum intensity for cosmic ray photons near sea level, and (c) time behavior of the diurnal variation during the eleven consecutive solar rotation periods (i.e. time variation of the diurnal amplitude and time of maximum). In any discussion of the above three problems, care must be taken in using the computed results. On examination of Fig. 4.1, Fig. 4.2 and Table 4.1, one can easily see that not all the values are statistically meaningful on account of large standard errors. Whenever possible, values obtained during period 12 or for the photons of energy range 17 should be used as the basis for

reliable conclusions. Whenever applicable, neutron data during the same period of time as recorded at Deep River station (geomagnetic coordinates: 46° 6' N, 77° 30' W) are utilized for comparison with our photon results.

D. Significance of the Second and Third Harmonics

For a daily variation with twenty four experimental points, a finite Fourier analysis can yield mathematical results for the amplitude and the time of maximum intensity up to the twelfth harmonic. However, in the previous reports on the harmonic analysis of the daily variation, nothing has been mentioned about harmonics higher than the second. The amplitude of the second harmonic is usually very small, and for some occasions can be entirely neglected. In our present work, the third harmonic is also included. To estimate the significance of the second and the third harmonics, amplitude ratios of the second to the first (designated as R_2) and of the third to the first (designated as R_3) are calculated from Table 4.1 for every energy range and for each of the twelve periods. Respectively, R_2 and R_3 indicate the relative contributions of the second and the third harmonics to the daily variation of cosmic rays as compared with the first harmonic. They are illustrated in Fig. 4.2 for six time periods (in rows) and for seventeen energy ranges (in columns). For a particular period and energy range, the solid line represents the first harmonic and its height is taken as unity. The dashed line and the dotted line are scaled to the values of R_2 and R_3. From Fig. 4.2, the following can be stated:

1. In all six periods, range 17 gives coherent features for the contributions of the second and the third harmonics.

2. In period 12, tolerable (i.e. reasonable) ratios (R_2 and R_3) appear only in energy ranges 1 to 8.

3. In periods of short time duration (i.e. periods 1, 3, 5, 7, 9), with the exception of energy ranges 1, 2, 17, the various energy ranges do not have a dominant first harmonic throughout.

4. The emergence of either the second or the third harmonic, or both, as the main or important contributor does not necessarily mean that the corresponding daily variation is essentially composed of the second and the third harmonics. On the contrary, we conclude that they are not useful for our present purpose because of the poor statistics which are reflected by the wide scattering of points with large standard deviations.

In order to draw some conclusions, we must confine ourselves to photons of energy ranges 2 and 17. A seasonal variation of their R_2 and R_3, together with those for neutrons (Deep River) is shown in Fig. 4.3. Their standard deviations are also estimated. Again, there is not much we can say definitely about photons of energy range 2 as the large standard deviations make conclusions impossible. However, it does show the existence of the second harmonic for neutrons and for photons of energy range 17. The second harmonic of the neutrons has an amplitude varying from 10% to as high as 45% of the first. In the case of the integral photon intensity($J \geq 17$), R_2 may have values as high as 0.5. Therefore, the second harmonic seems to be more important in the daily variation for certain periods of time.

As for the third harmonic, the neutron data demonstrates that it is not as negligible as one might have thought. Only on one occasion (March 1963), R_3 is close to zero. It goes up as high as 0.3 in September 1963; however, this unusually high value may be the consequence of a Forbush decrease which occurred in this month and disturbed greatly the character of the mean daily variation. Conservatively speaking, R_3 can reach a value at least as high as 0.1, that is to say, the amplitude of

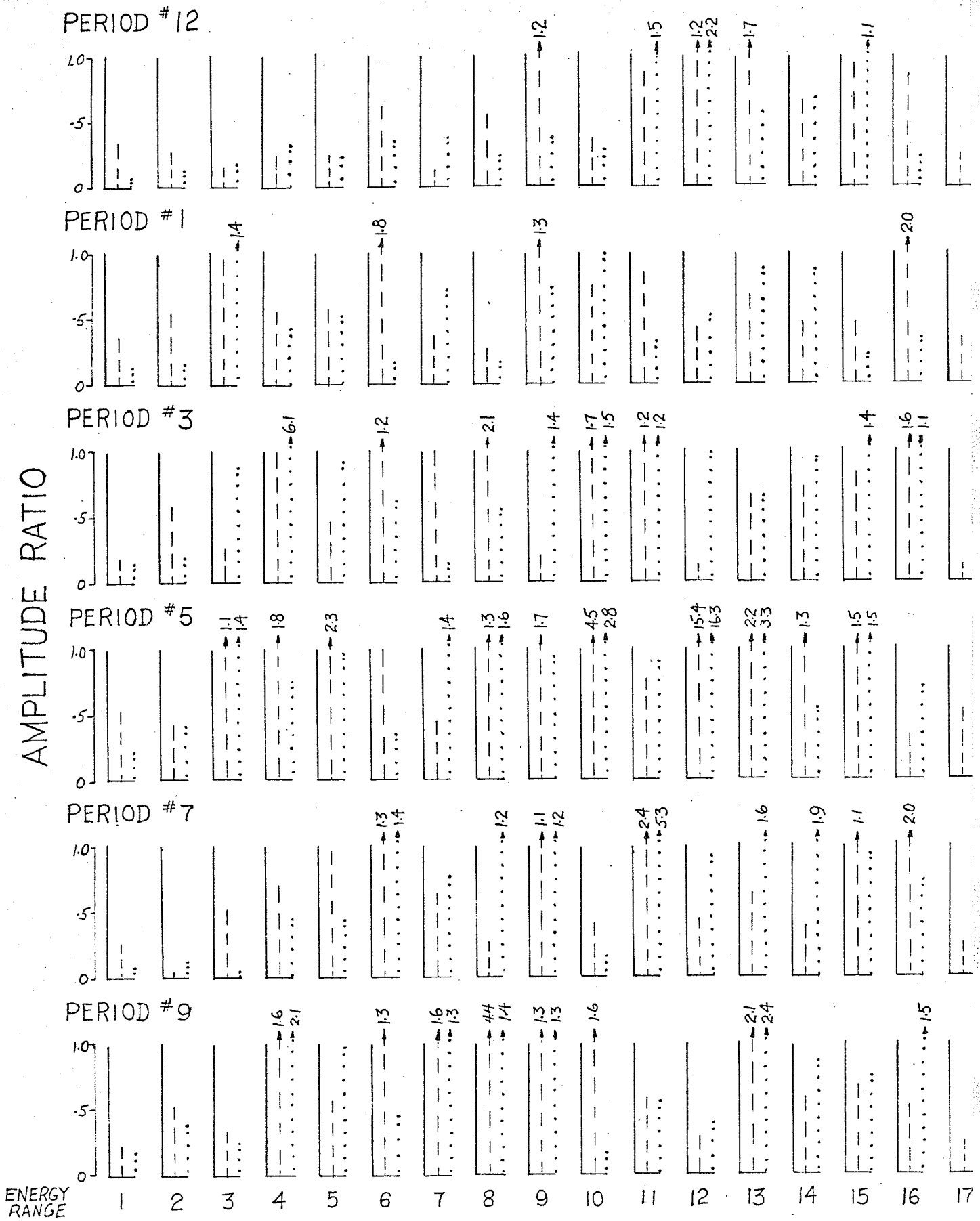

FIG. 4.2 AMPLITUDE RATIOS OF 2ND AND OF 3RD TO 1ST HARMONICS FOR SIX PERIODS

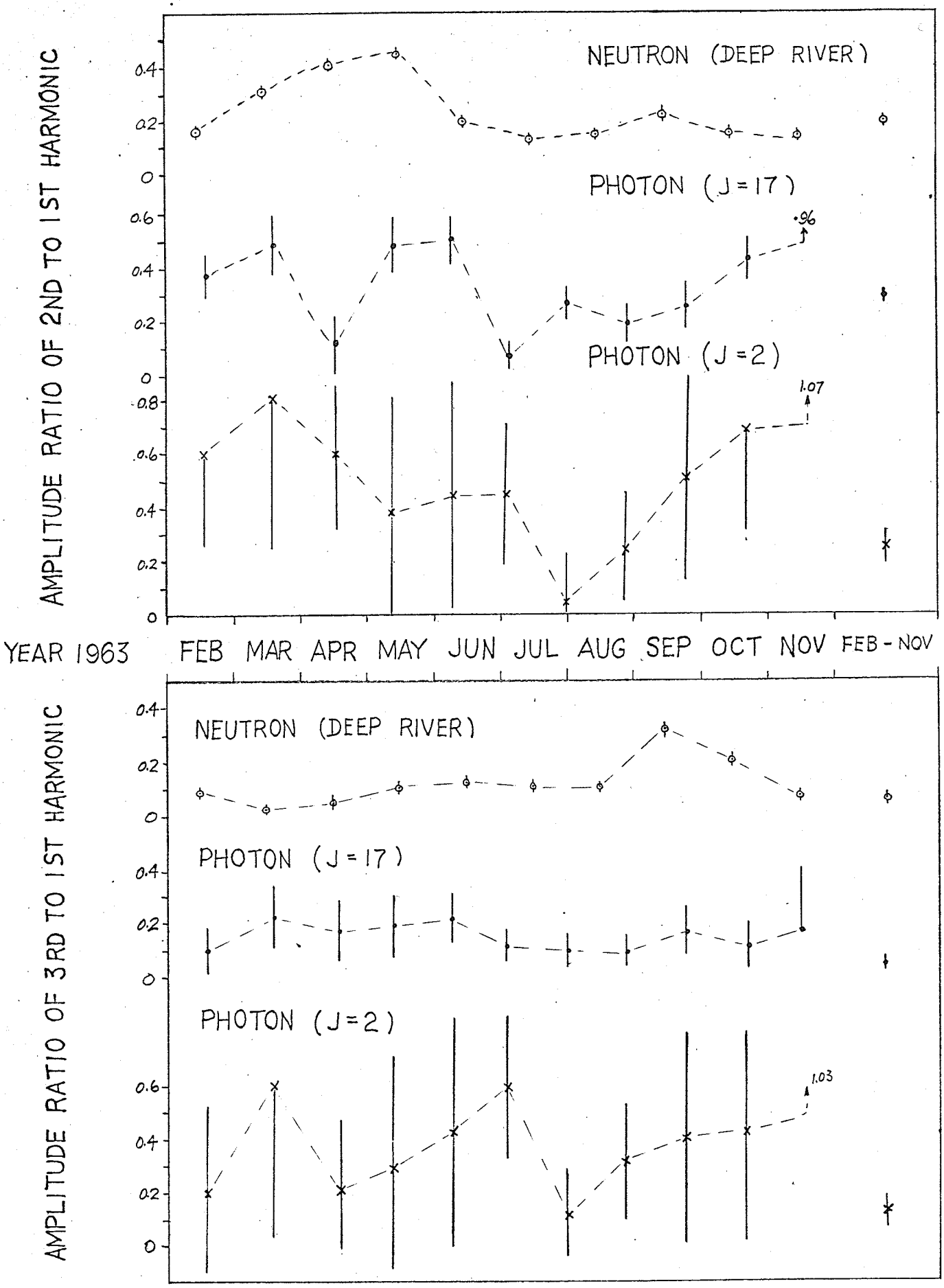

FIG. 4.3 SEASONAL VARIATION OF AMPLITUDE RATIOS

the third harmonic can be 10% that of the first. Again, the integral photon intensity yields a similar conclusion. Its R_3 can reach a value as high as 0.2.

Taking ten months (February - November 1963) as a single period, the values of R_2 and R_3 are tabulated in Table 4.2.

TABLE 4.2

	Amplitude Ratio		
	Photon J=17	Photon J=2	Neutron
R_2	0.28 ± 0.02	0.25 ± 0.06	0.20 ± 0.01
R_3	0.04 ± 0.02	0.12 ± 0.06	0.06 ± 0.01

Results R_2 and R_3 for photons agree fairly well with neutrons within statistical errors. This again shows the appreciable contributions of both the second and the third harmonics in the average solar daily variation of cosmic radiation over a long period of ten months.

The physical meaning of the second harmonic is quite obscure and is not to be found in the literature. The third harmonic is not even mentioned. At present, it is impossible to understand their real characters since the nature of the first is not yet completely understood. Analytically, any impure sinusoidal curve can be resolved into a series of harmonics. The contribution of the higher harmonics will be more significant if the curve deviates farther away from the pure fundamental harmonic. It is possible that the higher harmonics are the result of some fluctuation in the source of the first harmonic. Or, they may in part be caused by other processes operating in interplanetary space or inside the terrestrial atmosphere. For our photon data, we conclude that the significance of the higher harmonics is greatly exaggerated in a

period of twenty seven days and in the high energy ranges by the large statistical errors as a result of low counting rates. For the longer period, however, our results are in qualitative agreement with the corresponding neutron monitor results.

E. Energy Dependence of Diurnal Amplitude and Time of Maximum Intensity

Results of the harmonic analysis on the photon data collected during a period of ten months (i.e. period 12) have been utilized to study the average characteristics of the energy dependence of the solar diurnal amplitudes and phases. In Fig. 4.4, amplitudes and times of maximum intensity of the first and the second harmonics are plotted against photon energies up to 183 MeV.

Fig. 4.4 enables the following remarks to be made about the energy dependence of the first harmonic component of the solar diurnal variation of cosmic ray photons near sea level.

1. Between energy ranges 1 to 5, two definite tendencies can be clearly observed: namely, the time of maximum intensity advances towards later hours with increasing photon energy and the amplitude decreases with energy (except for energy range 5).

2. In general, from energy range 6 to 16, no definite trend for the energy relationship can be established on account of the poor statistics. Within statistical deviations, a straight line, either horizontal or inclined, can be passed through all experimental points for the diurnal amplitudes and for the time of maximum.

Before attempting to explain the above two facts, it is necessary to know the relationship between the secondary photons and the primary cosmic rays incident on the top of the terrestrial atmosphere. However, the quantitative aspects of the coupling processes between the

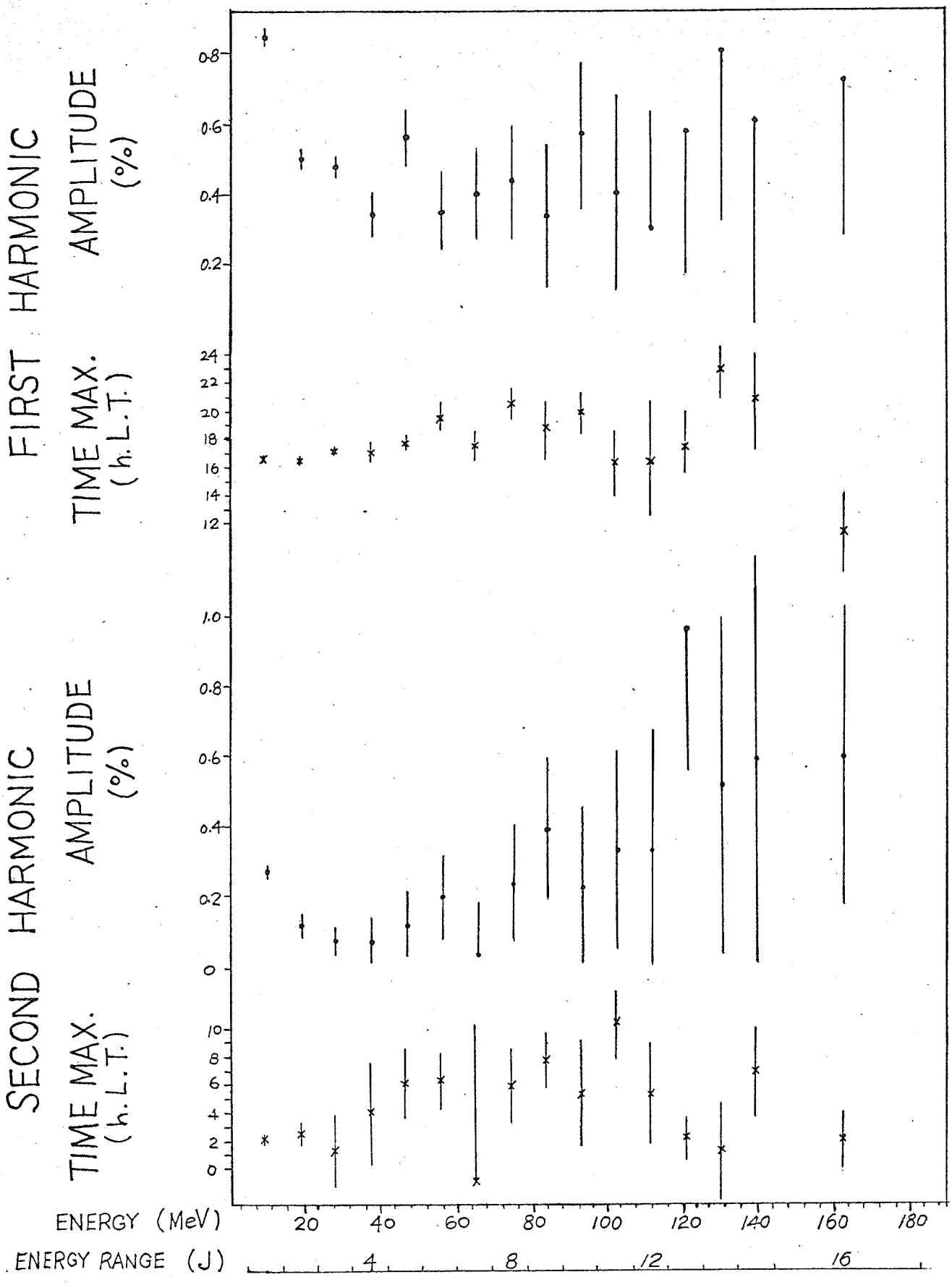

FIG. 4.4 ENERGY DEPENDENCE OF 1ST AND 2ND HARMONIC AMPLITUDE AND PHASE

(FOR PERIOD #12, FEB. 6 - NOV. 29, 1963)

sea level photons and the primaries are not at all well known and a mathematical formulation of this relationship between their differential energy spectra, if possible, would be an enormous task. In an attempt to explain qualitatively the experimental fact as stated in (1) above, a simple concept is employed here. Even though there is surely no one-to-one correspondence between the sea level photon energy and the responsible primary energy, we assume (a) that photons in a certain energy range of the experimental spectrum are produced by primaries of some "effective" energy, and (b) that observed photons in a higher energy range correspond to primary cosmic rays with a higher "effective" energy. Of course, this concept of a simple relationship between the primaries and the secondary photons is very crude but its validity can be tested by seeing if it can lead to a plausible qualitative explanation of the observed results.

According to the effect of the earth's magnetic field on the path of a charged particle (Brunberg et al. 1953), the primary cosmic radiation observed vertically by a station at medium latitude comes from a certain asymptotic longitude to the east of the station. (In fact, the asymptotic direction of the charged particle is specified by asymptotic latitude as well; however, this can be neglected for the present study.) Such asymptotic longitude (relative to the station), in general, increases with diminishing primary energy. Fig. 4.5 shows the asymptotic longitude east of the Winnipeg station as a function of the momentum of the vertically incident particle (These calculations were supplied through the courtesy of Dr. M. Bercovitch at Chalk River).

As suggested both by Parker (1964) and Axford (1965), the origin of the observed diurnal variation is an azimuthal streaming of cosmic rays and consequently there is a continuous streaming of cosmic rays around the orbit of the earth in the direction of 1800 h L.T. as

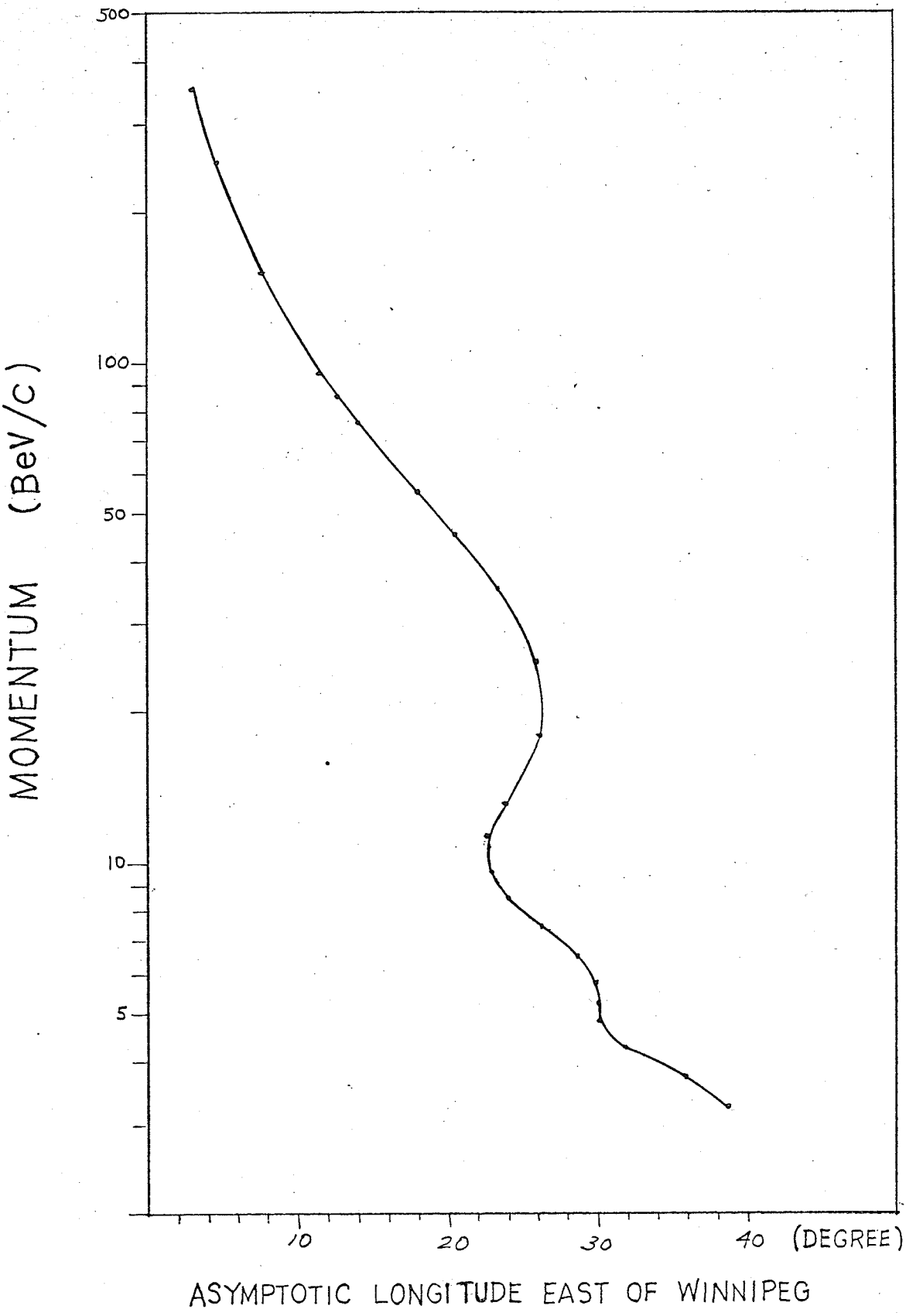

FIG. 4.5 ASYMPTOTIC DIRECTION OF APPROACH, WINNIPEG

observed at the earth. However, those cosmic rays which take part in the co-rotation with the sun are also subject to deflection in the geomagnetic field. As a result, we would expect the low energy primaries to be observed earlier than 1800 h L.T. and the times of maximum intensity for the higher energy primaries will converge to 1800 h L.T. as the limit. This is the general trend shown by the energy dependence of the time of maximum intensity for cosmic ray photons with energy below range 5 (Fig. 4.4).

Taking advantage of the results on the energy dependence of the time of maximum, we can estimate the "effective" energy of the primaries responsible for each photon energy range by using the energy dependence of the asymptotic longitude to the east of the station. Assuming that the solar diurnal anisotropy is a streaming towards the earth at 1800 h L.T., the difference between 1800 h and the observed time of maximum of the photon intensity will indicate the longitude to the east of station which in turn will give the "effective" energy of the corresponding primary particles using Fig. 4.5. Table 4.3 shows the values of the primary "effective" energy responsible for photon energy ranges from 1 to 5 and for range 17 as well.

TABLE 4.3

Photon Energy Ranges J	(MeV)	Time of Maximum of Photon Intensity (h L.T.)	Longitude East of Station (degree)	Effective Energy of Primary (BeV)
1	3.8- 13.2	16.45 ± 0.08	23.2 ± 1.2	$9 \,^{+30}_{-0.8}$
				$12 \,^{+27}_{-4}$
2	13.2- 22.6	16.39 ± 0.26	24.2 ± 3.9	$33 \,^{+12}_{-26}$
3	22.6- 32.1	16.97 ± 0.42	15.5 ± 6.3	$66 \,^{+8}_{-26}$
4	32.1- 41.5	16.86 ± 0.79	17.1 ± 11.8	$58 \,^{+168}_{-52}$
		(17.26 ± 0.79)	(11.0 ± 11.8)	$(102 \,^{+?}_{-66})$
5	41.5- 50.9	17.49 ± 0.64	7.7 ± 9.6	$148 \,^{+?}_{-91}$
17	3.8-183.0	16.56 ± 0.08	21.6 ± 1.2	$40 \,^{+2}_{-4}$

A few remarks are now made concerning the "effective" primary energies as listed in Table 4.3.

1. The probable errors of the times of maximum introduce a great uncertainty in the values of the "effective" primary energy. There is a large difference between the positive and the negative standard error for the "effective" energy owing to the characteristics of the curve as shown in Fig. 4.5.

2. In the range of 22.5° to 26.5° (see Fig. 4.5), there are multiple energy values corresponding to a single value of the asymptotic longitude east of station. Taking into account the reasonable order of the primary energy values with respect to the J values, we have "guessed" that photon energy range 2 should be related to a primary with "effective" energy of about 33 BeV while either 9 or 12 BeV is an equally suitable value for photon energy range 1.

3. As for photon energy range 4, the value for the time of maximum leads to an effective primary energy of 58 BeV which is a poor value in our sequence of the primary energy values as against photon energy. If we plot the values of the time of maximum against J values of 1, 2, 3 and 5, and interpolate a reasonable value at J = 4 (about 17.26 h), this then gives an "effective" energy of about 102 BeV. In view of the large error in our time of maximum for J = 4, we have adopted this value as the "effective" energy of the primary responsible for photon energy range 4.

4. The integral intensity of the photon component (J = 17) corresponds to a primary with "effective" energy around 40 BeV.

The "effective" primary energy values thus obtained are consistent with the upper and the lower limiting energies of the primaries participating in the solar diurnal variation as estimated by so many workers. In spite of its crudeness, this concept of a one-to-one correspondence

between the secondary photon energy range and an "effective" primary energy can provide a reasonable qualitative explanation for the energy dependence of the time of maximum for the photon component.

Further, the same concept can be employed to interpret the experimental fact that the diurnal amplitude decreases with increasing photon (or "effective" primary) energy. According to the method of coupling constants (see Appendix A), the diurnal amplitude of a secondary component depends on the integration of an integrand which is the product of the energy spectrum of the primary diurnal variation and the differential coupling coefficient between the primary and the secondary. The energy spectrum of the primary diurnal variation has been assumed to obey a power law and many workers have reported that the exponent is either negative or zero for the averaged diurnal variation over a long period of time. Therefore, the energy spectrum of the primary diurnal variation will either be a constant or decrease with increasing energy. If the differential coupling constant for the photon component varies with primary energy also in a decreasing mammer and if each of the photon energy range corresponds to approximately the same interval of primary energy, the diurnal amplitude of the photons will be diminished with photon energy. Unfortunately, the coupling constants between the primary and the secondary photon component have not yet been determined; therefore, there is no way to definitely justify this experimental fact. However, the differential coupling constants of the nucleonic and the ionizing components at medium latitudes do exhibit a decline with primary energy for primary energy greater than 9 BeV (Dorman 1957, Webber et al. 1959). If the photon coupling constants have similar characteristics, then the decrease in diurnal amplitude with photon energy will be satisfactorily explained. However, the abnormally high diurnal amplitude for photon

energy range 5 remains a puzzle if it is real and not just "statistical".

The nature of photons from energy range 6 to 16 can not be clearly established. The statistics for these energies are poor. However, some arguments can be brought forth against the existence of a prominent solar diurnal variation in this range.

1. Energy range 5 has been ascribed to primary cosmic rays with "effective" energy about 148 BeV. Bearing in mind that Jacklyn et al. (1965) have determined a mean upper limiting rigidity of about 100 BV for the solar diurnal variation, it can be concluded that there should be a negligible solar diurnal variation for photon energy ranges with J greater than or equal to 6 if our assumptions (a) and (b) are approximately valid.

2. Within the limits of standard errors, the times of maximum for J greater than or equal to 6 are later than 1800 h L.T. (Fig. 4.4). This contradicts the theory on the origin of the solar diurnal variation as suggested by Parker (1964) and Axford (1965).

3. Beyond photon energy range 5, there is no apparent decline of the diurnal amplitude with photon energy; on the contrary, it may rise. If assumptions (a) and (b) are approximately true, this is not consistent with the negative exponent of the differential spectrum of the primary diurnal variation and the highly probable decrease in the values of the differential coupling constants with primary energy for the photon component.

4. The 24 hour daily variations in these photon energy ranges do not seem to be "typically" diurnal in nature.

In spite of the above arguments, one cannot state that our assumptions (a) and (b) must hold for photon energy ranges beyond 5. It is probable that a considerable number of the photons in these energy ranges is contributed by primary cosmic rays within the energy limits of the solar diurnal variation if we take into account that

(a) photons detected near sea level of energy from 50 to 183 MeV can be generated by primaries with energies less than 100BeV through a great many processes and

(b) within standard deviations, the times of maximum intensity for photon energy ranges 7, 9, 11, 12, 13, 15 and 16 can be regarded as earlier than 1800 h L.T.

The second harmonic of the solar diurnal variation also shows an energy dependence of the amplitude and of the phase, strikingly similar to that of the first harmonic for photon energy ranges from 1 to 5 (see Fig. 4.4). Since very few theories have been proposed for the solar semi-diurnal variation, and since a detailed quantitative model for the origin of the solar diurnal variation does not yet exist, it is impossible at present to interpret our results for the second harmonic. However, the decrease of semi-diurnal amplitude and the advance of its time of maximum towards later hours with increasing photon energy seem to suggest that the semi-diurnal effect is also a result of some perturbation in the interplanetary electromagnetic conditions or through a variation of atmospheric conditions.

The energy dependence of the amplitude and the time of maximum for the third harmonic (with very large statistical errors) does not show any correlation with the solar diurnal variation. These results may be simply the byproduct of our Fourier analysis. At any rate, the third harmonic can hardly be discussed meaningfully until we have better experimental data and until we can understand the nature of the first and the second harmonics.

F. Comparison of Solar Diurnal Results of Photon and Nucleonic Components

At present, the neutron monitor data is regarded as the most reliable source of information in connection with the time variation study

of the primary cosmic radiation. A comparison of the results of the mean diurnal effects as observed by the photon spectrometer and the neutron monitor at Deep River will shed some light on the compatibility of the concept of the "effective" primary energy in the interpretation of the photon results. As the neutron detects the integral effect of the primary cosmic rays, the integral intensity of the photon component (J = 17) will be used for comparison. The mean diurnal amplitude and the time of maximum of both components as obtained from data covering the whole period from February to November 1963 are tabulated in Table 4.4.

TABLE 4.4

Cosmic Ray Component	Station	Coordinates		Diurnal Variation	
		Geomagnetic	Geographic	Amp. (%)	T.M. (h L.T.)
photon	Winnipeg	59.8° N 37.2° W	49.9° N 97.2° W	.71±.015	16.56±.08
neutron	Deep River	57.4° N 9.8° W	46.1° N 78.0° W	.29±.002	14.89±.03

Strictly speaking, the phase and the amplitude of the solar diurnal variation observed by the same cosmic ray monitor at various stations bear no simple relationship with their latitude and longitude (geographic or geomagnetic) on account of the difference in the asymptotic cones of acceptance at various stations. However, for stations lying in a narrow region, there still exists some trend relating the geomagnetic longitudes to the times of maximum intensity. Table 4.5 lists the theoretical and experimental values of the solar diurnal amplitude (designated as A) and the time of maximum intensity (designated as M) for neutron monitors at four stations as reported by Rao et al. (1963). The theoretical diurnal amplitudes are relative in nature.

TABLE 4.5

Station	Coordinates: Geomagnetic	Coordinates: Geographic	Theoretical: A (%)	Theoretical: M(L.T.) h m	Experimental: A (%)	Experimental: M(L.T.) h m
Ottawa	56.7° N, 7.4° W	45° N, 76° W	82.9	15 21	.29	14 48
Deep River	57.4° N, 9.8° W	46° N, 78° W	82.9	15 22	.31	15 00
Churchill	68.7° N, 35.6° W	59° N, 94° W	74.8	16 23	.33	15 48
Resolute	83.0° N, 68.6° W	75° N, 96° W	35.1	17 13	.16	17 18

From Table 4.5, it can be seen that the geomagnetic and geographic longitudes of the four stations are of the same order. The time of maximum intensity moves towards later hours with increasing geomagnetic longitude for both theoretical and experimental values. (While the theoretical values of the diurnal amplitudes also decrease with increasing geomagnetic longitude, the experimental results do not confirm this trend.) Hence, a neutron monitor at Winnipeg (geomagnetic longitude 37.2° W) should observe the maximum intensity at a time later than 16 h 23 m theoretically and 15 h 48 m experimentally. Indeed, the time of maximum of the integral photon intensity occurs at 16 h 33 m; this fits into the trend of the values of the time of maximum as a function of the geomagnetic longitude. However, 16 h 33 m seems to be much later than one would expect, taking into account that Winnipeg is located to the west of Churchill by only 1 to 3 degree in longitude (geomagnetic and geographic) but the difference in the time of maximum at these two places amounts to 10 minutes theoretically and 45 minutes experimentally. This implies (in agreement with our previous results on the "effective" primary energies) that the photon component corresponds to a higher energy region of the primary cosmic rays as compared with the neutron component.

The diurnal amplitude of the photon component is greater than that of the neutron by a factor of 2.4 as seen in Table 4.4. Such a large

difference in amplitude values cannot be explained by geomagnetic effects alone. Most probably, as already implied, the photon and the neutron monitors have different responses to the primaries. It is well known that the neutron monitor is highly sensitive to low energy primaries on account of its large differential coupling constants for primary energies as low as 2 BeV (Lockwood et al. 1966). At Deep River, the vertical threshold rigidity is about 1 BV; hence, most of the counts recorded by the neutron monitor are essentially contributed by low rigidity primaries (the primary spectrum decreases with a power law of the form E^{-r}). However, there is a lower limiting value for the primary energy in the solar diurnal variation. Firor et al. (1954), in their latitude study of solar diurnal variation of the nucleonic component, have found a slight change in the diurnal amplitude from equator to medium latitude and concluded a lower limiting energy value as being around 10 BeV. From the determination of the primary variation spectrum responsible for the solar diurnal variation, many workers (Dorman 1957, Quenby et al. 1960, Kuzmin 1960, Kuzmin et al. 1963) have obtained a lower bound of 7 to 15 BeV. Therefore, a neutron monitor at Deep River actually records secondaries due to a large number of low energy primaries which do not take part in the solar diurnal variation. As a result, its percentage diurnal amplitude will be diminished. This explanation is further strengthened by the evidence (Kane et al. 1960) that a decrease in diurnal amplitude from 0.35% to 0.15% in transition from medium latitude to high latitude has been observed from IGY data of nucleonic component. From Table 4.3, the integral photon intensity (J = 17) responds to the primaries with "effective" energy about 40 BeV. Its lower limiting primary energy can be roughly estimated from photon energy range 1 which corresponds to an "effective" primary energy of about 9 to 12 BeV. Considering the rapid decline in primary spectrum with increasing energy, the integral photon

intensity as observed may not include events due to primary cosmic rays with energy below about 7 BeV. Consequently, the contribution due to low energy primaries is very small in the integral photon intensity and hence, its diurnal amplitude will appear to be much greater than that of the Deep River nucleonic component.

G. Seasonal Variation of Solar Diurnal Amplitude and Phase

The seasonal variation of the solar diurnal effects as observed for the photon component has been investigated for the purpose of examining (a) the variation of the diurnal amplitude and time of maximum intensity for different photon energy ranges, (b) the variation of the diurnal vector of the integral photon component ($J = 17$) during the eleven consecutive solar rotation cycles, and (c) the relationship between the diurnal amplitude and phase of the integral photon component and solar and geomagnetic activities. The neutron component observed at Deep River is utilized as a reference whenever possible.

Since the existence of the solar diurnal variation in cosmic ray photons near sea level with energy beyond range 5 is obscure, they are neglected entirely in the present seasonal variation study. For photons of energy ranges 1 to 5, the seasonal variations of their diurnal amplitudes and times of maximum intensity are plotted respectively in Fig. 4.6 and Fig. 4.7. As presently believed, the solar diurnal variation arises from a cosmic ray anisotropy originating in interplanetary space due to the interplanetary magnetic field, the solar plasma and the rotation of the sun. The diurnal vectors of the eleven consecutive solar rotation periods are presented in a harmonic dial as shown in Fig. 4.8 for the integral photon component. Correlation between cosmic ray solar diurnal effects and various solar solar and geomagnetic indices (These data were obtained from the

Solar Geophysical Data complied monthly by U. S. Department of Commerce etc., Boulder, Colorado, U. S. A.) is illustrated in Fig. 4.9. Results are stated as follows:

1. Among the five photon energy ranges, the seasonal variation patterns of their diurnal amplitude and phase are different. For energy range number higher than 3, the standard deviations are so large that no definite conclusions can be reached(Fig. 4.6 and Fig. 4.7).

2. The diurnal vector of the integral photon component varies considerably in magnitude and direction within the eleven solar rotation cycles. Its pattern of variation is quite different from that of the nucleonic component (Fig. 4.8).

3. Neglecting the month of November, the diurnal amplitude of the integral photon component fluctuates with time rather like that of the neutron component. The first minimum and maximum of the photon component seem to lead those of the neutron by about one month (Fig. 4.9).

4. Between March and October, the photon amplitude is negatively correlated to R_A (American relative sunspot number). The maximum of the former occurs with the minimum of the latter in July. However, the neutron data generally shows a better correlation with R_A; the two minima of the neutron amplitude coincide with the two maxima of R_A (Fig. 4.9).

5. To some extent, the photon amplitude is rather weakly correlated to the C index (preliminary international character figure of geomagnetic activity). (see Fig. 4.9)

6. The time of maximum of the photon component remains fairly constant between 16 and 17 h L.T. except for three periods out of eleven. Its seasonal variation pattern is not obviously related to any other variations. On the other hand, the time of maximum of the neutron component shows relatively larger fluctuations (Fig. 4.9).

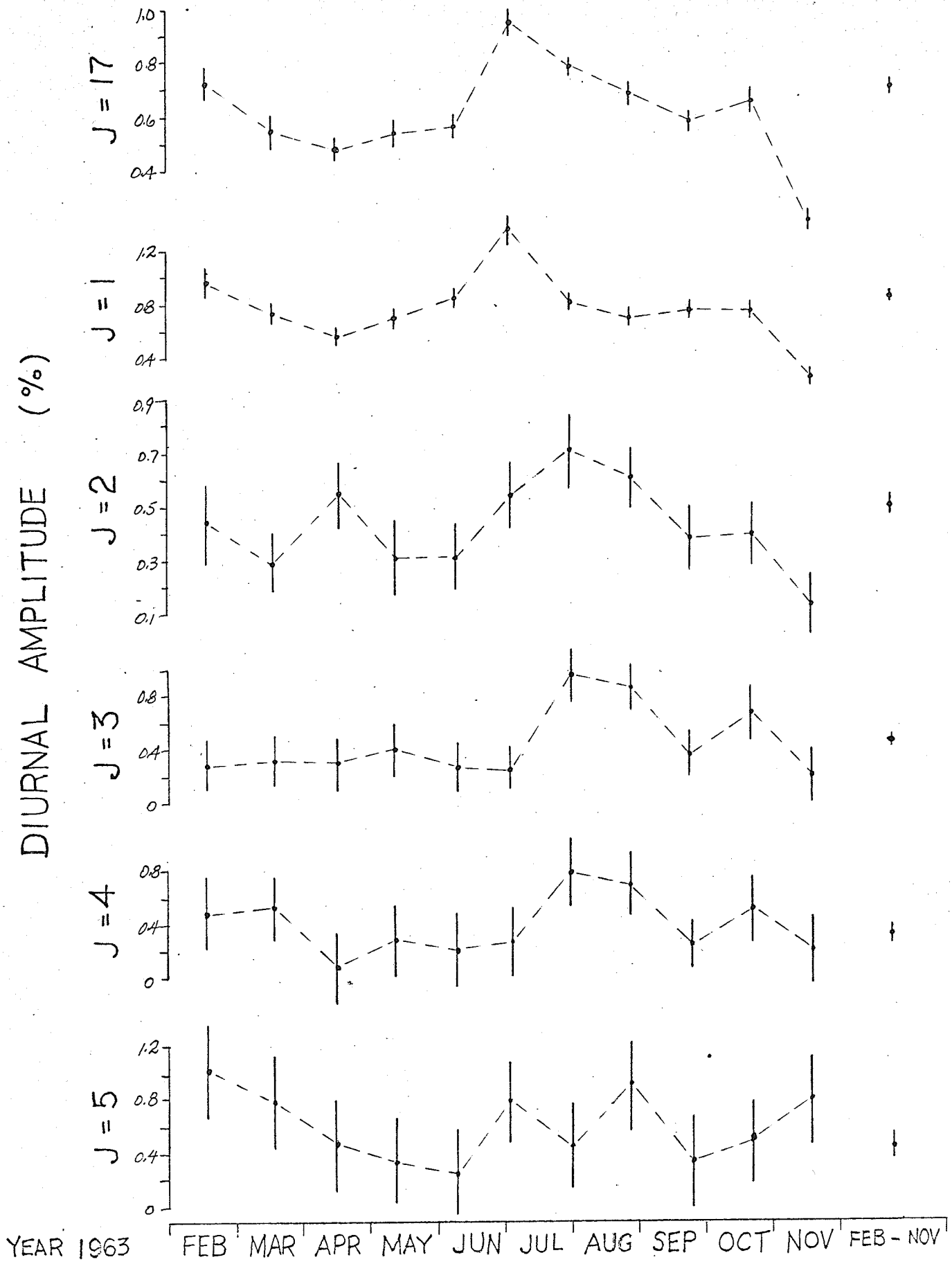

FIG. 4.6 SEASONAL VARIATIONS OF DIURNAL AMPLITUDE OF PHOTON COMPONENT FOR 6 ENERGY RANGES

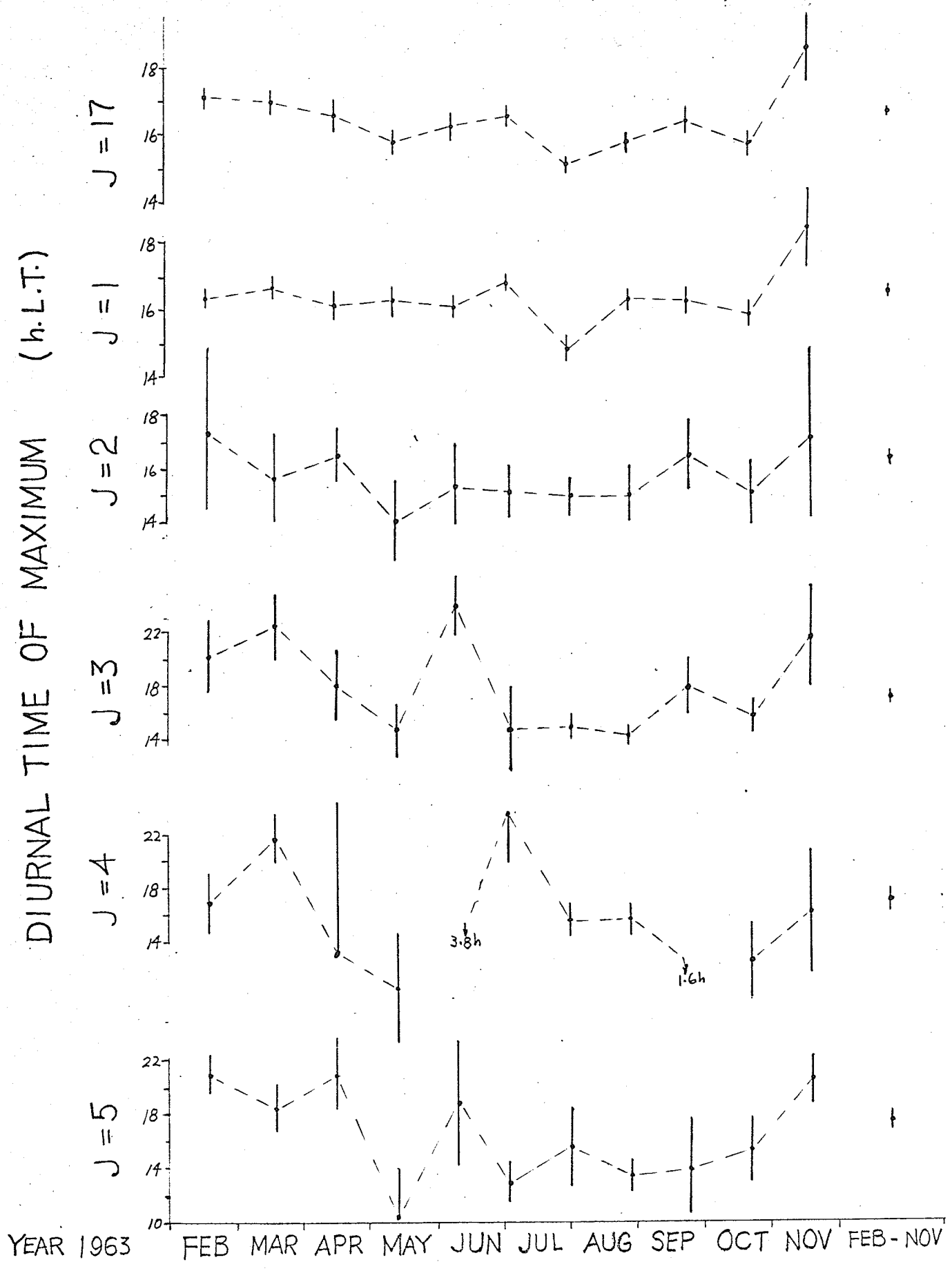

FIG. 4.7 SEASONAL VARIATIONS OF DIURNAL TIME OF MAXIMUM FOR 6 PHOTON ENERGY RANGES

PHOTON (J = 17)

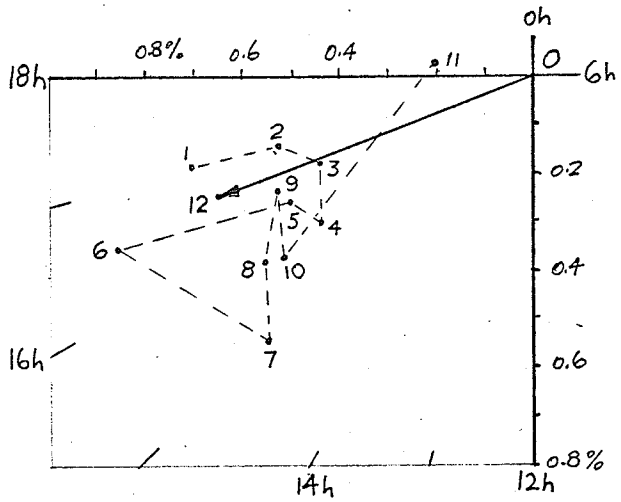

NEUTRON (DEEP RIVER)

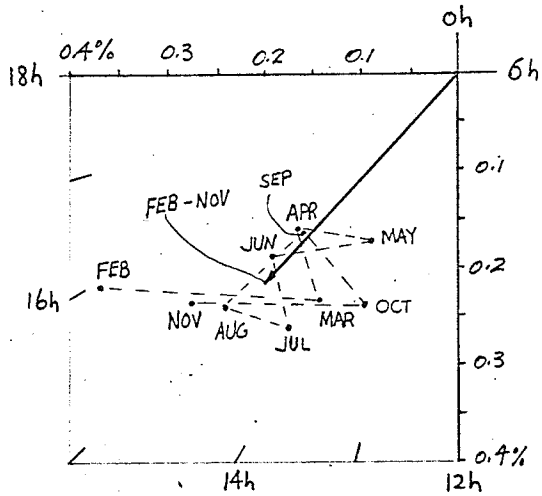

FIG. 4.8 HARMONIC DIALS OF SEASONAL DIURNAL VECTORS OF PHOTON AND NEUTRON (FOR YEAR 1963)

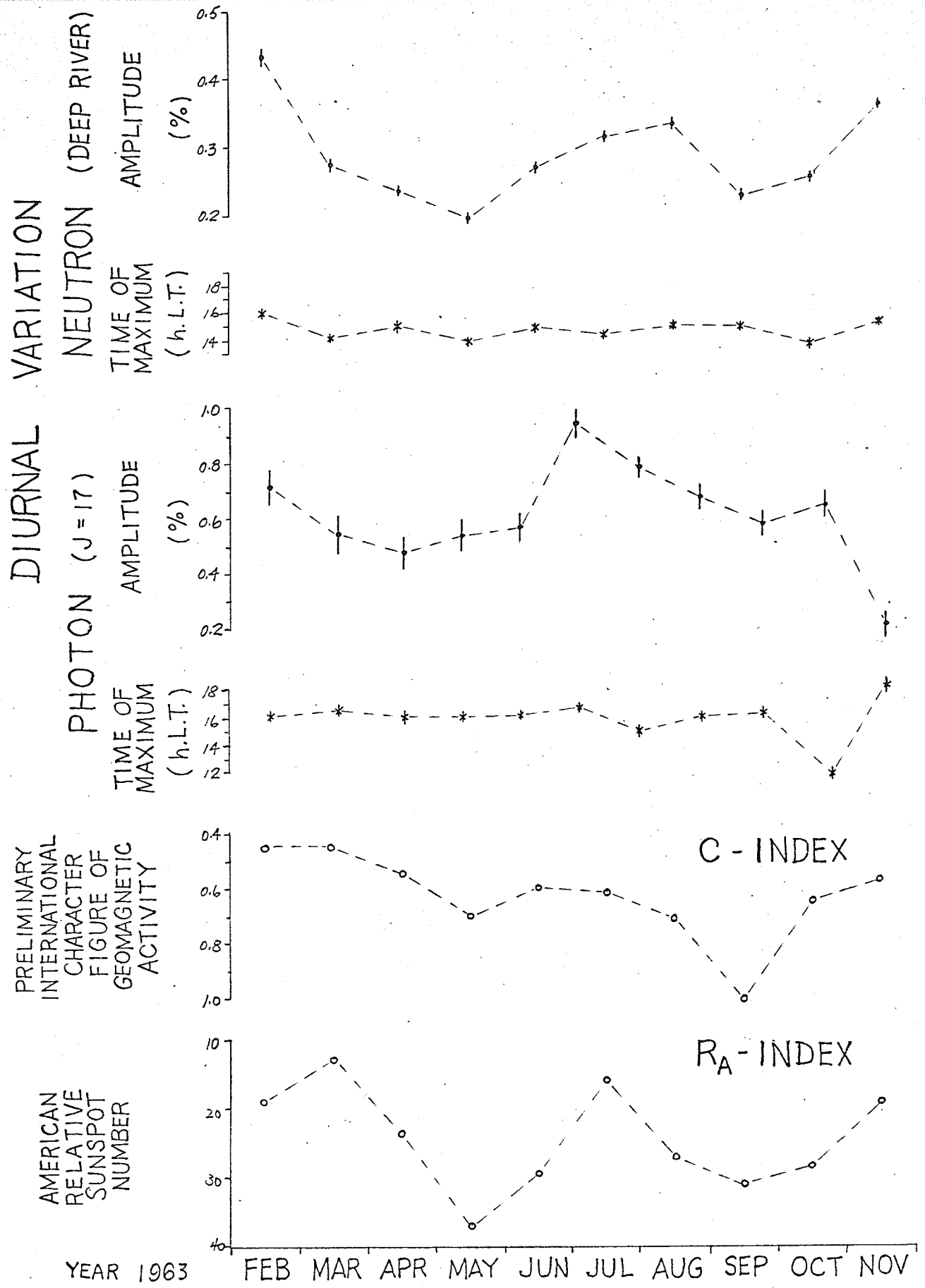

FIG. 4.9 CORRELATION AMONG COSMIC RAY DIURNAL EFFECTS AND SOLAR AND GEOMAGNATIC ACTIVITIES

During the period from February to November 1963, the considerable seasonal variability in the diurnal amplitude and phase (Fig. 4.6 and Fig. 4.7) simply suggests that the source of the diurnal variation is time varying. Conventionally, the energy spectrum of the primary diurnal variation is assumed to obey a power law with a constant exponent through all primary energies within upper and lower bounds. Owing to the absence of any common seasonal variation patterns for photons with different energy ranges, this exponent does not seem to be constant for all primary energies concerned, and its value varies with time. Also, the direction of the diurnal anisotropy (as implied by the time of maximum) changes with time. This is consistent with the results of the day-to-day study of the solar diurnal variation of cosmic rays as reviewed in section A of this chapter.

The diurnal vector of the integral photon component as shown in the harmonic dial (Fig. 4.8) does not show any orderly variation from one solar rotation cycle to another. However, the diurnal amplitude of the integral photon component ($J = 17$) does show some systematic variation as illustrated in Fig. 4.6.

The correlation between the American relative sunspot number R_A and the intensity of the cosmic ray components shows a strong influence of solar activity on the primary cosmic radiation. The degree of correlation as shown by the neutron component and photons of various energy ranges demonstrates that the primary cosmic rays of lower energy are more sensitive to the variation of the sunspot number. Correlation also exists between cosmic ray intensity and the geomagnetic disturbance as measured by the C index which is in phase with the American relative sunspot number.

H. Summary

In this chapter, a study on the solar diurnal variation has been conducted for various photon energy ranges. A solar diurnal variation for photon energies above 50 MeV is not unambiguously established because of very low counting rates. Graphically, the wave forms for these daily variations do not clearly show periodicity of 24 hours. Analytically, the concept of the "effective" primary energy suggests that these photons may correspond to the high energy primaries beyond the influence of the solar diurnal mechanism.

The existence of the higher harmonics has been investigated. The integral photon component shows a large second harmonic, the amplitude of which amounts to 28% that of the first. Even the third harmonic reaches a value as high as 4%. This result agrees with similar results for the neutron data collected during the same period of time. As yet, we do not know much about the nature of these higher harmonics.

Using ten months' data, the energy dependence of the diurnal amplitude and of the phase have been established for the sea level cosmic ray photons. These energy relationships are statistical in nature as they have been determined by a long-term observation. The diurnal amplitude decreases with increasing photon energy and the time of maximum intensity advances towards later hours with photon energy. The latter has been explained qualitatively in terms of a one-to-one correspondence between a photon energy range and an "effective" primary energy, the effect of the geomagnetic field and the current theories on the direction of the solar diurnal anisotropy. However, a similar interpretation of the amplitude results is much less certain because of a lack of knowledge on coupling constants for the secondary cosmic ray photons. With the above concepts, we conclude that a study of the integral photon component gives

information about primaries of higher energy than a corresponding study of the nucleonic component (i.e. neutron monitors).

The seasonal variation of the diurnal effect of the cosmic ray photons implies that the diurnal source is time varying. If the energy spectrum of the primary diurnal variation can be represented by a power law, then all the parameters involved are subject to alteration with time. The exponent of the spectrum does not seem to be a constant all through the entire primary energy region concerned. Even the direction of the diurnal anisotropy changes considerably with time. The correlation between the solar diurnal amplitudes of cosmic ray components and the American relative sunspot number in their seasonal variation shows that the diurnal variation of the primary cosmic radiation of lower energy are more readily modulated by the solar activities.

CHAPTER V

CONCLUSIONS

In the foregoing chapters, the function of the large NaI (Tl) total absorption spectrometer with its associated electronics as a photon monitor has been described in detail; for the first time results of studies on the atmospheric effect and the solar diurnal variation of sea level photons have been presented together with discussions and conclusions. In this chapter we comment briefly on the characteristics of this type of photon monitor time variation study.

The NaI crystal, coupled with the plastic shield, effects a separation of the totally absorbed neutral particles from the total component of cosmic radiation. These neutral particles have been identified experimentally as photons and recorded in the form of a differential energy spectrum.

The atmospheric effect on the sea level cosmic ray photons appears to be quite complicated in a short period of time. However, our results suggest that the average effect of the atmosphere can be removed by suitable pressure corrections. The energy dependence of the barometric coefficients is interpreted in terms of a simple absorption model. However, atmospheric effects due to other meterological factors (possibly temperature) cannot be entirely neglected if one recalls the considerable variability in the values of the monthly mean barometric coefficient.

Our present spectrometer has a major weakness as far as time variation studies of cosmic radiation are concerned. Its counting rate is too low on account of the relatively small sensitive volume of the

NaI crystal. This could be improved by using a crystal (and corresponding shield) of much larger size. The hypothesis of a one-to-one correspondence between photon energy range and an "effective" primary energy is justified by a reasonably successful interpretation of the solar diurnal results (Chapter IV). If the validity of this hypothesis is confirmed, then this type of photon spectrometer is a particularly useful device for time variation studies, its principal advantage being the ability, on account of energy discrimination, to respond to different primary energies in the one experiment. Presently popular cosmic ray monitors are integral rather than differential recording devices, and lack this important feature.

APPENDIX A

THE METHOD OF COUPLING CONSTANTS

The method of coupling constants is used to determine the primary variation of cosmic radiation from the secondary variation (see Dorman 1957). Assuming a vertical incidence of the primary cosmic rays on the atmosphere boundary, the total intensity N of a secondary cosmic ray component as observed at a station of specified latitude, longitude and elevation will be

$$N = \int_e^\infty D(E)m(E)dE \qquad (1)$$

where E is the primary energy, D(E) is the primary differential energy spectrum, m(E) is the multiplicity function and e is the vertical geomagnetic threshold energy. The time variation of the secondary component is a result of variations in geomagnetic cutoff, primary differential spectrum and the multiplicity.

A variation of equation (1) will lead to

$$\delta N = -\delta e D(e)m(e) + \int_e^\infty \delta D(E)m(E)dE + \int_e^\infty D(E)\delta m(E)dE \qquad (2)$$

and the relative variation of the observed secondary intensity (in percentage) will be

$$\frac{\delta N}{N} = -\delta e W(e) + \int_e^\infty \frac{\delta D(E)}{D(E)} W(E)dE + \int_e^\infty \frac{\delta m(E)}{m(E)} W(E)dE \qquad (3)$$

where

$$W(E) \equiv \frac{D(E)m(E)}{N} \qquad (\%/\text{BeV}) \qquad (4)$$

and is called the differential coupling constant. $\frac{\delta D(E)}{D(E)}$ is the energy spectrum of the primary variation. The first, second and third terms on the right hand side of equation (3) indicate respectively the variations in the secondary component due to changes in geomagnetic cutoff, primary spectrum and atmospheric conditions.

After the data have been corrected for the geomagnetic and atmospheric influences, the remainder will be due to variations of the primary energy spectrum outside the earth represented by

$$\frac{\partial N}{N} = \int_e^\infty \frac{\delta D(E)}{D(E)} W(E) dE \tag{5}$$

Using the concept of "effective" angles, the position of the primary variation source can be determined as follows:

$$\bar{X} = \frac{\int_e^\infty X(E) W(E) \frac{\delta D(E)}{D(E)} dE}{\int_e^\infty W(E) \frac{\delta D(E)}{D(E)} dE} \tag{6}$$

$$\bar{Y} = \frac{\int_e^\infty Y(E) W(E) \frac{\delta D(E)}{D(E)} dE}{\int_e^\infty W(E) \frac{\delta D(E)}{D(E)} dE} \tag{7}$$

where X is the angle between the direction of motion of the particle at infinity and the plane of geomagnetic equator, and Y is the angle between the projection of the direction of motion at infinity onto the plane of geomagnetic equator and the projection, onto the same equatorial plane, of the radius of vector produced from the center of the earth to the point on the earth's surface where the particle should impinge (called the angle of "drift"). $\bar{X}$ and $\bar{Y}$ are "effective" angles indicating the "effective"

direction to the source of variation. For a station specified by a set of longitude and latitude, X and Y are functions of the direction of arrival (specified by the zenith angle and azimuth angle) and the primary energy.

APPENDIX B

IBM 1620 SOURCE PROGRAMS

(a) Source Program for Calculation of Barometric Coefficients (in UTO Fortran language)

```
      DIMENSION Y(43),SY(43),SY2(43),SPY(43),A(43),R(43),G(43),T(43)
      DIMENSION B(43)
    4 FORMAT (F7.0,F7.0,F7.0,F7.0,F7.0,F7.0,F7.0,I3,I3,F7.2,I4,F5.1)
    9 FORMAT (I3,I4,I3,5X,F10.4,F10.4,F10.4,F7.0,F10.2,F7.2)
   30 FORMAT (F7.0)
   34 FORMAT (I5)
    7 CTR=0.0
      SP=0.0
      SP2=0.0
      DO 1 J=1,43
      SY(J)=0.0
      SY2(J)=0.0
    1 SPY(J)=0.0
      READ 34, KUM
   21 DO 15 J=1,29,7
   15 READ 4, Y(J),Y(J+1),Y(J+2),Y(J+3),Y(J+4),Y(J+5),Y(J+6),L,M,P,K,Q
      IF (KUM-K) 22,18,18
   18 DO 16 J=1,35
   16 Y(J)=Y(J)*51.2/Q
      Y(36)=Y(27)+Y(28)
      Y(37)=Y(29)+Y(30)+Y(31)
      Y(38)=Y(32)+Y(33)+Y(34)+Y(35)
      Y(39)=Y(1)+Y(2)+Y(3)+Y(4)
      Y(40)=Y(5)+Y(6)+Y(7)+Y(8)+Y(9)+Y(10)
      Y(41)=Y(11)+Y(12)+Y(13)+Y(14)+Y(15)+Y(16)+Y(17)+Y(18)+Y(19)
      Y(42)=Y(39)+Y(40)+Y(41)
      Y(43)=Y(20)+Y(21)+Y(22)+Y(23)+Y(24)+Y(25)+Y(26)+Y(36)+Y(37)+Y(38)
      SP=SP+P
      SP2=SP2+P**2
      CTR=CTR+1.0
      DO 55 J=1,43
      SY(J)=SY(J)+Y(J)
      SY2(J)=SY2(J)+Y(J)**2
   55 SPY(J)=SPY(J)+Y(J)*P
      GO TO 21
   22 PRINT 30, CTR
      H=CTR*SP2-SP**2
      DO 6 J=1,43
      B(J)=SY(J)/CTR
      G(J)=CTR*SY2(J)-SY(J)**2
      A(J)=(CTR*SPY(J)-SP*SY(J))/H
      R(J)=A(J)*(SQRT(H/G(J)))
      T(J)=SQRT((G(J)-A(J)*A(J)*H)/((CTR-1.0)*H))
```

```
      T(J)=100.*T(J)/B(J)
    6 A(J)=100.*A(J)/B(J)
      SPA=SP/CTR
      DO 5 J=1,43
    5 PUNCH 9, M,K,J,A(J),T(J),R(J),CTR,B(J),SPA
      PAUSE
      GO TO 7
      END
```

(b) Source Program for Determination of 24 Hour Daily Variations (in Fortran II language)

```
      DIMENSION SYHM(24,24),AM(24),Z(25)
      DIMENSION Y(43),CTRH(24),SPH(24),INTEN(40)
      COMMON INTEN
    8 FORMAT (6I6)
    9 FORMAT (6F10.2)
   19 FORMAT (7F10.2)
    6 FORMAT (8F8.4)
   28 FORMAT (5HKM = ,I3,8H   MM = ,I2,8H   NM = ,I2,7H   N = ,I2,
     19H   CTR = ,F7.0)
   27 FORMAT (6HNSECT=,I6,5H   K=,I4,5H   M=,I3,6H CTRM=,F7.0,5H CTR=,
     1 F7.0,6H   NG=,I3)
    4 FORMAT (8F8.1,I3,I2,I3)
    5 FORMAT (4HSPH=,F7.2,7H  CTRH=,F7.0,4H  K=,I4,5H  ML=,I3,6H CTRM=,
     1 F8.0,4H  M=,I3)
   26 FORMAT (24HEND OF JOB   LAST NSECT=,I6,5H   K=,I4,5H   M=,I3,
     1 6H   NG=,I3)
   30 READ 8,NSECT,NSECL,KLD,KHL,KGD,NM
      READ 8,MSECF,MSECL,NG,N
      READ 6, (AM(I),I=1,24)
    7 CTR=0.0
      CTRM=0.0
      DO 40 M=1,24
      SPH(M)=0.0
   40 CTRH(M)=0.0
      DO 41 I=1,24
      DO 41 M=1,24
   41 SYHM(J,M)=0.0
      MSECT=MSECF
  124 READ 9, (Z(I), I=1,18)
      READ 19, (Z(I), I=19,25)
      Z(25)=Z(25)*100.0
      DO 125 I=1,25
  125 INTEN(I)=Z(I)
      IY=DSKWF(MSECT)
      MSECT=MSECT+2
      IF(MSECL-MSECT) 126,126,124
  126 MSECT=MSECF
   53 IX=DSKRF(MSECT)
      DO 131 I=1,24
  131 Z(I)=INTEN(I)
      PA=INTEN(25)
      PA=PA/100.0
```

```
    MSECT=MSECT+2
10  IX=DSKRF(NSECT)
    DO 55 I=1,35
55  Y(I)=INTEN(I)
    M=INTEN(36)
    P=INTEN(37)
    P=P/100.0
    K=INTEN(38)
    Q=INTEN(39)
    Q=Q/10.0
    Y(36)=Y(27)+Y(28)
    Y(37)=Y(29)+Y(30)+Y(31)
    Y(38)=Y(32)+Y(33)+Y(34)+Y(35)
    Y(39)=Y(1)+Y(2)+Y(3)+Y(4)
    Y(40)=Y(5)+Y(6)+Y(7)+Y(8)+Y(9)+Y(10)
    Y(41)=Y(11)+Y(12)+Y(13)+Y(14)+Y(15)+Y(16)+Y(17)+Y(18)+Y(19)
    Y(42)=Y(39)+Y(40)+Y(41)
    Y(43)=Y(20)+Y(21)+Y(22)+Y(23)+Y(24)+Y(25)+Y(26)+Y(36)+Y(37)+Y(38)
    PD=P-PA
    IF (KLD-K) 16,15,15
15  IF (KGD-K) 18,14,14
14  IF (KHL-K) 99,17,17
17  CTR=CTR+1.0
    CTRM=CTRM+1.0
    CTRH(M)=CTRH(M)+1.0
    DO 56 I=1,24
56  Y(I+19)=Y(I+19)*(51.2/Q)-Z(I)*PD*(AM(I)/100.0)
    DO 1 I=1,24
 1  SYHM(I,M)=SYHM(I,M)+Y(I+19)
    SPH(M)=SPH(M)+P
    NSECT=NSECT+2
    KL=K
    ML=M
    GO TO 10
16  PRINT 28,KL,ML,NM,N,CTR
    NM=NM+1
    IF (8-NM) 84,83,84
83  N=0
84  IF (N) 81,81,82
81  N=N+1
    KLD=KLD+31
    GO TO 53
82  N=N-1
    KLD=KLD+30
    GO TO 53
18  NSECT=NSECT-1
    PRINT 27, NSECT,KL,ML,CTRM,CTR,NG
    NG=NG+1
    NSECT=NSECT+1
    DO 68 M=1,24
    DO 67 I=1,24
67  SYHM(I,M)=SYHM(I,M)/CTRH(M)
    SPH(M)=SPH(M)/CTRH(M)
    PUNCH 4, (SYHM(I,M), I= 1, 8),I,M,KL
```

```
      PUNCH 4, (SYHM(I,M), I= 9,16),I,M,KL
      PUNCH 4, (SYHM(I,M), I=17,24),I,M,KL
      DO 64 I=1,24
   64 SYHM(K,M)=SQRTF(SYHM(I,M))/SQRTF(CTRH(M))
      PUNCH 4, (SYHM(I,M), I= 1, 8),I,M,KL
      PUNCH 4, (SYHM(I,M), I= 9,16),I,M,KL
      PUNCH 4, (SYHM(I,M), I=17,24),I,M,KL
   68 PUNCH 5, SPH(M),CTRH(M),KL,ML,CTRM,M
     ,KGD=KGD+27
      CTRM=0.0
      DO 61 M=1,24
      SPH(M)=0.0
   61 CTRH(M)=0.0
      DO 62 I=1,24
      DO 62 M=1,24
   62 SYHM(I,M)=0.0
      GO TO 10
   99 PRINT 26, NSECT,KL,ML,NG
      PAUSE
      GO TO 30
      END
```

(c) Explanations

In the present studies, data were processed by means of IBM 1620 computer. A set of five cards contains readings of cosmic ray intensities and presure as recorded every hour. There are 19 pieces of data (indicated by J from 1 to 19 in the source programs) for the charged particles of various energies and 16 pieces (indicated by J from 20 to 35) for the photons. Each card is also labelled with card number, hour number, day number and the time interval of data recording. For source program (a), above informations were read into the computer directly from cards whenever they were needed in the computation. However, these informations were stored in a disk pack prior to the execution of the source program (b). Tables are given to define the meanings of the variables used in the input and output statements as follows.

(i) Table for Source Program (a)

(1) Input Variables:

Y(J) - cosmic ray intensity of energy range J
L - card number

M - hour number
P - pressure
K - day number
Q - time interval of data recording
KUM - a day number which is used to terminate further data readin

(2) Output Variables:

CTR - number of intensity-pressure pairs (i.e. number of hourly data) which has been used in the calculation
J - energy range number of cosmic ray intensity
A(J) - barometric coefficient of J
T(J) - standard deviation of J
R(J) - correlation coefficient of J
B(J) - average counting rate of J
SPA - average pressure

(ii) Table for Source Program (b)

(1) Special Variables and Functions for Using the Disk Pack

IY,IX - dummy variables which are used to initiate the executions of functions DSKWF and DSKRF
INTEN(40) - a subscripted variable, the size of whose array is 40.
DSKWF(NS) - a function which is used to write all the members of INTEN onto the two sectors of the disk with NS being the number of the first sector
DSKRF(NS) - a function which is used to read all the data from the two sectors of the disk (specified by the first sector number NS) into the memory locations specified for INTEN

(2) Input Variables:

NSECT - sector number
KLD - the last day number of a month
KHL - a day number which is used to terminate further data readin
KGD - a day number which is used to initiate the calculation of the average daily variation over a period of 27 days
NM - month number
MSECF - number of the first sector used to store Z(I)
MSECL - number of the last of the two sectors used to store Z(I)
NG - period number (a period consists of 27 days)
N - a number which is used to control the value of KLD
AM(I) - barometric coefficient (weighted average

rapid-pressure-change) of J = I + 19

Z(I) - monthly average counting rate of J = I + 19 (for I = 1 to 24)

Z(25) - monthly average pressure

J - energy range number of cosmic ray intensity

Y(J) - cosmic ray intensity of J

M - hour number

P - pressure

K - day number

Q - time interval of data recording

(3) Output Variables:

SYHM(I,M) - average counting rate (in a period of 27 days) of J = I + 19 for the specified hour M

SYHM(I,M) - (the second meaning) standard deviation of the average counting rate of J for M

SPH(M) - average hourly pressure (in a period of 27 days) for hour M

CTRH(M) - number of intensity-pressure pairs for hour M which has been used in the period of 27 days

ML - the number of the last hour of the last day in the period

CTRM - number of intensity-pressure pairs which has been used in the period

REFERENCES

Ables, J.G., K.G. McCracken and U.R. Rao, 1965, Proc. Int. Conf. Cosmic Rays, London, 1, 208.

Abraham, F., K. Kidd and M. Koshiba, 1963, Nuovo Cim., 28, 221.

Ahluwalia, H.S. and A.J. Dessler, 1962, Planet. Space Sci., 9, 195.

Ahluwalia, H.S., V.I. Escobar, M. Zubieta, R. Anda, M. Schreier and O. Troncoso, 1965, Proc. Int. Conf. Cosmic Rays, London, 1, 190.

Alfven, H., 1947, Phys. Rev., 72, 88.

Alfven, H., 1951, Cosmic Electrodynamics (Oxford, Clarendon).

Alfven, H., 1954, Tellus, 6, 232.

Alfven, H. and K.G. Malmfors, 1943, Ark. Mat. Astr. Fys., 29A, 24.

Axford, W.I., 1965, Planet. Space Sci., 13, 115.

Barton, J.C. and J.H. Stockhausen, 1958, Phil. Mag., 3, 55.

Bercovitch, M., 1963, J. Geophys. Res., 68, 4366.

Bercovitch, M., 1966, Can. J. Phys., 44, 1329.

Bercovitch, M. and B.C. Robertson, 1965, Proc. Int. Conf. Cosmic Rays, London, 1, 489.

Bercovitch, M., J.F. Steljes and H. Carmichael, 1963, Proc. Int. Conf. Cosmic Rays, Jaipur, 2, 327.

Blackett, P.M.S., 1938, Phys. Rev., 54, 973.

Brunberg, E.A. and A. Dattner, 1953, Tellus, 5, 135, 269.

Brunberg, E.A. and A. Dattner, 1954, Tellus, 6, 73.

Bukata, R.P., 1958, Summer Thesis, University of Manitoba.

Bukata, R.P., 1960, Master's Thesis, University of Manitoba.

Bukata, R.P., F.K. Chin and S. Standil, 1962, Can. J. Phys., 40, 348.

Carmichael, H., M. Bercovitch and J.F. Steljes, 1963, Proc. Int. Conf. Cosmic Rays, Jaipur, 2, 350.

Carmichael, H., M. Bercovitch and J.F. Steljes, 1965, Proc. Int. Conf. Cosmic Rays, London, 1, 492.

Cernigoi, G. and G. Poiani, 1954, Nuovo Cim., 11, 41.

Chasson, R.L., 1954, Phys. Rev., 96, 1116.

Chin, F.K., 1961, Master's Thesis, University of Manitoba.

Chin, F.K., R.P. Bukata and S. Standil, 1962, Can. J. Phys., 40, 380

Chou, C.N., 1953, Phys. Rev., 90, 473.

Chudakov, A.E., V.L. Dadykin, V.I. Zatsepin and N.M. Nesterova, 1963, Proc. Int. Conf. Cosmic Rays, Jaipur, 4, 199.

Clay, J. and E. van Alphen, 1951, Physica, 17, 711.

Cocconi, J., 1960, Trans. Int. Conf. Cosmic Rays, Moscow, 2, 327.

Coleman, P.J.Jr, L. Davis and C.P. Sonett, 1960, Phys. Rev. Letters, 5, 43.

Davisson, C.M., 1965, Beta- and Gamma-Ray Spectroscopy, Ed K. Siegbahn (Amsterdam: North-Holland).

Dawton, D.I. and H. Elliot, 1953, J. Atm. Terrest. Phys., 3, 295.

Dolbear, D.W.N. and H. Elliot, 1951, J. Atm. Terrest. Phys., 1, 215.

Dorman, L.I., 1955, Dissertation, NIZMIR FIAN, Moscow.

Dorman, L.I., 1957, Cosmic Ray Variations (Moscow: State Publishing House).

Dorman, L.I., A.I. Kuzmin, G.V. Tyanutova, Y.L. Feynberg and Y.G. Shafer, 1954, Zhur. Eksp. Teor., Fiz., 26, 537.

Dorman, L.I., V.I. Ivanov, I.E. Koshkarev, E.V. Kolomeets, L.A. Mirkin, V.T. Pivneva, G.A. Sergeeva and R.A. Chumbalova, 1963, Proc. Int. Conf. Cosmic Rays, Jaipur, 2, 356.
Drying, E. and B. Sporre, 1965, Proc. Int. Conf. Cosmic Rays, London, 1, 478.
Duperier, A., 1946, Nature, 158, 196.
Duperier, A., 1948, Proc. Phys. Soc., A61, 34.
Duperier, A., 1949, Proc. Phys. Soc., A62, 684.
Ehmert, A. and A. Sittkus, 1951, Z. Naturforsch., 6a, 618.
Elliot, H., 1960, Phil. Mag., 5, 601.
Elliot, H., 1962, J. Phys. Soc. Japan, 17 (Suppl. A-II), 588.
Elliot, H. and D.W.N. Dolbear, 1950, Proc. Phys. Soc., 63, 137.
Elliot, H. and D.W.N. Dolbear, 1951, J. Atm. Terr Phys., 1, 215.
Faller, A.M. and P.L. Marsden, 1965, Proc. Int. Conf. Cosmic Rays, London, 1, 231.
Firkowski, R., J. Gawin, A. Zawadzki and R. Maze, 1962, Nuovo Cim., 26, 1422.
Firkowski, R., J. Gawin, A. Zawadzki and R. Maze, 1963, Nuovo Cim., 29, 19.
Firor, J.W., W.H. Fonger and J.A. Simpson, 1954, Phys. Rev., 94, 1031.
Forbush, S.E. and D. Venkatesan, 1960, J. Geophys. Res., 65, 2213.
Fowler, P.H., 1963, Proc. Int. Conf. Cosmic Rays, Jaipur, 5, 182.
Gawin, J., J. Hibner, J. Wdowczyk, A. Zawadzki and R. Maze, 1965, Proc. Int. Conf. Cosmic Rays, London, 2, 639.
Gawin, J., J. Hibner, A. Zawadzki and R. Maze, 1963, Proc. Int. Conf. Cosmic Rays, Jaipur, 4, 180.
Glokova, E.S., 1952, Trudy NIIZM, 8, 59.
Glokova, E.S., 1956, Izv. AN SSSR, (Ser. Fiz.) 20, 47.
Glokova, E.S., 1960, Trans. Ya FAN, (Ser. Fiz.) 3, 84.
Glokova, E.S., L.I. Dorman, N.S. Kaminer and G.V. Tyanutova, 1955, Otchet NIIZM (report).
Glokova, E.S., N.S. Kaminer, N.A. Mishina, 1957, Trudy Ya FAN (Ser. Fiz.) 2.
Glokova, E.S., N.A. Mishina and N.S. Kaminer, 1958, Trans. Ya FAN (Ser. Fiz.) 2, 95.
Greenstadt, E.W., 1965, TRW Report 9890-6001-RU000.
Grigorov, N.L., 1955, Dissertation, FIAN.
Heitler, W., 1954, Quantum Theory of Radiation, 3rd ed. (Oxford: Clarendon).
Hogg, A.R., 1949, Memoirs of Commonwealth Observatory, Canberra, 10.
Inozemtseva, O.I., 1964, Geomagn. and Aeronomy, 4, 222.
Janossy, L., 1937, Zs. Phys., 104, 430.
Janossy, L. and G.D. Rochester, 1944, Roy. Soc. London, A182, 186.
Janossy, L. and B. Rossi, 1940, Proc. Roy. Soc., A175, 88.
Jacklyn, R.M. and J.E. Humble, 1965, The Upper Limiting Primary Rigidity of the Cosmic Ray Solar Anisotropy (Hobart: University of Tasmania).
Kameda, T., 1960, J. Phys. Soc. Japan, 15, 1175.
Kaminer, N.S., S.F. Ilgatch and T.S. khadakhanova, 1965, Proc. Int. Conf. Cosmic Rays, London, 1, 486.
Kane, R.P., 1963, Nuovo Cim., 29, 801.
Kane, R.P., 1964, Nuovo Cim., 32, 273.
Kane, R.P. and S.R. Thakora, 1960, Proc. Ind. Acad. Sci., A52, 122.
Kanno, T., 1963, Proc. Int. Conf. Cosmic Rays, Jaipur, 2, 370.
Kanno, T., Y. Ishida and S. Iseki, 1965, Proc. Int. Conf. Cosmic Rays, London, 1, 221.
Katzman, J. and D. Venkatesan, 1960, Can. J. Phys., 38, 1011.
Kird, J.M., 1963, Nuovo Cim., 27, 57.
Kitamura, M., 1965, Proc. Int. Conf. Cosmic Rays, London, 1, 201.

Kolomeets, E.V., G.A. Sergeeva, A.N. Nemolochuov, R.A. Chumbalova and A.G. Zusmanovich, 1965, Proc. Int. Conf. Cosmic Rays, London, 1, 224.
Kraushaar, W.L., G.W. Clark, M. Agagino, G. Garmire, H. Helmken and P. Higbie, 1963, Proc. Int. Conf. Cosmic Rays, Jaipur, 3, 184.
Kuzmin, A.I., 1955a, Zhur. Eksp. Teor., Fiz. 28, 614.
Kuzmin, A.I., 1955b, Trudy Ya FAN (Ser. Fiz.) 1, 19.
Kuzmin, A.I., 1960, Trans. Ya FAN (Ser. Fiz.) 3, 99.
Kuzmin, A.I., G.F. Krymsky and G.V. Skripin, 1963, Proc. Int. Conf. Cosmic Rays, 2, 460.
Kuzmin, A.I. and G.V. Skripin, 1958, Trans. Ya FAN (Ser. Fiz.) 2, 107.
Lange, I. and S.E. Forbush, 1948, Carnegie Institution of Washington Publication 175.
Lapointe, S.M. and D.C. Rose, 1962, Can. J. Phys., 40, 697.
Lindholm, 1928, Gerl. Beitr. Z. Geophys., 20, 466.
Lingren, S., 1962, Tellus, 14, 44.
Lockwood, J.A., W.R. Webber and H. Carmichael, 1966, Bull. Amer. Phys. Soc. (Ser.11) 11, 399.
Maeda, K., 1953, J. Geomagn. Geoelect., 5, 105.
Maeda, K., 1960, J. Atmos. Terr. Phys., 19, 184.
Malmfors, K.G., 1948, Ark. Mat. Astr. Fys., 32A, No. 8.
Mathews, P.M., 1959, Can. J. Phys., 37, 85.
Maze, R. and A. Zawadzki, 1960, Nuovo Cim., 17, 625.
McCracken, K.G. and U.R. Rao, 1965, Proc. Int. Conf. Cosmic Rays, London, 1, 213.
McCracken, K.G., 1962, J. Geophys. Res., 67, 447.
Mercer, J.B. and B.G. Wilson, 1965, Nature, 208, 477.
Mori, S., H. Ueno and K. Nagashima, 1965, Proc. Int. Conf. Cosmic Rays, London, 1, 498.
Mori, S., H. Ueno, K. Nagashima and S. Sagisaka, 1964, Rep, Ionosphere Space Res. Japan, 18, 275.
Mori, S., H. Ueno, S. Sagisaka, K. Nagashima and Y. Sekido, 1963, Proc. Int. Conf. Cosmic Rays, Jaipur, 2, 33.
Murakami, K. and S. Kudo, 1965, Proc. Int. Conf. Cosmic Rays, London, 1, 219.
Myssowsky, L.V. and L. Tuwin, 1926, Z. Phys., 39, 146.
Ness, N.F. and J.M. Wilcox, 1964, Phys. Rev. Letters, 13, 461.
Olbert, S., 1953, Phys. Rev., 92, 454.
Parker, E.N., 1958, Astrophys. J., 128, 664.
Parker, E.N., 1964, Planet. Space Sci., 12, 735.
Perlow, G.J. and C.W. Kissinger, 1951, Phys. Rev., 84, 572.
Peterson, L.W. and J.R. Winckler, 1959, J Geophys. Res., 64, 697.
Quenby, J.J. and T. Thambyahpillai, 1960, Phil. Mag., 5, 585.
Rao, U.R., K.G. McCracken and D. Venkatesan, 1963, J. Geophys. Res., 68, 345.
Regener, V.H., 1940, Ricerca Scient., 11, 66.
Rose, D.C., 1951, Can. J. Phys., 29, 97.
Sandström, A.E., 1955, Tellus, 7, 204.
Sandström, A.E., E. Dyring and S. Lindgren, 1960, Nature, 187, 1099.
Sarabhai, V. and P.D. Bhavsar, 1958, Nuovo Cim., 8 (Suppl.), 299.
Sarabhai, V., V.D. Dessai and D. Venkatesan, 1953, Nature, 171, 122.
Sarabhai, V., V.D. Dessai and D. Venkatesan, 1954, Phys. Rev., 96, 969.
Sarabhai, V., V.D. Dessai and D. Venkatesan, 1955, Phys. Rev., 99, 1490.
Sarabhai, V., G.L. Pai and M. Wada, 1965, Nature, 206, 703.
Sarabhai, V. and G. Subramanian, 1963a, Proc. Int. Conf. Cosmic Rays, Jaipur, 2, 307.
Sarabhai, V. and G. Subramanian, 1963b, Proc. Int. Conf. Cosmic Rays,

Jaipur, 2, 405.
Sastry, C.V., 1964, Current Sci., 33, 676.
Schwacheim, G., 1960, J. Geophys. Res., 65, 3149.
Sekido, Y., M. Kodama and T. Yagi, 1950, Rep. Ion. Res. Japan, 4, 207.
Sekido, Y. and S. Yoshida, 1950, Rep. Ion. Res. Japan, 4, 37.
Sekido, Y. and S. Yoshida, 1951, Rep. Ion. Res. Japan, 5, 43.
Simpson, J.A., W.H. Fonger and S.B. Treiman, 1953, Phys. Rev., 90, 934.
Sittkus, A., 1955, J. Atmos. Terr. Phys., 7, 80.
Smith, E.J., 1964, Space Physics, Eds D.P. leGalley and A. Rosen (New York: John Wiley).
Snyder, C.W., M. Neugebauer and U.R. Rao, 1963, Proc. Int. Conf. Cosmic Rays, Jaipur, 1, 185.
Standil, S. and W.D. Loveridge, 1959, Rev. Sci. Instr., 30, 931.
Standil, S., R.P. Bukata and F.K. Chin, 1961, Can. J. Phys., 39, 229.
Steinmauer, R. and H. Gheri, 1955, Naturwissenschaften, 42, 294.
Stepanyan, A.A., 1962, Geomagn. and Aeronomy, 2, 443.
Stern, D., 1964, Planet. Space Sci., 12, 973.
Swann, W., 1954, Phys. Rev., 93, 905.
Thambyaphillai, T. and H. Elliot, 1953, Nature, 171, 919.
Trefall, H., 1953, Nature, 171, 888.
Trefall, H., 1955, Proc. Phys. Soc., A68, 625, 893, 953.
Treiman, S.B., 1954, Phys. Rev., 93, 544.
Trumpy, B., 1953, Physica, 19, 645.
Venkatesan, D. and A. Dattner, 1959, Tellus, 11, 116.
Vladimirsky, B.M., A.K. Pankratov and A.A. Stepanyan, 1965, Proc. Int. Conf. Cosmic Rays, London, 1, 229.
Wada, M., 1957, J. Sci. Res. Inst., 51, 201.
Wada, M., 1960, Jap. Inst. Phys. Chem. Res., 54, 335.
Wada, M., 1961, Jap. Inst. Phys. Chem. Res., 55, 7.
Webber, W.R. and J.J. Quenby, 1959, Phil. Mag., 4, 654.
Yagi, T. and H. Veno, 1956, J. Geom. Geoelectr., 8, 93.
Yoshida, S. and I. Kondo, 1954, J. Geom. Geoelectr., 6, 15.
Compton, A.H. and R.N. Turner, 1937, Phys. Rev., 52, 799.